Polylactide microcapsules and films:

preparation and properties

Hassan Ismaiel Mahmoud Sawalha

Polylactide microcapsules and films:

preparation and properties

**Polylactide microcapsules and films:
preparation and properties**

Contents

Chapter 1

Introduction

Introduction

In this thesis, microparticles and films made of the biopolymer polylactide (PLA) are investigated (see Figure 1). The structure in these systems was induced by dissolving this polymer in a mixture of solvents and inducing phase separation.

In this introduction, first the properties of polymer itself are discussed, followed by those of the two main products which were investigated: films and solid and hollow particles (microbubbles).

We will then discuss the main target of this thesis, which is to prepare PLA-based products with specific properties, followed by an outline of the chapters of the thesis.
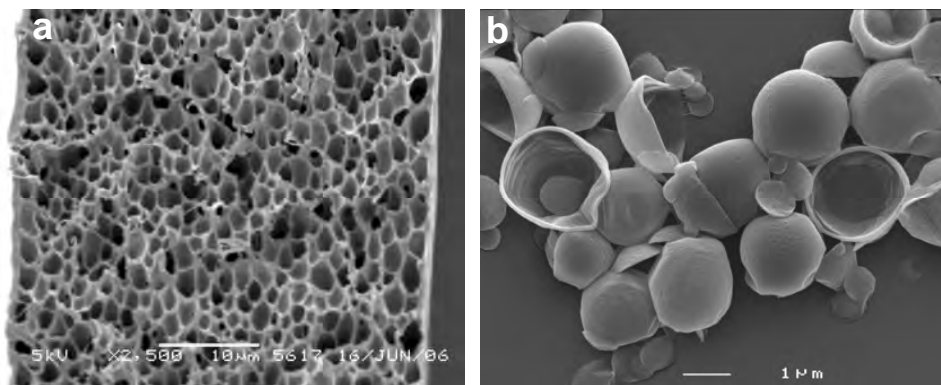
Figure1: examples of PLA films (a) and hollow-microcapsules (b) prepared in this study

Polylactide

PLA is a linear aliphatic thermoplastic polyester that can be derived from renewable resources [1, 2]. Production of PLA starts with fermentation of food stocks like starch, corn, or sugar beets into lactic acid (2-hydroxy propionic acid), which is the basic building block of PLA [3, 4]. After fermentation and separation, the lactic acid is converted into the cyclic di-ester lactide, using a combined process of oligomerization and cyclization [3, 4]. The lactide is then polymerized through ring-opening into polylactide [3, 4].

There are two optical isomers of lactide, the L (*Levorotary*) isomer, and the D (*Dexterotary*) isomer [1, 3, 5]. Polymers prepared from the L and D isomers are usually called poly(L-lactide), PLLA, and poly(D-lactide), PDLA, respectively. Both homopolymers are highly (semi-)crystalline, while the random copolymer poly (DL-lactide) PDLLA is completely amorphous (see Figure 2 for structural formulae). Hence, the properties of DL-based products are very different from those made of one of the homopolymers [1, 3, 5].
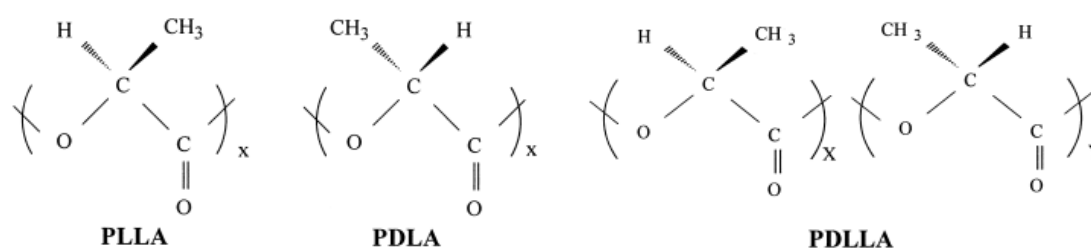
Figure 2: structural formulae of PLLA, PDLA and PDLLA [13].

The unique properties of PLA such as high mechanical strength and good biodegradability and biocompatibility have made it a popular polymer for many applications in the biomedical, pharmaceutical, as well as environmental fields [5-11]. In the biomedical field, PLA is used in different types of biomaterials; i.e. sutures, scaffolds for heart, bone and cartilage tissue engineering [8-10]. Besides, it is also used in films and membranes for cell culturing [11], and in microcapsules for controlled delivery of several types of drugs, antigens, and vaccines [7, 12]. Another big application area is in packaging, where PLA serves as an environmental-friendly alternative for conventional petrochemical-based packaging materials [6].

The mechanical and thermal properties of PLA are important for its application. PLA is generally brittle and stiff at room or body temperature with a glass transition temperature of around 60 $^{\circ}$C [14, 15]. The lack of toughness is a bottleneck for expanding the fields of applications of PLA. Its flexibility can be improved by using different techniques such as copolymerization, blending, and plasticization with other polymers and low molecular weight compounds [14, 16-

23]. Even though some interesting materials were reported in literature, it is obvious that optimization of the mechanical properties of PLA for the application in mind is still of prime importance.

Preparation of PLA films

PLA films have found different applications like cell scaffolding and packaging material [6, 11, 24, 25]. PLA films can be fabricated with melt or solution processing [4, 26, 27]. In melt processing, PLA is heated above its melting point, shaped into the desired shape, and then cooled to solidify the product. The techniques used for melt processing include extrusion, film blowing, injection moulding, and (thermal) compression [4]. A disadvantage of melt processing is that PLA degrades at elevated temperature [4]. The solution processing involves dissolving the polymer in a proper solvent, casting of the solution into a mold (e.g., a film), and subsequent solidification by removing the solvent or by reducing the solvent quality. The most commonly used techniques for PLA films and membranes are immersion precipitation and film casting; both techniques will be discussed more elaborately in the following chapters. In evaporative film casting, the polymer solution is cast on a flat mold and then exposed to air to evaporate the solvent. With immersion precipitation, the cast film is immersed in a coagulation bath filled with a nonsolvent for the polymer which is however miscible with the solvent. The solvent diffuses out of the film into the nonsolvent bath, while the nonsolvent diffuses into the polymer solution. This exchange results in a net reduction of the overall solvent quality in the polymer solution which induces nucleation and subsequent growth of a polymer poor phase, and enrichment and ultimately solidification of the solution of the solution surrounding these nuclei [27]. The polymer poor droplets eventually form the pores in a polymeric matrix. The properties of the resulting films, i.e. morphology, porosity, and mechanical and thermal properties are strongly dependent on the polymer concentration, polymer crystallinity, and thermodynamic and kinetic interactions between polymer solvent and nonsolvent [27] (see chapters 2 and 3). Mixtures of solvents and nonsolvents instead of a single solvent and a single nonsolvent can be therefore used to modify the properties of the films [28, 29].

Preparation of PLA microbubbles and particles

PLA microparticles (and bubbles) have received increased attention in recent years because of their applications in the pharmaceutical field. Microparticles have been widely investigated as delivery carriers for bioactive therapeutic agents and vaccines [7, 12]. In addition, hollow microparticles (bubbles) can be used as contrast agents in ultrasound imaging. Ultrasound contrast agents (UCA's) are small gas bubbles stabilized with a thin polymer or protein shell [30]. These agents are efficient ultrasound reflectors when subjected to an acoustic field: they enhance the ultrasound signal and consequently can facilitate visualization of organs and (soft) tissues of the body during ultrasound treatment [30, 31]. The mechanical and chemical properties of microparticles and UCA's are very important in medical applications. For example, when particles are small and have uniform size they are more biocompatible and induce less inflammatory response from the tissues compared to larger and more polydisperse particles [32, 33]. Furthermore, small particles can pass easier through narrow blood vessels and have longer circulation time in the blood than big particles, since they are taken up less quickly by liver and/or pancreas [34]. Preparation of microparticles and UCA's with well-defined properties is therefore very relevant, and it is obvious that preparation techniques and conditions need to be chosen carefully.

Microparticles or microbubbles can be prepared using different techniques such as solvent extraction/evaporation, coacervation, and spray-drying [35]. The solvent extraction/evaporation method, which is a crossover between evaporative casting and immersion precipitation, gives better control over the size and size distribution of the particles than the other techniques [35]. Preparation of microparticles through solvent extraction/evaporation starts with emulsification of a homogenous polymer solution in a continuous phase that consists of nonsolvent (*e.g.,* water), which is immiscible with the solvent, and possibly a stabilizer to keep the droplets apart. After emulsification, the solvent slowly diffuses out of the particles and through the nonsolvent bath, and then evaporates at the surface of the bath (see Figure 3). Removal of the solvent causes the polymer to solidify by glassification or crystallization [35].

The final particle size is determined by the initial droplet size and the concentration of the polymer in the casting solution. It is thus important to start with a narrowly dispersed emulsion of the casting solution. Standard emulsification techniques such as sonication, high-pressure homogenizers and colloid mills, have as main disadvantage that they give poor control over the size and size distribution of the particles, and are energy intensive, which may result in damage when fragile components are present in the droplets [36]. With newer emulsification methods such as membrane emulsification, monodisperse emulsions and particles can be effectively prepared [36], as is also the case for microchannel based emulsification techniques [37, 38].
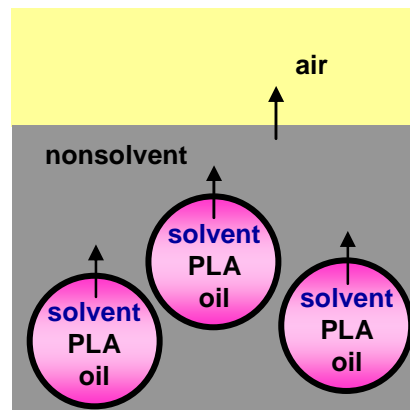
Figure 3: schematic representation of the extraction and evaporation of the solvent after emulsification.

For this study we decided to use premix membrane emulsification which combines high throughput with good control on droplet size. In premix membrane emulsification, a course pre-mix emulsion of the casting solution in the nonsolvent continuous phase is pressed through a complex network of branching and joining microchannels (e.g., a porous membrane matrix) (see Figure 4). The branching of the channels causes large droplets to divide over the channels, and slowly reduce in size, approximately down to the diameter of the channels [39]. Passage of the emulsion through the membrane is repeated several times (see also chapters 4 and 5) [36].
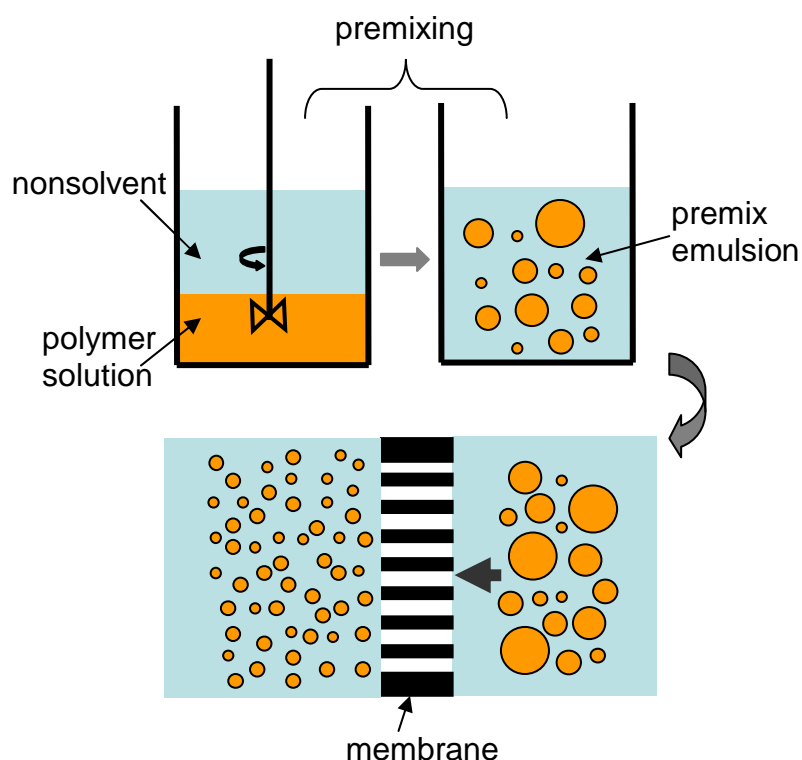
Figure 4: Schematic representation of premix membrane emulsification process.

When microbubbles are to be produced (see Figure 5), a mixture of a good and a poor solvent is used in the casting solution, both poorly soluble in the nonsolvent bath. Unlike the solvent for the polymer, the second, poor solvent (often called oil) does not diffuse out, since it is not volatile, and remains in the polymer droplet. As the good solvent slowly diffuses out of the droplets and evaporates, the concentrations of polymer and the oil become higher and higher, until the solution becomes unstable. The oil now forms a droplet inside the original droplet (being poorly compatible with the nonsolvent bath, it will be at the inside of the droplet), while the polymer will be in between the internal oil droplet and the outside nonsolvent bath. This will ultimately form a solid shell around the oil droplet, which can be removed by freeze-drying [40].

The shell properties are dependent on the precipitation process, which is strongly determined by the solvent removal rate and on the choice of oil (see chapters 2, 3, 4, 7 and 8).
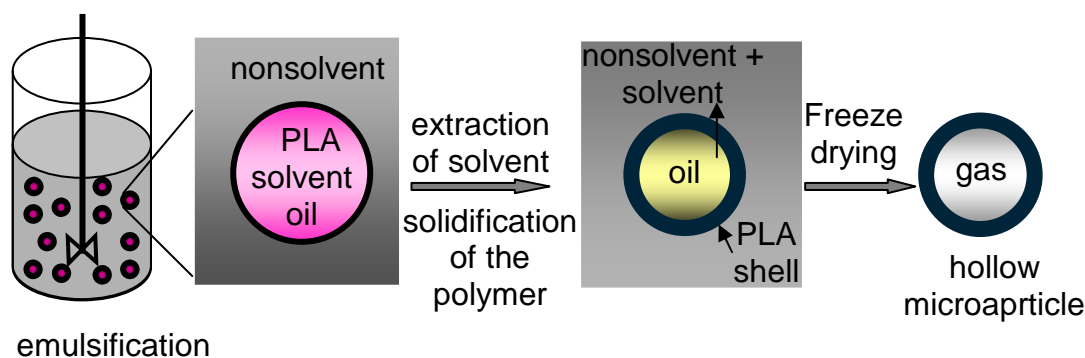
Figure 5: Schematic representation of the evaporative immersion precipitation process of hollow PLA microparticles.

The shell properties are dependent on the precipitation process, which is strongly determined by the solvent removal rate and on the choice of oil (see chapters 2, 3, 4, 7 and 8).

Aim and outline of the thesis

The aim of this study is to design PLA microbubbles (ultimately for use as UCA's) with well-defined size, size distribution, structure and mechanical properties. For this purpose, the phase behavior of PLA, solvent, oil, and nonsolvent was first studied using thin PLA films. The morphology and the mechanical properties of the films were investigated, and the insight obtained was used as a tool to improve the properties of films and microparticles and microbubbles.

Chapter 2 mainly focuses on the effects of nonsolvent, on the morphology of thin PLA films prepared through immersion precipitation and the results are discussed in relation to the phase separation behaviour of PLA.

In **Chapter 3** the mechanical properties, structure, and porosity of PLA films prepared through immersion precipitation and film casting are evaluated for various nonsolvents. Amongst others, the effect of addition of dodecane is discussed and potential uses for various biomedical applications are discussed.

Chapter 4 highlights the effects of solvent removal rates on the size, size distribution, and morphology of *solid* PLLA microspheres prepared with premix membrane emulsification. Both experimental and computer simulation results, based on a Maxwell-Stefan model for non-ideal, multi-component mass transfer, are presented.

The effects of the nonsolvent properties on the size and size distribution of *hollow* PLLA microparticles prepared with premix membrane emulsification are discussed in **chapter 5**, and linked to process conditions such as number of emulsification cycles and transmembrane flux.

In **chapter 6**, results are shown for mechanical, thermal and structure properties of PLLA films prepared through film casting when various oils were added to the polymer solution. The use of different oils for creating different film properties is discussed.

Chapter 7 summarizes the effects of the oils used in chapter 6 on the mechanical, thermal and structure properties of hollow PLLA microparticles.

In **chapter 8** the main results and conclusions obtained from the films and microparticles are highlighted, summarized, and compared. Furthermore, possibilities for future development in microparticle and film research based on the current results are discussed, together with possible options for other fields of research.

References

1.   Maillard, D., Prud'homme, R.E., *Chirality Information Transfer in Polylactides: From Main-Chain Chirality to Lamella Curvature.* Macromolecules, 2006. **39**(13): p. 4272.

2.   Vaidya, A.N., Pandey, R.A., Mudliar, S., Kumar, M.S., Chakrabarti, T., Devotta, S. , *Production and recovery of lactic acid for polylactide - An overview.* Critical Reviews in Environmental Science and Technology, 2005. **35**(5): p. 429.

3.   Jacobsen, S., Degée, Ph., Fritz, H.G., Dubois, Ph., Jérôme, R., *Polylactide (PLA) - a new way of production.* Polymer engineering and science, 1999. **39**(7): p. 1311.

4.   Lim, L.-T., Auras, R., Rubino, M., *Processing technologies for poly(lactic acid).* Progress in polymer science, 2008. **33**(8): p. 820.

5.   Wuisman, P.I.J.M., Smit, T.H., *Bioresorbable polymers: Heading for a new generation of spinal cages.* European spine journal, 2006. **15**(2): p. 133-148.

6.   Auras, R., Harte, B., Selke, S., *An overview of polylactides as packaging materials.* Macromolecular bioscience, 2004. **4**(9): p. 835.

7.   Mohamed, F., Van Der Walle, C.F., *Engineering biodegradable polyester particles with specific drug targeting and drug release properties.* Journal of Pharmaceutical Sciences, 2008. **97**(1): p. 71.

8.   Karageorgiou, V., Kaplan, D., *Porosity of 3D biomaterial scaffolds and osteogenesis.* Biomaterials, 2005. **26**(27): p. 5474.

9.   Lam, K.H., Nijenhuis, A.J., Bartels, H., Postema, A.R., Jonkman, M.F., Pennings, A.J., Nieuwenhuis, P., *Reinforced poly(L-lactic acid) fibres as suture material.* Journal of applied biomaterials, 1995. **6**(3): p. [d]191.

10.   Lee, S. H., Kim, B. S., Kim, S. H., Kang, S. W., Kim, Y. H., *Thermally produced biodegradable scaffolds for cartilage tissue engineering.* Macromolecular bioscience, 2004. **4**(8): p. 802.

11.   Luciano, R. M., Zavaglia, C. A. C., Duek, E. A. R., Alberto-Rincon, M. C., *Synthesis and characterization of poly(L-lactic acid) membranes: Studies in vivo and in vitro.* Journal of materials science. Materials in medicine, 2003. **14**(1): p. 87.

12.   Freiberg, S., Zhu, X. X., *Polymer microspheres for controlled drug release.* International Journal of Pharmaceutics, 2004. **282**(1-2): p. 1.

13. Zhu, B., Li, J., He, Y., Yamane, H., Kimura, Y., Nishida, H., Inoue, Y., *Effect of steric hindrance on hydrogen-bonding interaction between polyesters and natural polyphenol catechin.* Journal of Applied Polymer Science, 2004. **91**(6): p. 3565.

14. Ljungberg, N., Wesslén, B., *Preparation and properties of plasticized poly(lactic acid) films.* Biomacromolecules, 2005. **6**(3): p. 1789.

15. Martin, O., Avérous, L., *Poly(lactic acid): plasticization and properties of biodegradable multiphase systems.* Polymer, 2001. **42**(14): p. 6209.

16. Broström, J., Boss, A., Chronakis, I.S., *Biodegradable films of partly branched poly(L-lactide)-co-poly(ε-caprolactone) copolymer: Modulation of phase morphology, plasticization properties and thermal depolymerization.* Biomacromolecules, 2004. **5**(3): p. 1124.

17. Jacobsen, S., Fritz, H.G., *Plasticizing polylactide - the effect of different plasticizers on the mechanical properties.* Polymer engineering and science, 1999. **39**(7): p. 1303.

18. Jiang, L., Wolcott, M.P., Zhang, J. , *Study of biodegradable polylactide/poly(butylene adipate-co-terephthalate) blends.* Biomacromolecules, 2006. **7**(1): p. 199.

19. Ke, T., Sun, S.X., Seib, P., *Blending of poly(lactic acid) and starches containing varying amylose content.* Journal of applied polymer science, 2003. **89**(13): p. 3639.

20. Kulinski, Z., Piorkowska, E., Gadzinowska, K., Stasiak, M., *Plasticization of poly(L-lactide) with poly(propylene glycol).* Biomacromolecules, 2006. **7**(7): p. 2128.

21. Labrecque, L.V., Kumar, R.A., Davé, V., Gross, R.A., Mccarthy, S.P. , *Citrate esters as plasticizers for poly(lactic acid).* Journal of applied polymer science, 1997. **66**(8): p. 1507.

22. Lu, J., Qiu, Z., Yang, W., *Fully biodegradable blends of poly(l-lactide) and poly(ethylene succinate): Miscibility, crystallization, and mechanical properties.* Polymer, 2007. **48**(14): p. 4196.

23. Sheth, M., Kumar, R.A., Davé, V., Gross, R.A., Mccarthy, S.P., *Biodegradable polymer blends of poly(lactic acid) and poly(ethylene glycol).* Journal of applied polymer science, 1997. **66**(8): p. 1495.

24.   Zoppi, R. A., Contant, S., Duek, E. A. R., Marques, F. R., Wada, M. L. F., Nunes, S. P., *Porous poly(-lactide) films obtained by immersion precipitation process: morphology, phase separation and culture of VERO cells.* Polymer, 1999. **40**(12): p. 3275.

25.   Liu, H.-C., Lee, I.-C., Wang, J.-H., Yang, S.-H., Young, T.-H., *Preparation of PLLA membranes with different morphologies for culture of MG-63 Cells.* Biomaterials, 2004. **25**(18): p. 4047.

26.   Rhim, J.-W., Mohanty, A.K., Singh, S.P., Ng, P.K.W., *Effect of the processing methods on the performance of polylactide films: Thermocompression versus solvent casting.* Journal of applied polymer science, 2006. **101**(6): p. 3736.

27.   Van de Witte, P., Dijkstra, P. J., Van den Berg, J. W. A., Feijen, J., *Phase separation processes in polymer solutions in relation to membrane formation.* Journal of Membrane Science, 1996. **117**(1-2): p. 1.

28.   Chuang, W. Y., Young, T. H., Chiu, W. Y., Lin, C. Y., *The effect of polymeric additives on the structure and permeability of poly(vinyl alcohol) asymmetric membranes.* Polymer, 2000. **41**(15): p. 5633.

29.   Van de Witte, P., Esselbrugge, H., Peters, A. M. P., Dijkstra, P. J., Feijen, J., Groenewegen, R. J. J., Smid, J., Olijslager, J., Schakenraad, J. M., Eenink, M. J. D., Sam, A. P., *Formation of porous membranes for drug delivery systems.* Journal of Controlled Release, 1993. **24**(1-3): p. 61.

30.   Lathia, J. D., Leodore, L., Wheatley, M. A., *Polymeric contrast agent with targeting potential.* Ultrasonics, 2004. **42**(1-9): p. 763.

31.   Dayton, P. A., Chomas, J. E., Lum, A. F. H., Allen, J. S., Lindner, J. R., Simon, S. I., Ferrara, K. W., *Optical and acoustical dynamics of microbubble contrast agents inside neutrophils.* Biophysical journal, 2001. **80**(3): p. 1547.

32.   Chu, L. Y., Park, S. H., Yamaguchi, T., Nakao, S. I., *Preparation of Micron-Sized Monodispersed Thermoresponsive Core-Shell Microcapsules.* Langmuir, 2002. **18**(5): p. 1856.

33.   Liu, R., Ma, G., Meng, F.-T., Su, Z.-G., *Preparation of uniform-sized PLA microcapsules by combining Shirasu Porous Glass membrane emulsification technique and multiple emulsion-solvent evaporation method.* Journal of Controlled Release, 2005. **103**(1): p. 31.

34.   Gref, R. R., Minamitake, Y., Peracchia, M. T., Trubetskoy,V., Torchilin,V., Langer, R., *Biodegradable long-circulating polymeric nanospheres.* Science, 1994. **263**(5153): p. 1600.

35. Freitas, S., Merkle, H.P., Gander, B., *Microencapsulation by solvent extraction/evaporation: Reviewing the state of the art of microsphere preparation process technology.* Journal of Controlled Release, 2005. **102**(2): p. 313.

36. Vladisavljević, G. T., Williams, R. A., *Recent developments in manufacturing emulsions and particulate products using membranes.* Advances in colloid and interface science, 2005. **113**(1): p. 1.

37. Van Der Graaf, S., Steegmans, M.L.J., Van Der Sman, R.G.M., Schroën, C.G.P.H., Boom, R.M., *Droplet formation in a T-shaped microchannel junction: A model system for membrane emulsification.* Colloids and Surfaces A: Physicochemical and Engineering Aspects, 2005. **266**(1-3): p. 106.

38. Utada, A.S., Lorenceau, E., Link, D.R., Kaplan, P.D., Stone, H.A., Weitz, D.A., *Monodisperse Double Emulsions Generated from a Microcapillary Device.* Science, 2005. **308**(5721): p. 537.

39. Van Der Zwan, E., Schroën, K., Van Dijke, K., Boom, R., *Visualization of droplet break-up in pre-mix membrane emulsification using microfluidic devices.* Colloids and Surfaces A: Physicochemical and Engineering Aspects, 2006. **277**(1-3): p. 223.

40. Böhmer, M. R., Schroeders, R., Steenbakkers, J. A. M., de Winter, S. H. P. M., Duineveld, P. A., Lub, J., Nijssen, W. P. M., Pikkemaat, J. A., Stapert, H. R., *Preparation of monodisperse polymer particles and capsules by ink-jet printing.* Colloids and surfaces. A, Physicochemical and engineering aspects, 2006. **289**(1-3): p. 96.

Chapter 2

Polylactide films formed by immersion precipitation:

effects of additives, nonsolvent and temperature*

Abstract

The influence of nonsolvent, crystallinity of the polymer film, and addition of dodecane (a poor solvent for the polymer and for the nonsolvent), on the morphology of polylactides films has been investigated, and was related to phase separation behaviour. Both amorphous poly-DL-lactide (PDLLA) and crystalline poly-L-lactide (PLLA) were dissolved in dichloromethane (DCM), and subsequently films were made by immersion in non-solvent baths. PDLLA gave dense films without any internal structure, since the structure was not solidified by crystallization or glassification. PLLA films show varying structure depending on the non-solvent. With methanol, asymmetric morphologies were observed as a result from combined liquid-liquid demixing and crystallization, while with water symmetric spherulitic structures were formed.

As a next step, dodecane was added, which is not miscible with the nonsolvent; and we found it to have a strong influence on the morphology of the films. The PDLLA films with dodecane did not collapse: a closed cell structure was obtained. In PLLA films, dodecane speeds up phase separation and induces faster crystallization in the films, and the porosity, size of the pores, and interconnectivity increased. When the PLLA solutions were subjected to a heat pretreatment, crystallization could be postponed, which yielded a cellular structure around dodecane, which did not contain spherulites anymore.

Introduction

Phase separation of polymer solutions is one of the most popular techniques used for e.g. the preparation of porous polymeric membranes or dense or hollow particles. Different methods are known such as: thermally induced phase separation, air-casting of a polymer solution, precipitation from the vapour phase, and immersion precipitation [1, 2]. All these methods are used to produce commercial membranes. For the production of flat sheet membranes, a solution that consists of polymer and solvent is cast on an inert support and subsequently immersed in a coagulation bath filled with a non-solvent [3]. For the production of hollow fibre membranes, the support is not required because of the construction of the nozzle that shapes the membrane directly.

Due to the exchange of solvent and non-solvent, phase separation occurs. Two main types of phase transitions are responsible for this, liquid-liquid demixing, and solid-liquid demixing [4, 5]. Liquid-liquid demixing in polymer solutions that are relatively concentrated (typically > 10 weight %), generally takes place by nucleation and growth of the polymer poor phase. Solid-liquid demixing mainly happens in crystalline and semi-crystalline polymers, and occurs because of crystallization, gelation, or vitrification [1, 6, 7]. The resulting morphology is strongly determined by the aforementioned processes. Generally, liquid-liquid demixing produces porous and cellular structures, while crystallization forms interlinked particle-based structures [8-10]. Many parameters such as concentration of the polymeric solution, crystallinity of the polymer, temperature of the casting solution, and coagulation bath, type of solvent, and non-solvent, and their mutual diffusivities [5, 11-15] influence demixing, and consequently the final morphology. Some investigators have reported that additives in the casting solution can be used to modify the structure obtained. As additives, a second polymer, acids, alcohols, or inorganic salts have been reported. Obviously, the resulting morphology strongly depends on the type of additive and the interactions with the polymer, solvent, and non-solvent [13, 16-19].

In the study reported here, we chose Polylactic acid (PLA) which is a biodegradable polymer that has wide applications in the medical and pharmaceutical fields [20, 21]. PLA films were formed by means of immersion precipitation which has, for instance, been proposed as a method for the preparation of biodegradable scaffolds for blood vessels, but also for preparation of drug delivery devices [18]. Two types of PLA were used: Poly (D50,L50) lactide PDLLA, and(P(L)LA) PLLA. PDLLA is a random co-polymer that cannot crystallize and thus is either in the rubbery or in the glassy state, while PLLA is in optically pure form and crystallizes readily [11, 22, 23].

The effects of non-solvent quality and PLA crystallinity on the resulting film morphology were studied separately. Unlike most studies, in which additives are used, that are soluble in the non-solvent [9, 12, 18], we have used dodecane as an additive which is not soluble in the non-solvent. The effect on the resulting structures is unknown, but it is to be expected that different morphologies can be obtained. The morphology of the films was investigated visually with scanning electron microscopy. Light transmission experiments were performed to monitor and characterise the film formation process itself.

Experimental

Materials

Poly-L-lactide (PLLA) and poly-DL-lactide (PDLLA), with an intrinsic viscosity of 1.21 and 0.49 dl/g respectively, were supplied by PURAC Biochem B.V., Gorinchem, the Netherlands. Dichloromethane (DCM), (HPLC, gradient grade) was obtained from Merck and used as the solvent for the polymer. Dodecane (≥99%) was purchased from Sigma-Aldrich and added to the casting solution as a poor solvent for the polymer. Methanol (HPLC, gradient grade, ≥99.9%) (Aldrich) was used with Milli-Q water as a non-solvent. All chemicals were used as received.

Film preparation

The casting solutions were prepared by dissolving different amounts of polymer in various DCM-dodecane mixtures to obtain the desired concentrations. The solution

was kept at the required temperature under stirring for 1-2 days and then cooled down to room temperature before use. Solutions with concentrations (w/w/w) of 20:0:80, 20:5:75, and 20:10:70, or 20:0:80, and 20:10:70 PDLLA-dodecane-DCM were used. The polymer solution was cast in the form of a thin film on a glass plate, and subsequently immersed in the coagulation bath for 30 minutes, after which the films were ready. All the experiments were done at room temperature. As non-solvents, the following methanol-water mixtures were used: 100:0, 60:40, 30:70, 0:100.

Light transmission experiments

The experimental setup for light transmission measurements is shown in Figure 1[3]. As mentioned before, the film is cast on a glass plate. The plate is turned upside down, and placed on top of the coagulation bath as quickly as possible. A desk lamp is used as light source just above the coagulation bath. The setup was shielded from ambient light by an opaque plastic cover. The electric resistance was measured by a photocell fixed beneath the coagulation bath. The occurrence of inhomogeneities in the film due to demixing causes the electric resistance to increase; this increase is registered as a function of time.

The curves of resistance in time (an example is shown in Figure 2) are characterized with three parameters. The first one is the time at which the electric resistance starts to increase, which is considered the onset of demixing (delay time; t_d). The time, at which the resistance reaches a constant value, represents the final stage of phase separation in the film (t_f). In between t_d and t_f, the maximum rate of demixing can be found (r_{max}). The curves are analysed by fitting the logistic growth model, and minimising the residual sum of squares.

Scanning electron microscope (SEM)

The morphology of polymer films was investigated with SEM (JEOL, JSM-5600 LV). To prepare cross section samples, sections of the films were cut, dried, and fractured in liquid nitrogen. The top and bottom surfaces and the cross sections were coated with a very thin platinum layer using a sputter-coater (JEOL, JFC-1300) before viewing with SEM.
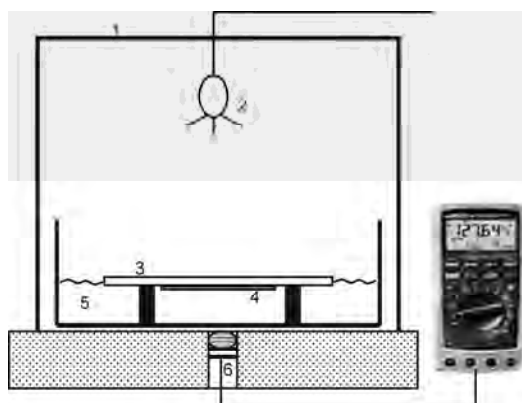
Figure 1: Experimental setup for light transmission measurement: 1- plastic cover, 2- light source, 3- glass plate, 4- polymer film, 5- coagulation bath, and 6- photocell.
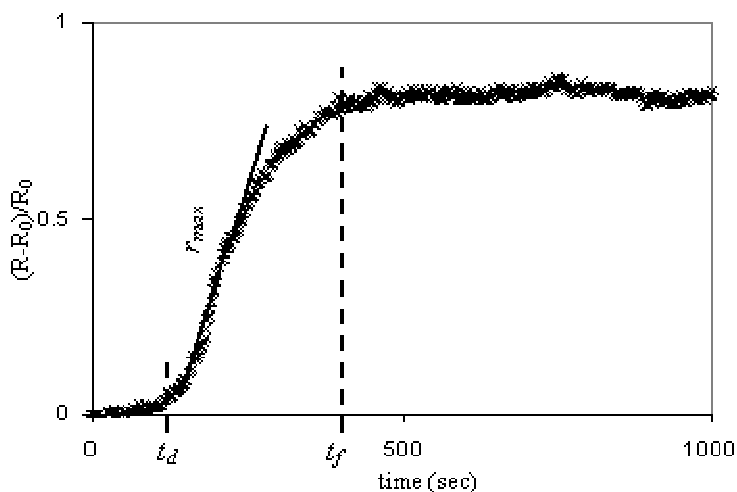
Figure 2: Interpretation of light transmission results; R is the electric resistance (Ω) at time t, R_0 the initial resistance (Ω), t_d the delay time of demixing (second), r_{max} the maximum demixing rate (1/second), and t_f is the time where demixing is complete (second). The actual data were measured for a film of 20:10:70 PLLA:dodecane:DCM immersed in a water bath.

Method - Calculation of phase diagrams

As many others, we have used the Flory-Huggins theory for evaluating the thermodynamics of the (quaternary) systems used [1,3,4,6,10,11]. The Gibbs energy of mixing is described by

$$\frac{\Delta G_m}{RT} = n_1 \ln \phi_1 + n_2 \ln \phi_2 + n_3 \ln \phi_3 + n_4 \ln \phi_4$$
$$+ \chi_{12} n_1 \phi_2 + \chi_{13} n_1 \phi_3 + \chi_{14} n_1 \phi_4 + \chi_{23} n_2 \phi_3 + \chi_{24} n_2 \phi_4 + \chi_{34} n_3 \phi_4$$

in which, n_i is the number of moles of component *i*, and φ_i is the volume fraction of component *i*, and χ_{ij} is the Flory-Huggins interaction parameter (see Table 1). Index 1 represents the nonsolvent, 2 = solvent, 3 = polymer and 4 = additive. Because of the complexity of such quaternary systems, we used constant interaction parameters. The main aim of the phase diagrams is to show the various trends that are present and not to quantitatively describe all the effects in detail.

The chemical potentials for each component were determined by taking the derivative of the Gibbs energy to n_i. Phase equilibria were calculated by equating the chemical potential of each component in each phase. This results for a two-phase equilibrium in m-1 equations (m is the number of components present), and for a three-phase equilibrium in 2m – 2 equations. Solving these equations yields the coexisting compositions, and therewith the binodals. The phase diagrams were shown as limiting ternary phase diagrams, linked together to form the sides of a folded-out pyramidal quaternary phase diagram. For the limiting ternary phase diagram, the volume fraction of the excluded component was set to zero. The ternary phase diagrams (without dodecane) are primarily used in the results section. The interested reader can find the quaternary phase diagrams in the appendix, together with a more elaborate explanation for the phase behaviour.

Table 1: Values of the input parameters used in the equations.

Parameter	Value	Parameter	Value
χ_{12} *(methanol-DCM)*	0.5 [24]	v_{1} *(methanol)*	40.46 cm^3/mol
χ_{12} *(water-DCM)*	3.3	v_{1} *(water)*	10.00 cm^3/mol
χ_{13} *(methanol-PLA)*	1.5 [24]	$v_{2(DCM)}$	64.10 cm^3/mol
			226.67
χ_{13} *(water-PLA)*	3.4 [24]	v_{4} *(dodecane)*	cm^3/mol
χ_{14} *(methanol-dodecane)*	2.5	$r*($ $v_{nonsolvent/}$ $v_{PLA)}$	0.00085 [24]
			81 - 140 J/g
χ_{14} *(water-dodecane)*	3.4	$\Delta H_{m\,PLA}$	[24]
χ_{23} *(DCM-PLA)*	0.2 [24]	$T_{m}^{0}{}_{PLA}$	480 K [24]
χ_{24} *(DCM-dodecane)*	0.5	T	298 K
χ_{34} *(PLA-dodecane)*	1.5		

* The value of *r* is based on the number average degree of polymerization of PLLA with respect to the molar volume of water. This value has to be calculated for each polymer-nonsolvent combination; but because these values have negligible influence in the location of the phase boundaries, r was taken as a constant value [24].

The crystallization equilibriums were described with the Flory equation for quaternary systems:

$$\frac{v_u}{v_1}\frac{\Delta H_m}{R}\left(\frac{1}{T_m^0}-\frac{1}{T}\right)=\frac{v_1}{v_3}\ln\phi_1+\frac{v_1}{v_3}\left(1-\phi_3\right)-\phi_1-\frac{v_1}{v_2}\phi_2-\frac{v_1}{v_4}\phi_4$$
$$+\left(\chi_{13}\phi_1+\frac{v_1}{v_2}\chi_{23}\phi_2+\frac{v_1}{v_4}\chi_{34}\phi_4\right)-\chi_{12}\phi_1\phi_2-\chi_{14}\phi_1\phi_4-\chi_{24}\phi_2\phi_4$$

in which v_3 is the molar volume of the repeating unit of component 3 (PLA), and v_i the molar volume of component *i*; ΔH_m is the melting enthalpy, and T_m^0 the melting temperature of pure PLA. Once more, for the limiting ternary phase diagrams, the

volume fraction of the excluded component was set to zero. Values of the parameters used are summarized in Table 1.

Results and discussion

PDLLA films: non-solvent effects

To investigate the effect of the type of non-solvent on the morphology of PDLLA films, a casting solution of 20% wt/wt PDLLA/DCM was immersed in 100% methanol, 60% w/w methanol/water, and water. The cross sections of all films were similar and consisted of a solid, dense film with no pores; the results for the extremes methanol and water are shown in Figure 3.

When water is used as non-solvent, the DCM is expected to slowly diffuse through the water phase and evaporate at the surface of the bath. As the miscibility of water with DCM and PLA is very low, one expects that water will hardly penetrate the casting solution. PDLLA is atactic, and therefore amorphous; its glass transition temperature is expected to be lower than 20 ^{0}C when it is at equilibrium with water. Therefore, when a PDLLA/DCM film is immersed in a water bath, and the DCM is slowly removed from the film, the PDLLA will not crystallize and the structure will slowly collapse, until all DCM is removed, and a dense film is obtained (see also Figure 4 for phase diagram).
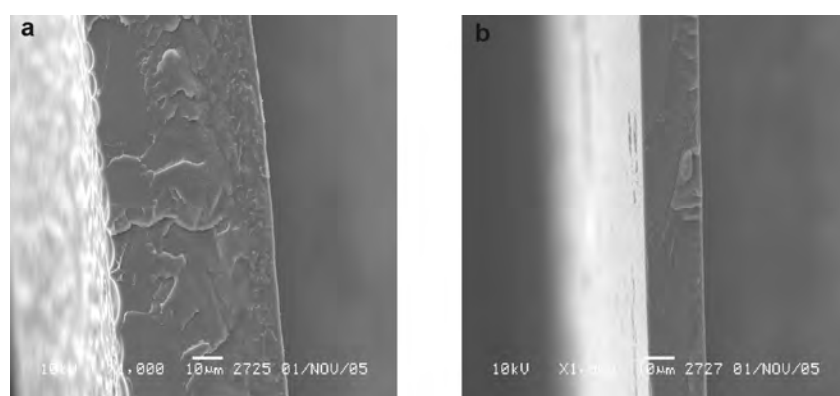
Figure 3: SEM images of cross sections of films prepared from 20:80 w/w PDLLA:DCM with different non-solvents: a) methanol, b) water; please note that the water film has been made out of film with less initial thickness than the one with methanol.
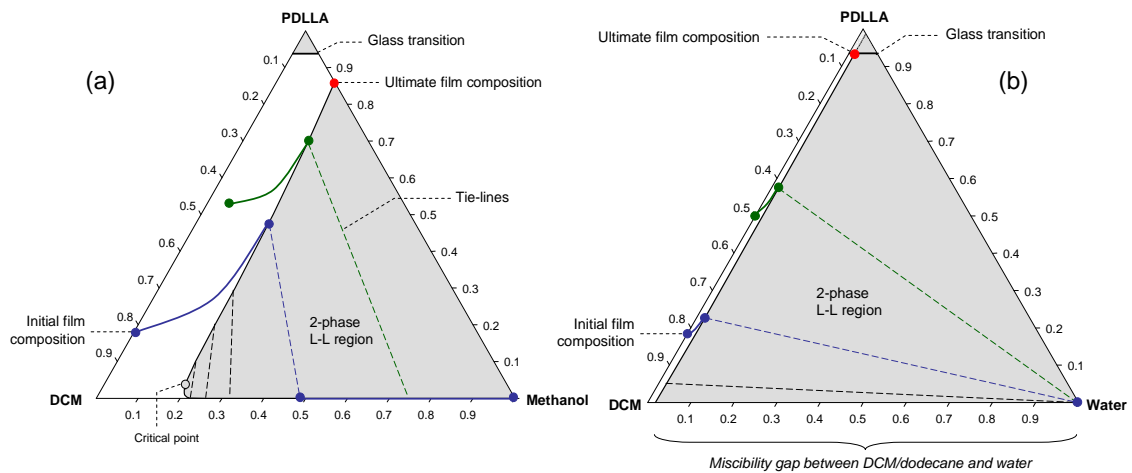
Figure 4: Schematic equilibrium phase diagram for: (a) PDLLA-DCM-methanol and (b) PDLLA-DCM-water. The phase diagrams were calculated with the parameters as mentioned in Table 1.

DCM is only marginally miscible with water but readily miscible with methanol. With methanol, a PDLLA-DCM solution will exhibit so-called delayed demixing (formation of droplets of a polymer lean phase inside the polymer solution, after some time for indiffusion has elapsed) [4]. Therefore, one would expect a film containing at least some closed-cell pores because of the presence of the polymer lean phase. This is not what we observed. We expect that the porous structure may have been formed during the process, but as the ultimately formed film is still highly swollen with methanol (PDLLA swells 22 % w/w in methanol), it will never reach the glass transition [11]. Thus, the film will never fixate, and the porous structure that is formed initially will have collapsed into a completely dense film when the residual DCM evaporates.

It is known from literature that fixation of the cellular structure obtained by liquid-liquid demixing requires a solidification step [11]. This can take place via solid-liquid demixing (i.e. crystallization), or via glassification. If neither of these transitions occurs, liquid-liquid demixing will proceed until two completely separated layers are obtained [11]. Since PDLLA cannot crystallize [11, 22], and its glass transition line does not cross the binodal for either methanol or water (this is illustrated in Figure 4), it will not be solidified but will collapse given sufficient time. Van de Witte an co-workers have shown with differential scanning calorimetry (DSC) that in a PDLLA-

chloroform-methanol system, phase transition occurred only by liquid-liquid demixing and no signs of crystallites or transitions due to verification were observed [25], which is in line with our findings.

For a film made out of 5% w/w PDLLA/Chloroform which was immersed and kept in methanol for one day or longer Van de Witte and co-workers [11] found that no structure was preserved. Comparison with our results shows that increasing the polymer concentration reduces the time required for phase separation, and results in faster loss of structure.

PLLA: non-solvent effects

In contrast to PDLLA, PLLA is a rapidly crystallizing polymer [11, 22, 25]. Therefore one may expect a strong influence of polymer crystallisation, which will influence the morphology of the films as was reported in the literatures [6, 9-11, 25]. Films with polymer concentrations of 20% w/w PLLA/DCM were prepared using 100% methanol, 60%, 30% w/w methanol/water and water as non-solvents; the cross sections of the films are shown in Figure 5. The film prepared with methanol as nonsolvent consists of dense blobs surrounded by semi-circular closed cells (Figure 5a). The top layer at the left of the image (the side in contact with the non-solvent) has a very densely packed structure without pores. During film formation (see also Figure 6 for the phase diagrams), the initial in-diffusion of non-solvent is much smaller than the out-diffusion of the solvent [3]. Therefore, the polymer concentration in the top layer of the film rises quickly, which will bring the composition in this layer far inside the crystallization region of the phase diagram. Thus, the polymer will crystallize rapidly.

The out-diffusion of DCM from the sublayer to the non-solvent bath is reduced significantly due to the additional mass transfer resistance created by the dense top layer. In spite of this, in time the concentration of DCM in the sublayer will be reduced, the solution will become more enriched with polymer, and the composition will approach the liquid-liquid miscibility gap. As soon as the miscibility gap is reached (after 16 seconds of immersion, see also Table 2), liquid-liquid demixing by nucleation and growth of a polymer-lean phase will take place and a cellular structure

is formed. The polymer concentration in the continuous phase will increase continuously until the solid-liquid demixing region is entered and crystallization of the polymer rich phase occurs, which will form the dense blobs, and pore walls. It is expected that these solid blobs contain spherulites to such an extent that no distinction of the individual spherulites is possible anymore. This becomes also clear from the top view of the film (Figure 5b), which shows a dense, non-porous film full of spherulites.

The occurrence of both phase separation processes (liquid-liquid demixing and crystallization) was observed for crystalline systems in general [6, 10] and specifically for PLLA. For the PLLA-chloroform-methanol system, Van de Witte and co-workers demonstrated by DSC the presence of crystallites during the formation of PLLA membranes, Further, they stated that at high PLLA concentration (>20%w/w) crystallization becomes the main demixing process, which affects to a large extent the morphology of the product [25]. Our results are in agreement with those of Van de Witte for the same polymer concentrations [11].

When water/methanol mixtures were used as non-solvent, the in-diffusion of methanol mixture and the out-diffusion of DCM are slowed down, and the crystallization process has more time to proceed. Thus, we see that for higher water concentrations, the spherulites are more pronounced, larger and further apart (Figure 5 c-f). Crystallization is expected to have taken place because of the slow exchange of the solvent and non-solvent; the time available was long enough to initiate growth of the solid crystals. This case is schematically illustrated in the phase diagram (see Figure 6); where the polymer concentration is slowly increased and after a relatively long time, the solid-liquid demixing region is entered and crystallization occurred in the film. The structure of the spherulites shows no signs of phase separation due to liquid-liquid demixing. It has been reported in literature that slow exchange rates between solvent and non-solvent promote solid-liquid demixing over liquid-liquid demixing [9, 10]; our findings are in line with this.
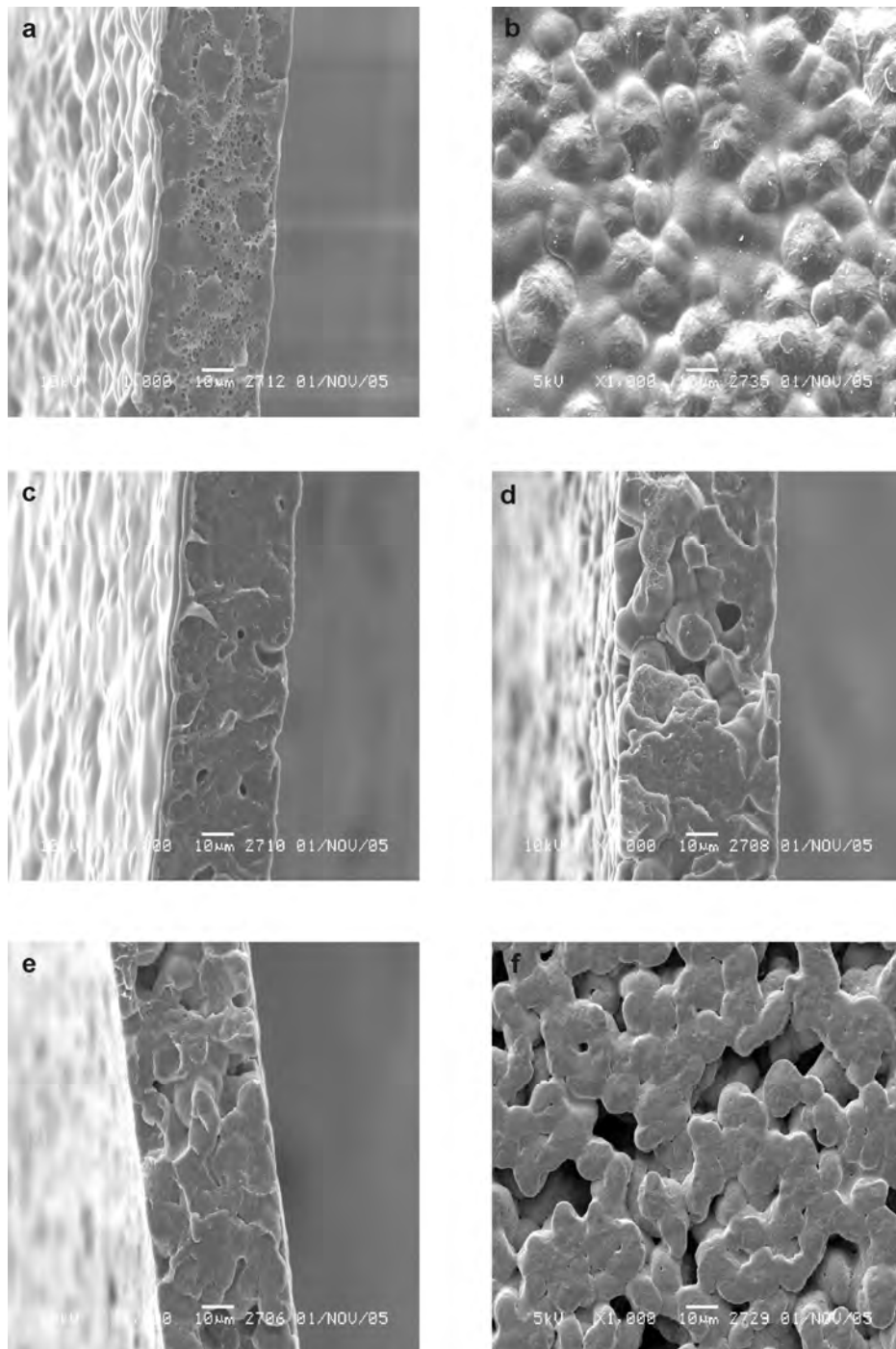
Figure 5: SEM images of cross sections of films prepared from 20:80 w/w PLLA:DCM with different non-solvents: a) methanol, b) methanol, top surface, c) 60:40 w/w methanol:water, d) 30:70 w/w methanol:water; e) water, f) water, top surface.

Even when only water was used in the coagulation bath, the cross section and the top view of the films were still similar (Figures 5e and f). The film shows a spherulitic, dense structure. In some places, the spherulites are fused at their point of contact or completely blended together, forming a solid blob. Apparently, also in this case phase separation has occurred by solid-liquid demixing, and perhaps some liquid-liquid demixing afterwards. The structure of films prepared with 60% and 30% w/w methanol/water (Figures 5c and d) resemble the structure of the water film (Figures 5 e and f), as was also expected from the demixing times, results not shown.

Table 2: Light transmission results for PLLA-dodecane-DCM casting solutions immersed into different methanol -water baths: t_d the delay time of demixing (second), r_{max} the maximum demixing rate (1/second), and t_f is the time where demixing is complete (second). Standard deviations of parameters t_d, and r_{max} are typically 10% or less.

| PLLA (wt%)	Dodecane (wt%)	DCM (wt%)	Temperature (^{0}C).	Non-solvent bath (wt%)	t_d (s)	r_{max}	t_f (s)
20	0	80	room	Methanol	15.9	0.076	82
20	5	75	room	Methanol	6.7	0.016	92
20	5	75	room	60% Methanol - 40% Water	27.4	0.018	116
20	5	75	room	Water	328.3	0.003	741
20	10	70	room	Methanol	2.2	0.023	84
20	10	70	room	60% Methanol - 40% Water	18.1	0.026	69
20	10	70	room	Water	140.1	0.006	358
20	10	70	62	Methanol	4.4	0.016	402
20	10	70	87	Methanol	9.4	0.015	766
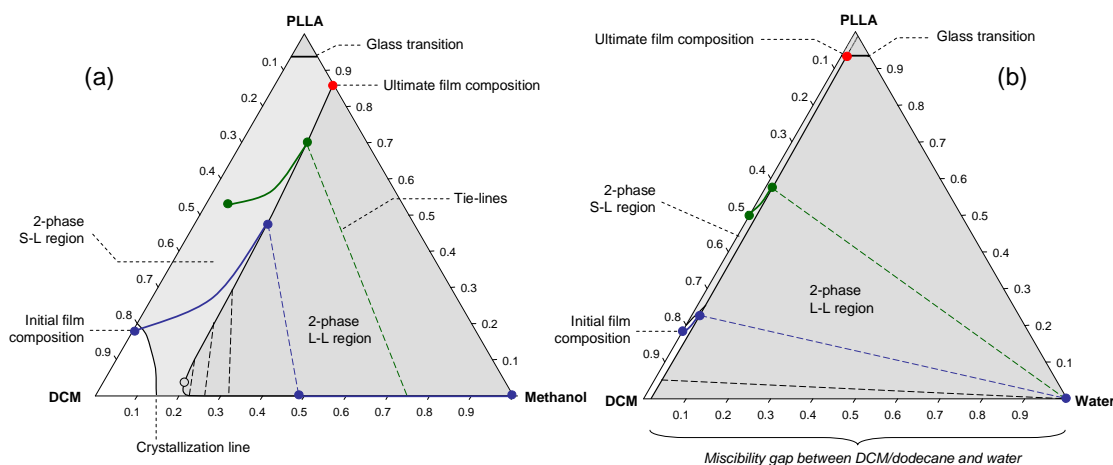
Figure 6: Schematic phase diagrams of (a) PLLA-DCM-methanol and (b) PLLA-DCM-water systems. The crystallization line indicates fixation of the polymer rich matrix by formation of crystals. The phase diagrams were calculated with the parameters as mentioned in Table 1.

Addition of dodecane

PDLLA

The effect of an additive that is not miscible with either the polymer or with the nonsolvent applied in the coagulation bath was investigated by addition of 10% w/w dodecane to the casting solution. Compared to the situation without dodecane, the morphology of the films dramatically changed into a typical asymmetric morphology. The cross sections of these films show a dense skin layer with only little, small pores, and a porous sublayer with a fairly uniform closed cellular morphology (Figure 7 a-d). In the film prepared from methanol, the dense skin is thicker and has no pores, while the porous sublayer contains big, irregular pores (Figure 7 a). The explanation is the high exchange rate between methanol and solvent compared to the other non-solvents. For methanol, the polymer concentration increased quickly at the film-bath interface resulting in a dense toplayer. In the sublayer, the diffusion of solvent and non-solvent slowed down because of the presence of the dense toplayer, however, slowly but surely the dodecane concentration increased in the sublayer. As PDLLA is an amorphous polymer, liquid-liquid demixing was the predominant phase separation

process, which resulted in the porous structure. As the methanol concentration inside the film slowly increased, the solubility of dodecane in the solution decreased accordingly, which ultimately resulted in the formation of droplets of dodecane; these droplets were the precursors of the cellular pores observed. It is remarkable that without dodecane the film collapses completely, while now some structure is preserved. The dodecane phase is trapped while the polymer solution surrounding it slowly becomes more viscous. As the out-diffusion of dodecane is extremely slow, the collapse becomes too slow. Thus, when we would have extended the residence time in the bath considerably, we would possibly have seen a slow reduction of the porosity as a function of the immersion time.
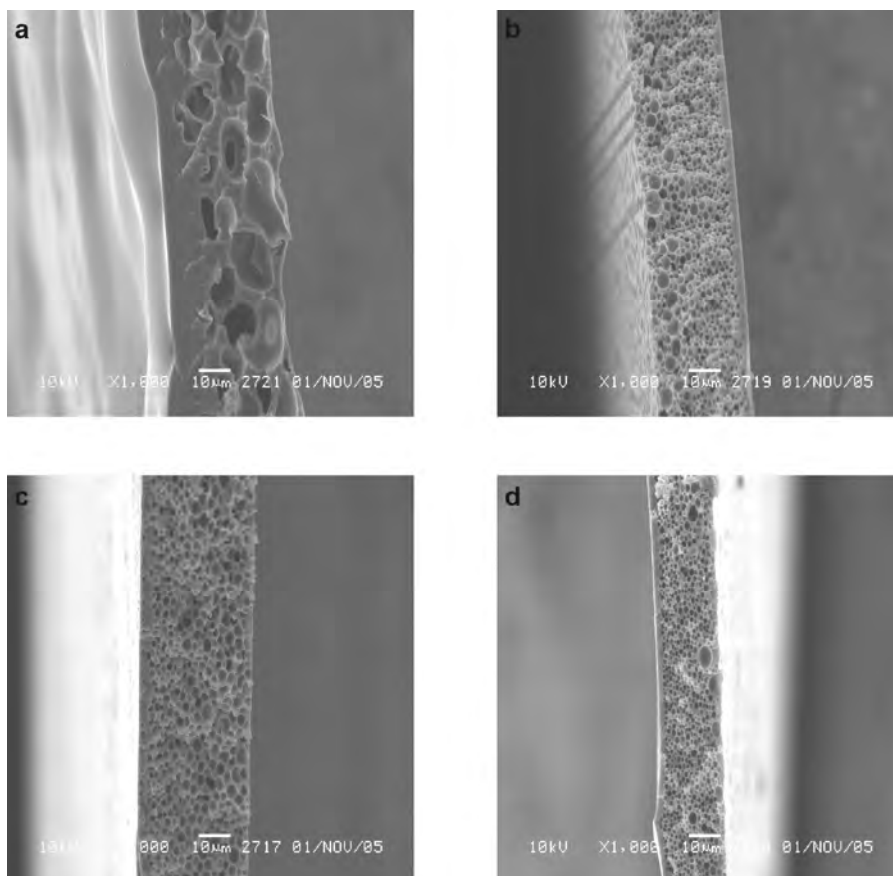
Figure 7: SEM images of cross sections of films prepared from 20:10:70 w/w PDLLA:dodecane:DCM with different non-solvents: a) methanol, b) 60:40 w/w methanol:water, c) 30:70 w/w methanol:water, d) water; please note that the water film has been made out of film with a thinner initial thickness than the other films.

If the dodecane in PDLLA solution was replaced with an additive that is miscible with the nonsolvent as conventionally used, one would expect that the additive will diffuse out of the film, along with the solvent. The film would have collapsed into a dense structure, as without using an additive; no stabilization of the structure could have taken place. The immiscibility of the additive ensures that it stays inside the film, forming the cellular pores. In the appendix, the addition of dodecane and its effect on the phase behaviour of the system is discussed in more detail for the interested reader.

PLLA

To investigate the effects by crystallinity of the polymer, also PLLA films with different dodecane concentrations were prepared. In Figures 8 and 9, the SEM micrographs are shown for dodecane concentrations of 5 and 10% (w/w), respectively. Figure 8 shows the cross sections of films prepared from 20:5:75 PLLA:dodecane:DCM. Compared to those without dodecane (e.g. Figure 5.a), the porosity of the films increased, the pores became larger and better connected, and consequently the structure was more open.

Demixing set in approximately 7 seconds after immersion into the methanol bath (see Table 2). The resulting film has an asymmetric structure consisting of a dense top layer and a porous sublayer, which consists of a bicontinuous network. The morphologies observed suggest a particular series of occurrences of liquid-liquid demixing and crystallization. We expect that initially, crystallization will set in, which depletes the surrounding solution of polymer, and which becomes more susceptible to liquid-liquid demixing, as they simultaneously become more concentrated in DCM and dodecane. This implies that the concentration of dodecane is expected to influence the structure as well.

When the same polymer solution was immersed in water, demixing occurred only very slowly (>6 minutes) as indicated in Table 2. The obtained film morphology differs strongly from the one formed with methanol (Figure 8c and d). The dense skin layer has disappeared and the structure consists of a few blobs embedded in a distorted,

bicontinuous porous matrix. The pores were more open, interconnected, and irregular in shape and size. When a solution of 60%w/w methanol in water was used as non-solvent, the delay time was in between those of methanol and water (see Table 2). The observed morphology was to some extent similar to the one obtained with water, but the structure is less porous and the pores are smaller, more closed, and less interconnected (Figure 8e).

The effect of the dodecane concentration was investigated further, because we expected it to have an important role in the formation of the films. Figures 9a-b shows the morphologies of films prepared with more dodecane (10% w/w) in the casting solution.

The porosity and the size of the pores increase by increasing the dodecane concentration. In case of methanol as nonsolvent (Figure 9a), pores can be observed in the top layer, and the film contains some dense areas embedded in a more regular cellular structure with bigger pores, compared to the film prepared with 5% dodecane (Figure 8a). With water, the film has a more open morphology with high interconnectivity and big spherical pores as shown in Figure 9b. This could be related to an increased probability of coalescence of dodecane droplets due to the long diffusion times, resulting in bigger pores. Similar effects as described for methanol occurred for the film prepared from 60% methanol (result not shown).

From the light transmission results, it is clear that increasing the amount of dodecane in the casting solution decreases the delay time for demixing (Table 2). As the solution is less stable with the non-solvent dodecane present (i.e., the starting composition is closer to the border of the demixing gap in the phase diagram), phase separation will start at an earlier stage, at which droplets of a dodecane rich phase will be formed (see Figure 9a). The remaining PLA-DCM solution will then demix according to a normal (delay of) demixing regime with methanol (Figure 6), which will result in smaller pores in the matrix surrounding the larger pores formed by the dodecane. In the appendix, the addition of dodecane and its effect on the phase behaviour of the system is discussed in more detail for the interested reader.
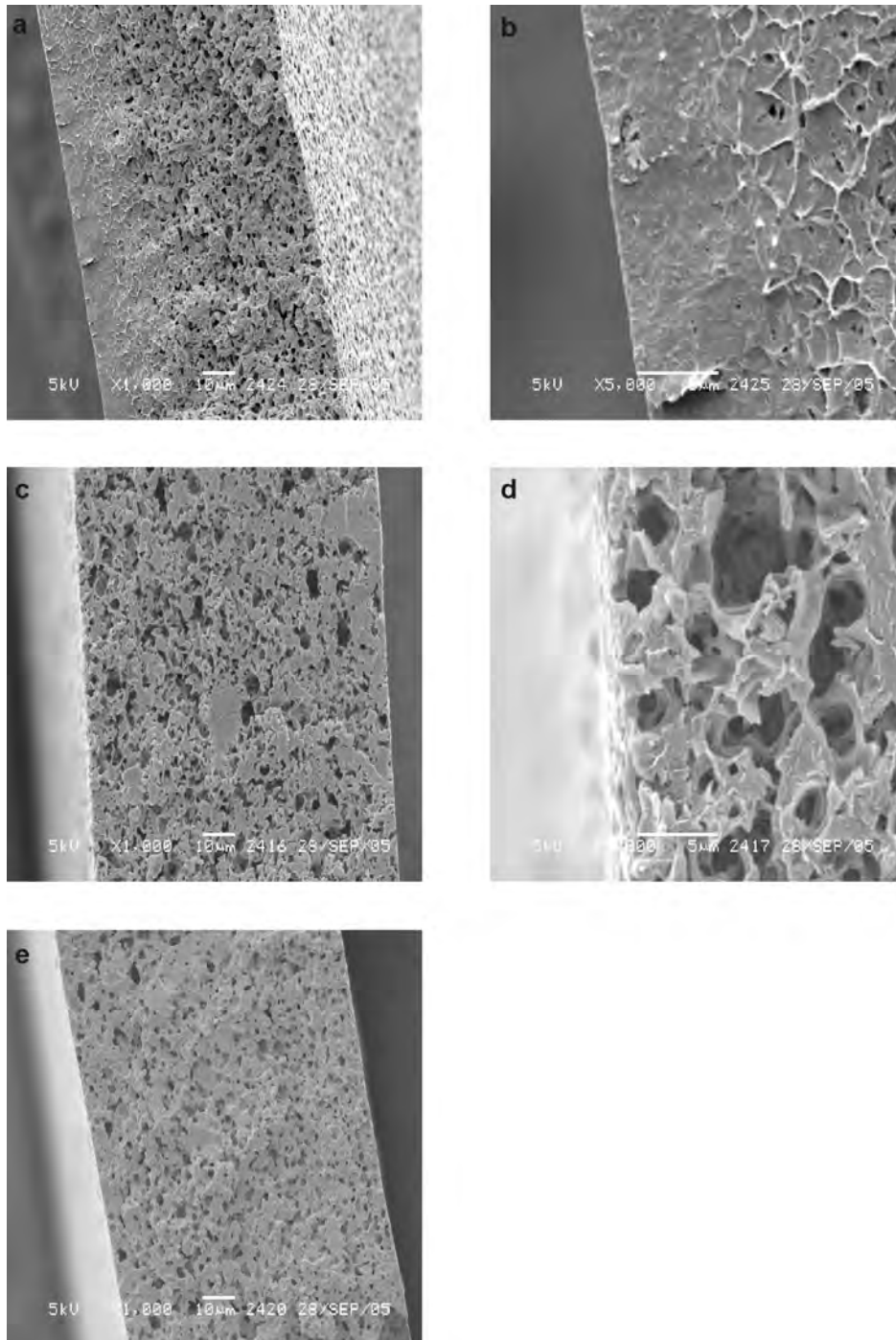
Figure 8: SEM images of cross sections of films prepared from 20:5:75 w/w PLLA:dodecane:DCM with different non-solvents: a) methanol, b) magnification of a, c) water, d) magnifications of c, and e) 60:40 w/w methanol:water.
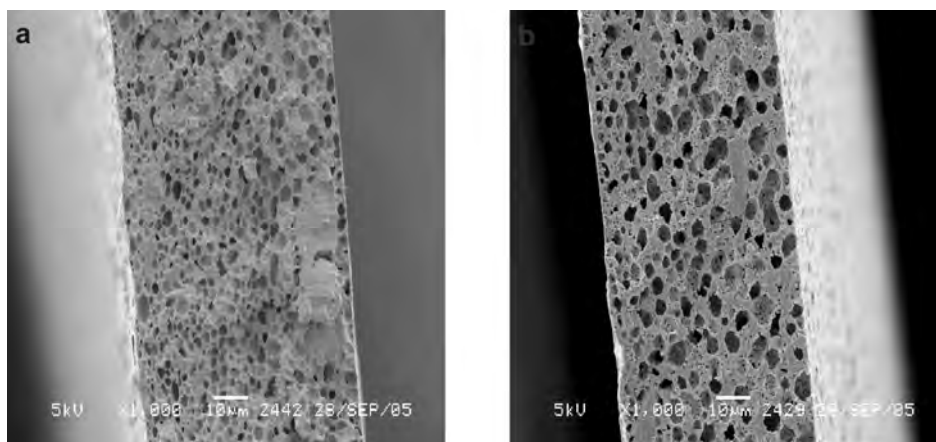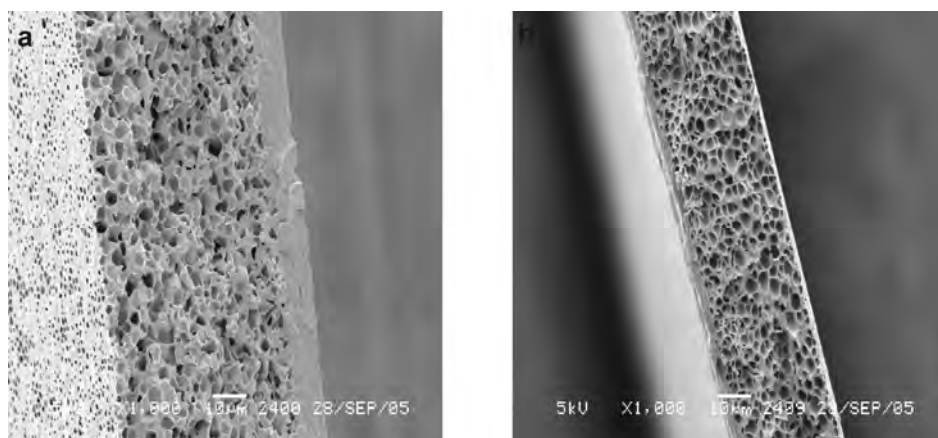
Figure 9: SEM images of cross sections of films prepared from 20:10:70 w/w PLLA:dodecane:DCM with different non-solvents: a) methanol, b) water.

Effect of temperature

Casting solutions with 10% w/w dodecane were heated up and after some time cooled down to room temperature, before immersion in the non-solvent bath. When the film was produced from a solution that was incubated at 87 $^{\circ}$C, crystallization set in after longer delay time (see Table 2) and the skin layer was thinner than with a solution that was incubated at 62 $^{\circ}$C. Besides that, the porous sublayer contained a closed cellular structure (see Figures 10a and b). This indicates that the crystallization process depends on nuclei already present in the casting solution. Heating the solution before casting, results in melting of many of the nuclei. This suppresses the crystallization process. Therefore, liquid-liquid demixing is relatively faster in these films. Therewith, a cellular morphology was obtained and the crystallization-associated structures, such as the observed solid blobs (compare with Figure 9a) were not present. We now see structures that are similar to the ones observed with the amorphous PDLLA; the structures are now fixated after some time by crystallization. This stresses the importance of control of crystallinity of the polymer in the production of structures with a desired morphology, especially in combination with the use of another non-solvent like dodecane in the polymer solution.

In general, it is clear that the use of dodecane as a non-soluble additive leads to new opportunities to influence porosity in polymeric films and structures. In combination with the choice of solvent, non-solvent, and other process conditions, this may open a new road to the design of highly porous structures.

Figure 10: SEM images of cross sections of films prepared from 20:10:70 w/w PLLA:dodecane:DCM solution heated at different temperatures and with methanol as non solvent: a) 62 C, b) 87 C.

Conclusions

Films formed from solutions of amorphous PDLLA show a dense structure; any porous structure formed during demixing collapses since fixation by crystallization, or vitrification, cannot take place. With crystalline PLLA specific morphologies are obtained. With methanol as non-solvent, a typical asymmetric structure formed by crystallization and (delayed) liquid-liquid demixing was found. With water as nonsolvent, which is hardly miscible with the solvent, the demixing rate was much lower. Liquid-liquid demixing was suppressed and crystallization dominated the formed, symmetric structure.

Next, the influence of an additive, dodecane, which is immiscible with the nonsolvent was investigated. Addition of dodecane speeds up demixing and increases the porosity

of the films. Remarkably, for PDLLA the film does not collapse, as a result of the presence of dodecane droplets, and retains a closed-cell structure. For PLLA films, addition of dodecane made the structure more open and better interconnected. This effect seems stronger than with miscible additives.

The differences in structure between PLLA and PDLLA became smaller when PLLA solution was given a heat pre-treatment before casting to remove nuclei for crystallisation. Liquid-liquid demixing became the dominant mechanism, and crystallization served to stabilize the obtained structure.

Acknowledgements

References

1.   Van de Witte, P., Dijkstra, P. J., Van den Berg, J. W. A., Feijen, J., *Phase separation processes in polymer solutions in relation to membrane formation.* Journal of Membrane Science, 1996. **117**(1-2): p. 1.

2.   Tanaka, T., Lloyd, D. R., *Formation of poly(-lactic acid) microfiltration membranes via thermally induced phase separation.* Journal of Membrane Science, 2004. **238**(1-2): p. 65.

3.   Reuvers, A. J., Smolders, C. A., *Formation of membranes by means of immersion precipitation : Part II. the mechanism of formation of membranes prepared from the system cellulose acetate-acetone-water.* Journal of Membrane Science, 1987. **34**(1): p. 67.

4.   Wienk, I. M., Boom, R. M., Beerlage, M. A. M., Bulte, A. M. W., Smolders, C. A., Strathmann, H., *Recent advances in the formation of phase inversion membranes made from amorphous or semi-crystalline polymers.* Journal of Membrane Science, 1996. **113**(2): p. 361.

5.   Young, T. H., Cheng, L. P., Lin, D. J., Fane, L., Chuang, W. Y., *Mechanisms of PVDF membrane formation by immersion-precipitation in soft (1-octanol) and harsh (water) nonsolvents.* Polymer, 1999. **40**(19): p. 5315.

6.   Bulte, A. M. W., Mulder, M. H. V., Smolders, C. A., Strathmann, H., *Diffusion induced phase separation with crystallizable nylons. II. Relation to final membrane morphology.* Journal of Membrane Science, 1996. **121**(1): p. 51.

7.   Cheng, L. P., Young, T. H., You, W. M., *Formation of crystalline EVAL membranes by controlled mass transfer process in water-DMSO-EVAL copolymer systems.* Journal of Membrane Science, 1998. **145**(1): p. 77.

8.   Lin, D. J., Chang, C. L., Chen, T. C., Cheng, L. P., *Microporous PVDF membrane formation by immersion precipitation from water/TEP/PVDF system.* Desalination, 2002. **145**(1-3): p. 25.

9.   Van De Witte, P., Esselbrugge, H., Dijkstra, P. J., Van Den Berg, J. W. A., Feijen, J., *A morphological study of membranes obtained from the systems polylactide-dioxane-methanol, polylactide-dioxane-water, and polylactide-N-methyl pyrrolidone-water.* Journal of Polymer Science, Part B: Polymer Physics, 1996. **34**(15): p. 2569.

10. Bulte, A. M. W., Folkers, B., Mulder, M. H. V., Smolders, C. A., *Membranes of semicrystalline aliphatic polyamide nylon 4,6: Formation by diffusion-induced phase separation.* Journal of Applied Polymer Science, 1993. **50**(1): p. 13.

11. Van De Witte, P., Esselbrugge, H., Dijkstra, P. J.,Van Den Berg, J. W. A., Feijen, J., *Phase transitions during membrane formation of polylactides. I. A morphological study of membranes obtained from the system polylactide-chloroform-methanol.* Journal of Membrane Science, 1996. **113**(2): p. 223.

12. Zoppi, R. A., Contant, S., Duek, E. A. R., Marques, F. R., Wada, M. L. F., Nunes, S. P., *Porous poly(-lactide) films obtained by immersion precipitation process: morphology, phase separation and culture of VERO cells.* Polymer, 1999. **40**(12): p. 3275.

13. Yeow, M. L., Liu, Y. T., Li, K., *Morphological study of poly(vinylidene fluoride) asymmetric membranes: Effects of the solvent, additive, and dope temperature.* Journal of Applied Polymer Science, 2004. **92**(3): p. 1782.

14. Cheng, L. P., *Effect of Temperature on the Formation of Microporous PVDF Membranes by Precipitation from 1-Octanol/DMF/PVDF and Water/DMF/PVDF Systems.* Macromolecules, 1999. **32**(20): p. 6668.

15. Cheng, L. P., Huang, Y. S., Young, T. H., *Effect of the temperature of polyurethane dissolution on the mechanism of wet-casting membrane formation.* European Polymer Journal, 2003. **39**(3): p. 601.

16. Chuang, W. Y., Young, T. H., Chiu, W. Y., Lin, C. Y., *The effect of polymeric additives on the structure and permeability of poly(vinyl alcohol) asymmetric membranes.* Polymer, 2000. **41**(15): p. 5633.

17. Chuang, W. Y., Young, T. H., Chiu, W. Y., *The effect of acetic acid on the structure and filtration properties of poly(vinyl alcohol) membranes.* Journal of Membrane Science, 2000. **172**(1-2): p. 241.

18. Van de Witte, P., Esselbrugge, H., Peters, A. M. P., Dijkstra, P. J., Feijen, J., Groenewegen, R. J. J., Smid, J., Olijslager, J., Schakenraad, J. M., Eenink, M. J. D., Sam, A. P., *Formation of porous membranes for drug delivery systems.* Journal of Controlled Release, 1993. **24**(1-3): p. 61.

19. Madaeni, S. S., Rahimpour, A., Barzin, J., *Preparation of polysulphone ultrafiltration membranes for milk concentration: Effect of additives on morphology and performance.* Iranian Polymer Journal (English Edition), 2005. **14**(5): p. 421.

20. Zhao, J., Yuan, X., Cui, Y., Ge, Q., Yao, K., *Preparation and characterization of poly(L-lactide)/poly(ε-caprolactone) fibrous scaffolds for cartilage tissue engineering.* Journal of Applied Polymer Science, 2004. **91**(3): p. 1676.

21. Pêgo, A. P., Siebum, B., Van Luyn, M. J. A., Gallego y Van Seijen, X . J., Poot, A. A., Grijpma, D. W., Feijen, J., *Preparation of Degradable Porous Structures Based on 1,3-Trimethylene Carbonate and D,L-Lactide (Co)polymers for Heart Tissue Engineering.* Tissue engineering, 2003. **9**(5): p. 981.

22. Tsuji, H. H., *Stereocomplex formation between enantiomeric poly(lactic acid)s. 6. Binary blends from copolymers.* Macromolecules, 1992. **25**(21): p. 5719.

23. Urayama, H., Kanamori, T., Kimura, Y., *Properties and biodegradability of polymer blends of poly(L-lactide)s with different optical purity of the lactate units.* Macromolecular Materials and Engineering, 2002. **287**(2): p. 116.

24. Van De Witte, P., Dijkstra, P.J., Van Den Berg, J.W.A., Feijen, J., *Phase behavior of polylactides in solvent-nonsolvent mixtures.* Journal of Polymer Science Part B: Polymer Physics, 1996. **34**(15): p. 2553.

25. Van de Witte, P., Boorsma, A., Esselbrugge, H., Dijkstra, P. J., Van den Berg, J. W. A., Feijen, J., *Differential Scanning Calorimetry Study of Phase Transitions in Poly(lactide)-Chloroform-Methanol Systems.* Macromolecules, 1996. **29**(1): p. 212.

26. Cheng, L. P., Shaw, H. Y., *Phase behavior of a water/2-propanol/poly(methyl methacrylate) cosolvent system.* Journal of Polymer Science Part B: Polymer Physics, 2000. **38**(5): p. 747.

27. Tao, C. T.,Young, T. H., *Phase behavior of poly(N-isopropylacrylamide) in water-methanol cononsolvent mixtures and its relevance to membrane formation.* Polymer, 2005. **46**(23): p. 10077.

28. Radovanovic, P., Thiel, S. W., Hwang, S. T., *Formation of asymmetric polysulfone membranes by immersion precipitation. Part I. Modelling mass transport during gelation.* Journal of Membrane Science, 1992. **65**(3): p. 213.

Appendix

Based on the results presented previously, one can conclude that the addition of dodecane to the casting solution has a big influence on the film structure. The presence of dodecane in the polymer solution has lowered the solvent quality of DCM; which will influence the phase separation mechanism. The presence of dodecane in the casting solution has brought the demixing gap much closer to the initial polymer cast composition. This is consistent with the light transmission results. Increasing the dodecane concentration from 0 to 5% reduces the delay time from 16 to 7 seconds. Upon further increase of the dodecane concentration, the delay time is reduced further until we have almost instantaneous demixing at 10% dodecane (Table 2).

A possible but very unlikely interpretation for the system is that the mixture of DCM and dodecane might actually function as a co-solvent for PLA. If the co-solvency holds, the phase diagram can have two demixing regions with two binodal curves sandwiching a miscibility region as described by Liao-Ping *et al* for the system of poly-(methylmethacrylate) in water-2-propanol co-solvent mixtures [26], and by Tao *et al* using poly(N-isopropylacrylamide) in water-methanol co-non-solvent mixtures [27]. In such a case, the demixing region in the phase diagram will increase in size, which will most probably facilitate phase separation. However, it should be kept in mind that dodecane is a poor solvent for PLA and it is not expected that dodecane/DCM mixtures can act as a co-solvent.

The incorporation of dodecane to the casting solution makes the system more complex as it has become a quaternary system. The principle is however the same as for the ternary one. Contacting the polymer solution with non-solvent will cause out-diffusion of solvent and a smaller in-diffusion of non-solvent, and consequently demixing will take place.

Figure 11 shows the folded-down quaternary phase diagrams – these are the ternary limiting systems of the full (3-dimensional) diagrams. Please note that only binodals and tie-lines are shown and not spinodals. Earlier research has shown that demixing by

immersion leads to metastable demixing and not spinodal decomposition – thus the binodals are most relevant for our purpose [28]. The PDLLA-DCM-methanol-dodecane system (a) shows three two-phase regions, indicating an equilibrium between a PLA concentrated and a PLA diluted phase. For truly quaternary solutions, these two-phase regions lead to a three-phase region, which is inside the quaternary phase diagram, and not visible in the limiting ternary diagrams. This can be illustrated by assuming a quaternary solution containing equal amounts of all four components. This solution will decompose into a PLA-rich and a PLA-poor phase. This PLA-poor phase would contain roughly equal amounts of the three low-molecular weight components. This phase is not stable (see limiting ternary DCM-dodecane-methanol diagram) and will itself decompose into a phase rich in methanol and a phase rich in dodecane. Thus, a three-phase region is present inside the quaternary phase diagram, as a result of the three two-phase regions in the limiting ternary diagrams. This same three-phase region is evident in the limiting ternary system methanol-dodecane-PDLLA: most of the phase diagram is occupied by a three phase region, indicating decomposition of the compositions enclosed by the region, into a methanol phase, a dodecane phase and a PDLLA-rich phase. Around this three-phase region, two two-phase regions are visible.

The system with water instead of methanol (b) shows a somewhat different phase diagram due to the relative immiscibility of water with the other components. Solutions of PDLLA with DCM are basically immiscible with water, leading to a large two-phase region in that limiting ternary diagram. Since dodecane is immiscible with water as well, a similar demixing gap is visible in the ternary system DCM-dodecane-water. The three two-phase regions in the systems PDLLA-DCM-water, DCM-dodecane-water and DCM, dodecane-PLA, once more lead to a three-phase region inside the quaternary phase diagram, which is evident in the limiting diagram for water-dodecane-PDLLA.

The systems with PLLA (c and d) show the same liquid-liquid demixing behavior as with PDLLA, but in addition show regions exhibiting demixing between a crystalline
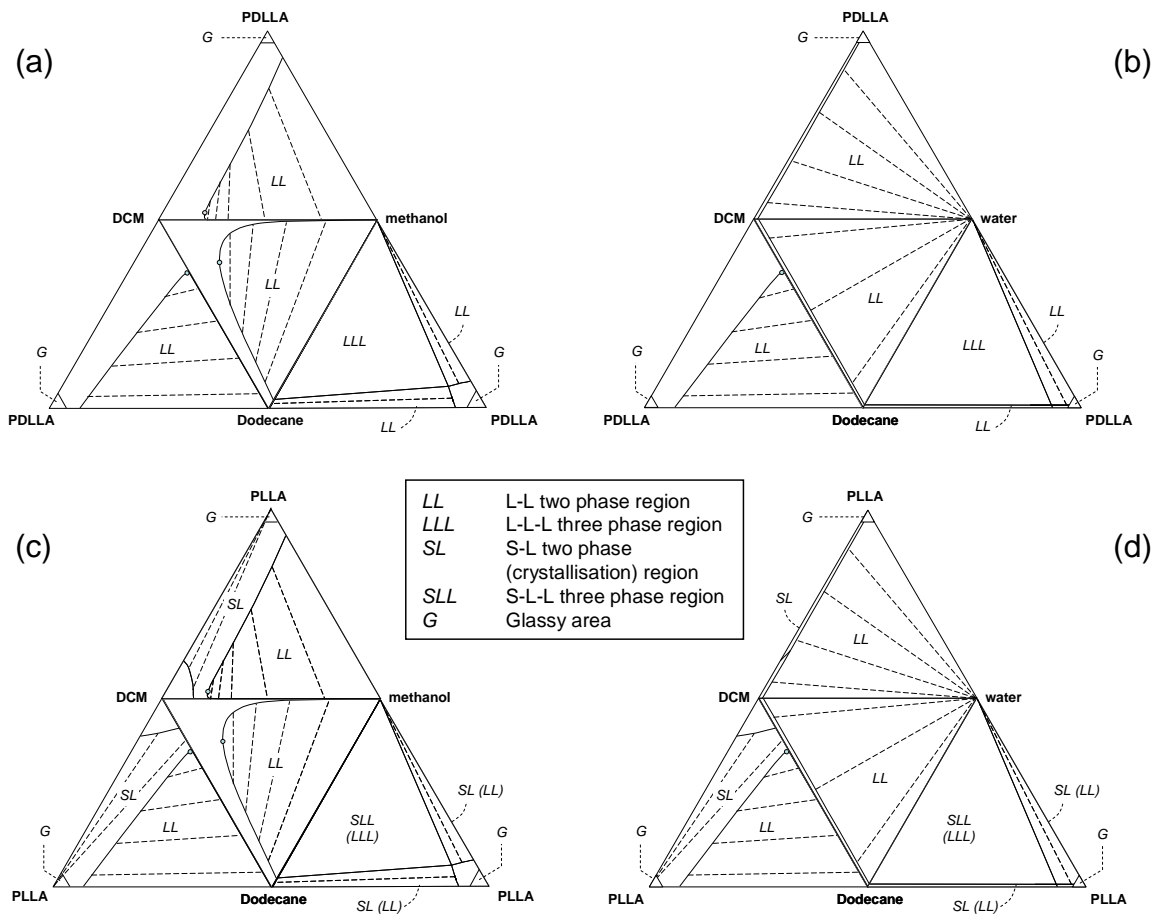
Figure 11: Full quaternary (folded-out) phase diagrams for (a) PDLLA-DCM-methanol-dodecane, (b) PDLLA-DCM-water-dodecane; (c) PLLA-DCM-methanol-dodecane, (d) PLLA-DCM-water-dodecane. The phase diagrams were calculated with the parameters as mentioned in Table 1.

PLLA phase and a liquid (PLLA poor) phase. They are visible in the limiting phase diagrams PLLA-DCM-methanol and PLLA-DCM-dodecane and PLLA-DCM-water and PLLA-DCM-dodecane: once more, these regions extend into the volume of the quaternary phase diagrams. Even though in the ternary systems PLLA-dodecane-methanol and PLLA-dodecane-water no crystallization areas are visible, one should bear in mind that the stable PLLA rich phases in the lower right corner of the diagram will be strongly crystallized. Below the liquid-liquid demixing gaps (two-phase and three-phase) a crystallization curve is present, which means that even though thermodynamically speaking the three-phase region is a liquid-liquid-liquid region, the

actual three phase equilibrium will be of type liquid-liquid-solid (water/methanol phase, dodecane phase and crystallized PLLA phase).

The phase diagrams show that PLLA systems have a strong tendency to crystallize, even before liquid-liquid demixing. However, crystallization is generally a slow process. Since liquid-liquid demixing is usually a fast process (except when the nonsolvent diffuses in very slowly), liquid-liquid demixing can still take place before crystallization can take place.

Chapter 3

Mechanical properties and porosity of polylactide for biomedical applications*

Abstract

In this study, strength, ductility, and porosity of polylactide films prepared by immersion precipitation and film casting in air were investigated. To induce extra porosity in the films, dodecane was added to the polymer casting solution.

The structure, porosity, and mechanical properties of the films were evaluated. The ultimate strength and elastic modulus of neat PLLA prepared by film casting were at least twice those of the same film prepared in methanol, whereas the ductility of these films was considerably higher than for air. The porosity, size of pores, and interconnectivity of pores increased gradually with increasing dodecane concentration. This dodecane-induced porosity (as high as 80%), progressively decreased the ultimate strength and modulus of practically all films, but remarkably improved the ductility of films prepared in air, and this can be related to a decrease in crystallization temperature. For films prepared in water, or PDLLA films in general, the ultimate strength, modulus, and ductility of films prepared in water were significantly lower than those of air-cast PLLA films.

In summary, the results obtained in this research show that it is possible to tailor the properties of the films for various biomedical applications, through the use of polymer type, preparation method, and dodecane-induced porosity as tools.

Introduction

Biodegradable polymers have received considerable attention in the last decades, because of their wide applications in pharmaceutical, biomedical and environmental fields [1, 2]. Typical examples of these polymers are aliphatic polyesters such as poly(butylene succinate) (PBS), poly[(butylene succinate)-co-adipate] (PBSA), poly(3-hydroxybutyrate) (PHB), poly(e-caprolactone) (PCL), and poly(lactide) (PLA) [3-6]. PLA is highly hydrolysable in the human body and has good mechanical strength, thermal plasticity, fabricability, biodegradability, and biocompatibility [7, 8], and that is why PLA has become one of the most popular biodegradable materials in the biomedical field. It has been used for sutures, bone screws, bone plates, tissue repair, and regeneration, and also for controlled delivery devices (e.g. microparticles or implants for drugs) [1, 9-16]. Also for applications outside the medical field, recent developments in processing technology make PLA more economically viable as an environmental-friendly substitute for the conventional synthetic packaging materials [2].

For many applications, the degradation and mechanical properties of PLA are important. The degradation behaviour of PLA plays a big role on its in vivo performance and may influence many processes i.e. tissue regeneration, cell growth and host response [17, 18]. Degradation of PLA mostly occurs by hydrolytic attack of the ester bonds in the polymer, after which lactic acid monomers are formed and eventually removed via normal metabolic processes in the body [19, 20]. There are many factors that can affect degradation rate of PLA including the polymer material properties such as: crystallinity, molecular weight, and monomer hydrophobicity [19]. Moreover, some researchers have reported that additives can also speed up or delay the degradation process of PLA [21-23].

Beside the degradation behaviour, which is beyond the scope of this paper, mechanical properties of PLA is of a great importance also, and in this respect some improvement of e.g. the brittle nature, lack in toughness and low deformation at break, is desirable [24-26]. One solution lies within the polymer itself, it is well known that the physical properties of PLA such as melting point, mechanical strength, and crystallinity, can be influenced considerably by the stereo-isomeric

L/D ratio of the lactide units [3, 5]. For instance, poly(L-lactide) (PLLA), which consists of pure L-lactide is an isotactic and crystallisable polymer, that gives strength to structures [3, 27]. In contrast, poly(DL-lactide) (PDLLA) produced from racemic mixtures of L-lactide and D-lactide, is atactic and completely amorphous resulting in more brittle structures [3, 27]. Also several other techniques to enhance flexibility and toughness have been reported, such as copolymerization or blending with other substances like polymers [3, 6, 28], plasticizers [24-26, 29], or fillers [4, 30].

Each application will have its own requirements, therefore, it is obvious that control over the mechanical properties of PLA is of great importance. However structure-related properties should not be disregarded because they will influence the mechanical properties; at the same time they may be required for a specific application (e.g. porosity for controlled release purposes). Part of the solution can be found within the polymer itself but obviously the production method will also play a role. Various production processes are reported for PLA such as injection moulding, extrusion, film blowing, fibre spinning, film casting, and immersion precipitation [2, 5, 9, 13, 24, 30, 31]. In the last process for instance, a dope consisting of polymer, solvent, and additives is immersed in a coagulation bath filled with a non-solvent and due to the subsequent exchange of the solvent and non-solvent, phase separation takes place and solidification of the polymeric product occurs [31]. Depending on the composition of the coagulation bath, completely different structures may be formed ranging from dense films, to highly porous structures. It can be expected that depending on the structures formed also different mechanical behaviour will be found, therewith co-determining the field of application [9, 32]. Therefore it is not strange that immersion precipitation has been proposed in very different fields including the preparation of polymeric membranes, and also for the preparation of biodegradable scaffolds for blood vessels, drug delivery devices, microparticles, implants, fibres, and films [13, 16, 31, 33].

In this study, we systematically investigate polylactide films (PLLA, PDLLA, and mixtures thereof) in order to correlate structure formation with mechanical behaviour. The films were fabricated via two processes, film casting and immersion precipitation. In the first method the film was cast and then exposed to the air,

while in the last one the film was immersed into different non-solvents (instead of air), which are known to influence the film structure considerably. Besides that, also dodecane was used as an immiscible additive to the polymer solution that is used to prepare the films in order to induce porosity in the films away from the porosity generated by regular phase separation processes. (The use of high alkanes, such as dodecane, has been described in literature among other things for the production of hollow polymeric particles [33]). In that way, we hope to combine structure related requirements, such as porosity, with mechanical strength. The results are summarized in an application graph that links (film) production conditions, mechanical properties and methods with application fields.

Experimental

Materials

Two types of PLA were used in this study: Poly-L-lactide (PLLA) and poly-D(50)L(50)-lactide (PDLLA), with intrinsic viscosities of 1.21 and 0.49 dl/g, respectively, and both were obtained from PURAC Biochem B.V., Gorinchem, the Netherlands. Dichloromethane (DCM), (HPLC, gradient grade) was purchased from Merck and used as the solvent for the polymer. Dodecane (≥99%) was supplied by Sigma-Aldrich and used as an additive. Methanol (HPLC, gradient grade, ≥99.9%) (Aldrich) was used with Milli-Q water as a non-solvent. All chemicals were used as received.

Methods

Film preparation

To form PLA films, solutions of weight ratios 10:0:90, 10:5:85, 10:10:80, 10:15:75, and 10:20:70 PLLA:dodecane:DCM; 10:0:90, and 10:5:85 PDLLA:dodecane:DCM; and 10:5:85 PLA mixture (1:1 PLLA:PDLLA):dodecane:DCM w/w/w were prepared. In the case of the films with 10% PDLLA, only one dodecane concentration is used, because at higher concentrations, no films could be formed with PDLLA. The polymer was first dissolved in DCM, and if needed, dodecane was subsequently added. The solution was kept under stirring for 1-2 days. The films were formed with two procedures:

i) Film casting: the polymer solution was cast onto a mould and left in a fume hood for evaporation of the solvent under ambient conditions.

ii) Immersion precipitation: the polymer solution was cast onto a mould and then immersed into a coagulation bath filled with non-solvent and kept there for around 40 min. As non-solvents, 100:0, 60:40, 30:70, and 0:100 (w/w) methanol:water mixtures were used in this study. The initial thickness of the cast layer was always 100 µm.

Mechanical properties

All films were left in the fume hood under ambient conditions for one day before use to ensure complete evaporation of the solvent. Out of films prepared by either film casting or immersion precipitation, samples with a dog–bone-like shape were cut. The total length of each sample was 37 mm; the gauge length of the samples was about 15 mm ($\pm$1); the width was 13 mm at the top and 7.2 mm (narrowest) at the middle of the sample in order to induce the fracture in the middle of the sample. Tensile testing of the films was performed with the Texture Analyzer T2 (Stable Micro Systems Ltd., Surrey, UK). The tensile tests were carried out at constant crosshead speed of 0.1mm/s until break. Stress-strain curves were calculated from load-elongation curves measured for 2-10 samples from films that were each separately produced under the various conditions described earlier. Tensile strength (σ), elongation at break (EB), and Young's modulus (E) were calculated from the stress-strain curves.

Differential scanning calorimetry (DSC)

The thermal properties of the films were measured using differential scanning calorimeter (Perkin Elmer DSC-7, with a TAC 7/DX thermal analysis controller). Scans of samples (about 8-10 mg) were run from 0 ^{o}C to 250 ^{o}C at heating rates of 10 ^{o}C/min. The glass transition temperature (T_g), crystallisation temperature (T_c), melting temperature (T_m), and enthalpies of crystallization and melting were determined.

Scanning electron microscopy (SEM)

Structures of the films before and after tensile testing (with special interest for the fracture surfaces) were investigated by SEM (JEOL, JSM-5600 LV). Cross

sections of the samples were cut, dried, and fractured in liquid nitrogen. Before viewing with SEM, the cross sections were coated with a thin platinum layer (~5 nm) using a sputter-coater (JEOL, JFC-1300).

Porosity and density of films

The porosity (ε) of the films was estimated by measurement of the mass and dimensions of the films as reported by Hu and co-workers, and others [16, 34, 35]. The porosity was defined as follows:

$$\varepsilon = 1 - \rho_{film} / \rho_{polymer} \tag{1}$$

Where, ρ_{film} and $\rho_{polymer}$ are the (bulk) densities of film and polymer, respectively. The densities of the films were measured by calculating the mass/volume ratio for three samples of each film. The film prepared without dodecane (Figure 1a) shows a porosity of zero, and therefore the density of this film was taken as the polymer density [16, 36].

For the theoretical description of the bulk density of the films and, therefore, the porosity as a function of the dodecane concentration, equation 2 was used.

$$\rho_f = \frac{X_{polymer}}{(X_{polymer} / \rho_{polymer}) + (X_{dodecane} / \rho_{dodecane})} \tag{2}$$

Where, $X_{polymer}$ and $X_{dodecane}$ are the mass fractions of polymer and dodecane, and $\rho_{polymer}$ and $\rho_{dodecane}$ are the densities of polymer, and dodecane respectively. It was assumed that the total volume fraction of the voids (porosity) in the film was equivalent to the volume fraction of the dodecane added to the film. This implies that the volume loss of the air-cast film is caused by evaporation; and the weight of the film is equivalent to the initial weight of the polymer in the cast. These assumptions are only true for air-cast films in Figure 1, as the porosity was mainly caused by dodecane, while for immersion precipitation films, these assumptions do not hold because part of the porosity in the films was generated by the phase inversion process.

Results and discussion

Film characterization

Morphology air casting

The morphologies of the cross sections of PLLA films prepared by air casting were investigated by SEM. In Figure 1, the results for different dodecane concentrations are shown. When no dodecane was present in the casting solution, a solid, dense, and nonporous film was obtained (Figure 1a). When the film was exposed to air, only evaporation of the solvent dichloromethane occurred because air can hardly diffuse into the polymer solution; no demixing takes place, and therefore a nonporous structure was observed.

When dodecane was added, the structures were entirely different; they became porous and porosity increased with increasing dodecane concentration (this is described in more detail in the porosity and density section). For 5 % dodecane, an asymmetric morphology consisting of a thin dense toplayer and a porous sublayer with a fairly uniform closed cellular structure was obtained (Figure 1b). With increasing dodecane concentration (i.e. >10% w/w), symmetric structures with more open morphologies were observed (Figures 1c-e). The overall pore fraction, size of the pores, and their interconnectivity gradually increases with increasing dodecane concentration. Based on these findings, one can say that the addition of dodecane is a novel and easy approach for production of porous structures by the film casting method.

The influence of dodecane on the structure can be explained as follows: when a film containing dodecane is exposed to the air, the solvent DCM will start to evaporate, and consequently the dodecane concentration in the film will increase. Because dodecane is a poor solvent for PLA, one expects that when dodecane reaches a certain concentration, demixing will start to occur in the film by nucleation and growth of the polymer [32]. The dodecane droplets are the precursors of the pores that were observed by SEM. The amount of these droplets is expected to increase when more dodecane is added to the polymer solution. Thus

the incidence of coalescence will become higher, which will eventually result in a structure with more and larger pores. This is in line with the SEM observations. The resulting structure is expected to be solidified by crystallisation of the polymer. How this influences the mechanical properties is discussed in a later section.

Morphology immersion precipitation

The structures in air-cast films are now compared with those obtained by immersion precipitation in various non-solvents (see Figure 2). With methanol the structures were to a certain extent similar to the ones obtained with air. When water/methanol mixtures were used, the porosity, the size of the pores, and their interconnectivity increased, with increasing water concentration.

During immersion precipitation, the phase separation process is different and more complex than that for air casting. Contacting the polymer solution with non-solvent will lead to out-diffusion of solvent into the non-solvent (instead of air) and in-diffusion of non-solvent into the polymer solution. When the polymer solution becomes saturated with non-solvent, phase separation will take place. In a previous study, we found that PLLA films are solidified by crystallization of the polymer, and depending on the non-solvent used, crystallization will set in early (methanol) or later (water), therewith allowing more or less time for solidification of the structure and/or structural rearrangements [32]. Furthermore, dodecane speeds up phase separation and induces faster crystallization in the films, depending on the non-solvent used. Even when we used PDLLA in combination with dodecane, the films did not collapse, and porous structures were obtained [32]. Thus, crystallization is not necessity for solidification in the film. For a more complete description of the effects involved, we refer readers to previous work [32].
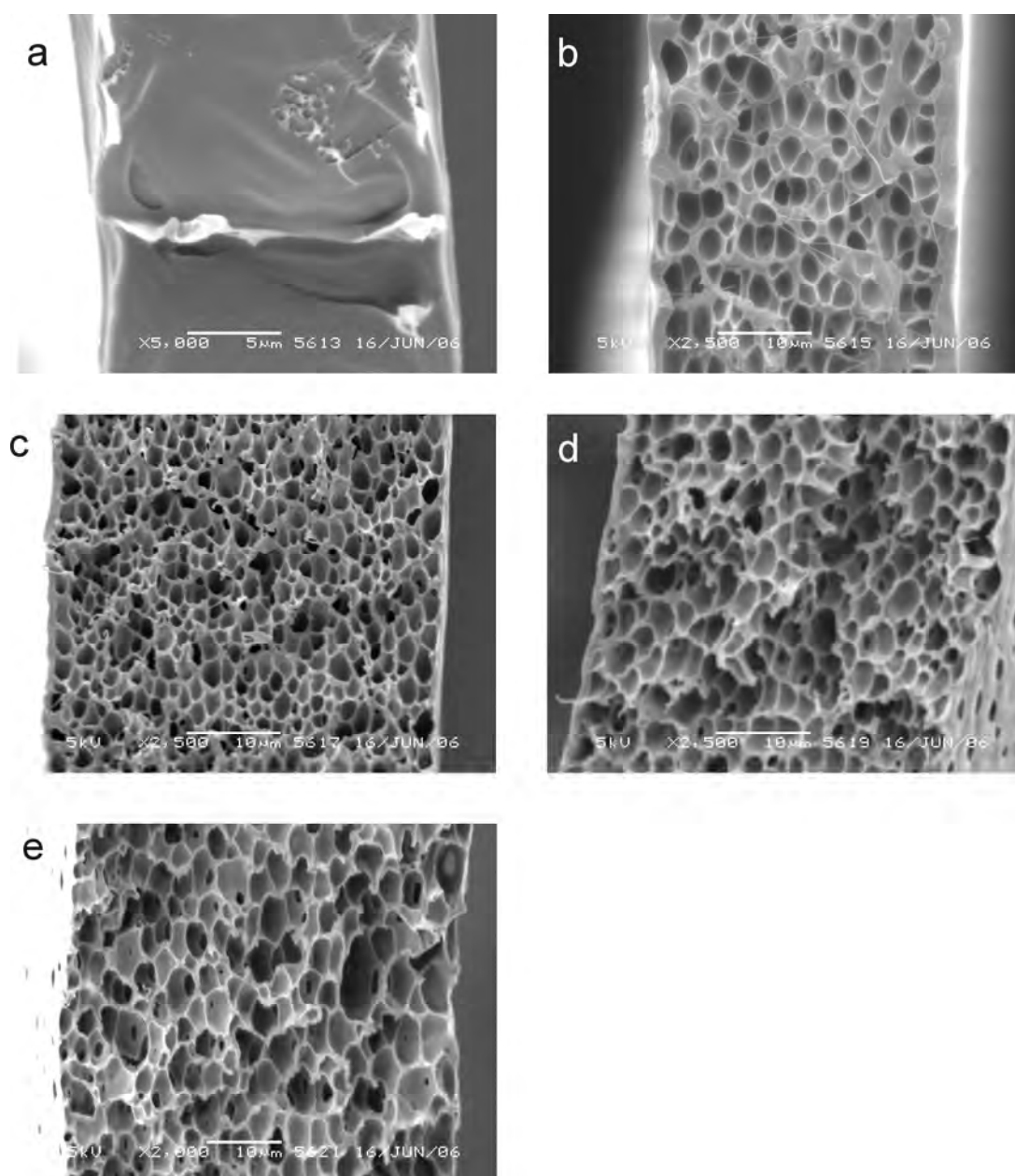
Figure 1: SEM images of cross sections of PLLA films prepared in air and with different dodecane concentration w/w in casting solution: a) 0%, b) 5%, c) 10% d) 15% and e) 20%. The initial polymer concentration in all films was 10%w/w.
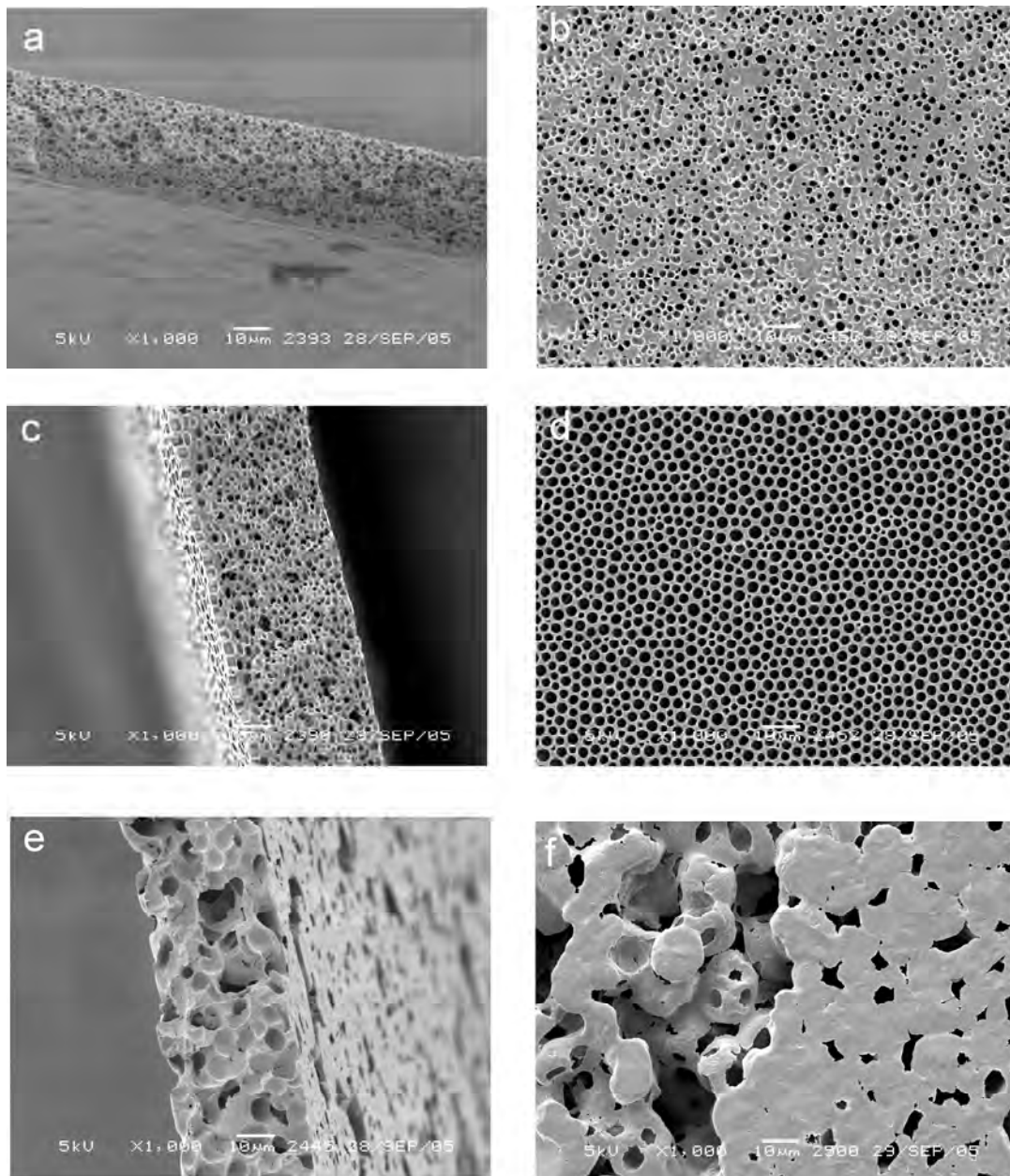
Figure 2: SEM images of cross sections of films prepared from 10:05:85 w/w PLLA:dodecane:DCM with different non-solvents: a) methanol, b) methanol, surface, c) 60:40 w/w methanol:water, d) 60:40 w/w methanol:water, surface, e) water, f) water, surface.

Film porosity and density

Figure 3 shows the porosity and density of films prepared in air as a function of dodecane concentration. The results were in line with the SEM observations; the higher the dodecane concentration the higher the porosity in the films. With increasing porosity, obviously the bulk density of the films decreases (see Figure

3a). Figure 3a shows that the theoretical model always overestimates the measured porosity, which points to partial collapse of the structure. This effect is, perhaps surprisingly, more pronounced at low dodecane concentrations (see Figure 3b). It is expected to be caused by the time scale of solidification in these films which was slow compared to high dodecane concentrations which solidify fast [32]. This is expected to lead to better preservation of the structure. Although part of the porosity that is induced by dodecane collapses, it is important to note that the largest part of this porosity remains, and more so at higher concentrations of dodecane (Figure 3b). This is true not only for air-cast films but also for films prepared by immersion precipitation [32]. This indicates an additional way to induce porosity in a film away from pores generated by regular phase separation. Whether this also leads to mechanically more interesting structures is discussed in the next section.
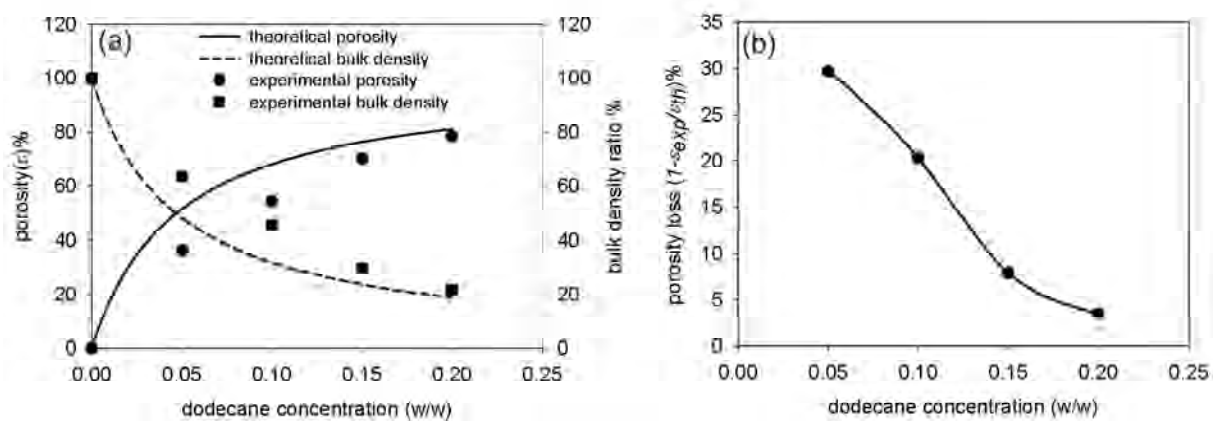
Figure 3: Influence of dodecane concentration on porosity and bulk density of PLLA films prepared in air, theoretical porosity and bulk density of the films were calculated using equations 1 and 2. The initial polymer concentration in all films was 10%w/w.

Mechanical properties

The ultimate tensile strength, elasticity modulus and the elongation at break were measured for all films described in the materials and methods section. The effects of dodecane, preparation method, and type of PLA on the mechanical properties of the films were investigated.
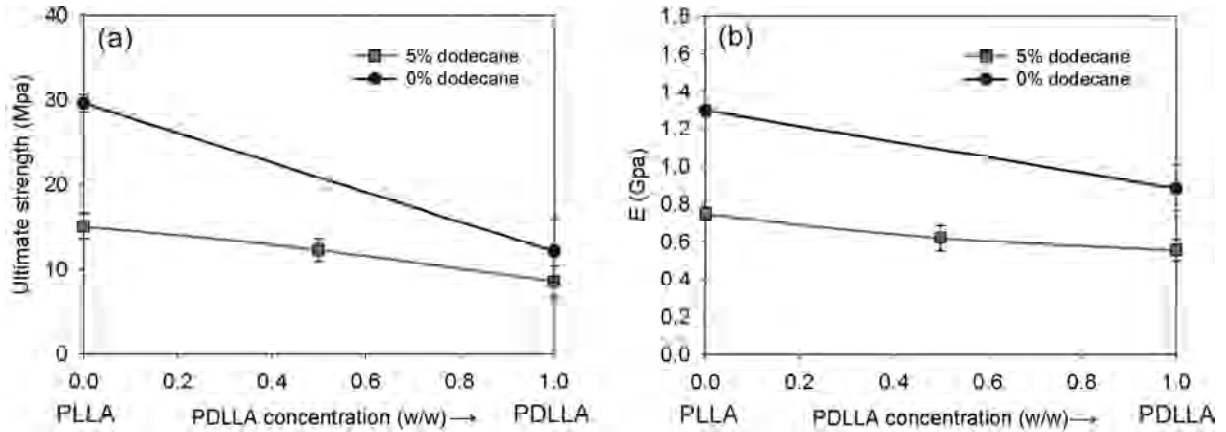
Ultimate tensile strength and elastic modulus

In Figures 4, the effect of dodecane on the ultimate tensile strength (Figure 4a) and elasticity modulus (Figure 4 b) of PLLA films prepared by either air casting or immersion precipitation with methanol or water is shown. The film without dodecane prepared by air casting shows a maximum tensile strength of approximately 70 Mpa and an elasticity modulus of approxmately 2.4 Gpa, which are, in fact, similar to those reported elsewhere for neat PLLA [5, 37]. When the same film was prepared by immersion into methanol, the tensile modulus and strength drop to around half of the original values (see Figure 4), and we expect that the presence of pores (less than if dodecane were added) has caused these effects. This conclusion is in line with the fact, that dodecane induced porosity leads to significant decreases in ultimate strength and elasticity modulus. Please note that these latter porosities can be as high as 80% (Figure 3).

When comparing films with dodecane prepared in air and methanol, we found it remarkable that the films show approximately the same ultimate strength, whereas the elasticity moduli of films prepared in air were higher than those in methanol (Figure 4b). When comparing with films prepared in water, it is obvious that both the ultimate strength and elasticity were considerably less than for methanol and air. This was investigated in more detail; with increasing water concentration in water/methanol mixtures, the films became gradually more fragile and weak (Figure 4c). This can be attributed to the formation of large pores, that are known to occur in films with dodecane cast in water (see Figures 2e and f), and which are generally considered weak spots within the structure [35]. In air-cast films, and films submerged in methanol, these large pores are not present (see Figures 1 b-e, and Figures 2 a, and b).

The results for crystalline PLLA are compared to those for amorphous PDLLA and 1:1 mixtures of both polymers. As expected, the higher the PLLA concentration in the films the higher the strength and modulus (see Figure 5). This is ascribed to the high load-bearing capacity of the crystalline domains in PLLA [27, 38].
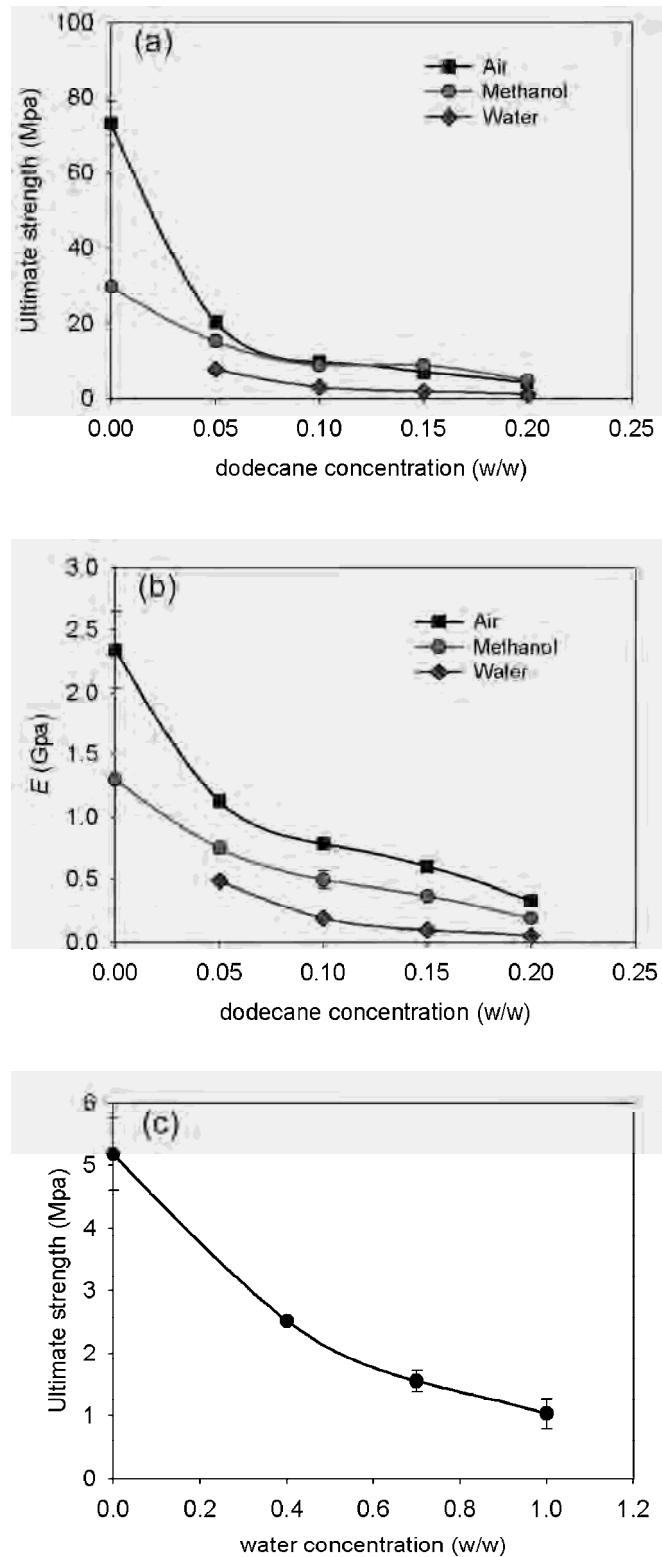
Figure 4: Influence of dodecane concentration and preparation method (air, methanol, and water) of 10% polymer films on: a) ultimate strength, b) elastic modules, of PLLA films., c) ultimate strength of 10:20:70 PLLA: dodecane:DCM films as a function of water concentration in the nonsolvent.

Figure 5: Influence of PLA type (PLLA and PDLLA) on: a) ultimate strength, b) elastic modules, of PLA films prepared in methanol and with different dodecane concentrations. The initial polymer concentration in all films was 10%w/w.

On the bases of these results, one can conclude that the mechanical properties of the films are dependent not only on the polymer type but even more so on their structure; the tensile strength and elasticity modulus decrease with increasing porosity, pore size, and interconnectivity. This is reasonable, if we keep in mind that fracture in films originates from local concentrations of stress at flaws, scratches or notches [39] and propagates by nucleation and growth of cracks or crazes inside structures. These cracks can easily propagate and grow in regions containing voids, and they become even easier to grow from larger pores or macrovoids within films. Furthermore, it is expected that the cross sectional area of the load-bearing polymer decreases with increasing porosity in the film which will reduce the tensile modulus and ultimate strength [11]. A first attempt to quantify these effects is given in the next section.

The reduction in strength and elasticity modulus with increasing porosity was also observed in other studies [35, 36, 40], and for highly porous materials, such as foams, a power-law relation between porosity and elasticity modulus was given [36, 40]:

$$E = E_o \, (1 - \varepsilon)^n \tag{3}$$

Where E_o is the modulus of the nonporous film, ε is the porosity, and n is a constant. For E_o, the E-value of a film prepared without dodecane was taken, and the model was fitted to our experimental data for films prepared in air using the least sum of squares. For a value for n of 1.326, the data points are described adequately (see Figure 6). The theoretical value of n for completely open cell foams was reported to be 2, whereas for closed cells this value is around one [40]. Our value is between these extremes; indicating partially open cells (see Figure 1).

The same model was explored to describe the ultimate tensile strength of the films as function of porosity (ε) and ultimate strength of the film prepared without dodecane (σ_o):

$$\sigma = \sigma_o \left(1 - \varepsilon\right)^n \tag{4}$$

Again the data were fitted using the least sum of squares method and for $n = 2.596$ the fit is reasonable (see Figure 7).
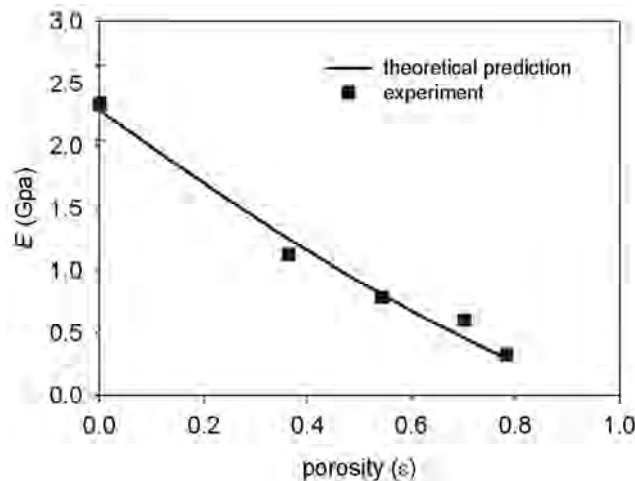
Figure 6: Influence of porosity on elastic modules of PLLA films prepared in air with different dodecane concentrations. The initial polymer concentration in all films was 10%w/w.
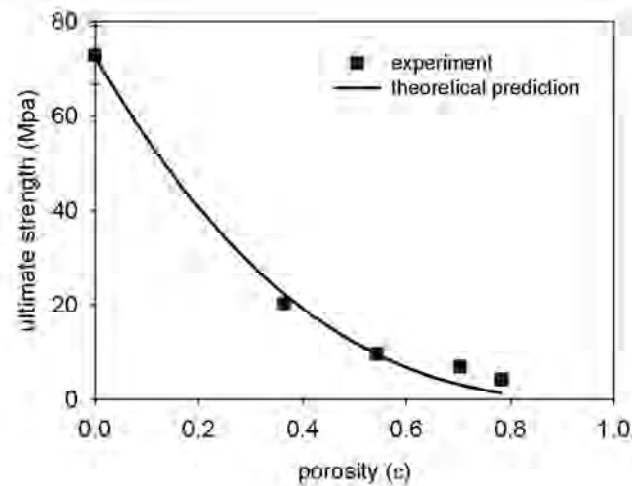
Figure 7: Influence of porosity on ultimate strength of PLLA films prepared in air with different dodecane concentrations. The initial polymer concentration in all films was 10%w/w.

Elongation at break

Besides the elasticity modulus and the ultimate strength, the elongation at break is also an important feature of a film. In Figure 8, results are shown for films prepared by air casting and immersion precipitation (with or without added dodecane). When no dodecane was added, the film formed in air showed typical stiff behavior of neat PLLA with a total elongation of 8%, which is close to values stated in other studies [26] . Remarkably, with methanol the flexibility of the film was significantly enhanced and an elongation at break of up to 35% was recorded. This may be due to the higher degree of deformation that a regular cell structure permits during elongation.
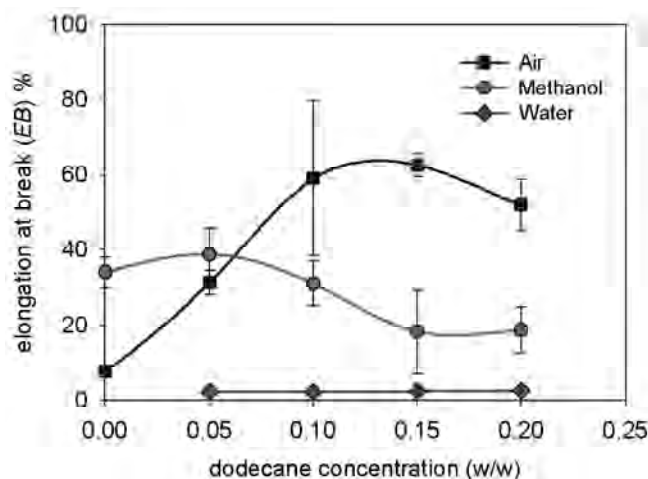
The effect of dodecane depends on the preparation method used. A remarkable improvement in ductility was observed for the films prepared in air (although strength and modulus decreased considerably), (see Figure 8). For example, the elongation of the film with 5% w/w dodecane was threefold that of a neat PLLA film; that of a film with 10% w/w dodecane was eightfold that of a neat PLLA film. This can be related to the structure of the films; in air-cast films with dodecane we observed the formation of the fairly large but uniform pores (Figure 1), which can deform during elongation and hence allow for a much larger maximum elongation

67

at break. This was investigated in more detail with DSC, and the results are shown in that section.

Figure 8: Influence of dodecane concentration and preparation method (air, methanol, and water) on elongation at break of PLLA films. The initial polymer concentration in all films was 10%w/w.

The effect of dodecane on the ductility of films prepared with methanol was different from those prepared with air. At 5% w/w dodecane, the elongation at break of the films was slightly enhanced in comparison with neat PLLA, but when higher concentrations of dodecane were used, a progressive reduction in the elongation at break was observed, as shown in Figure 8. At 5% the films still contained many small pores (Figure 2a), but at higher dodecane concentrations these films have many large pores with thin, fragile lamellae between them [32], and are therefore, more susceptible to break at less elongation.

For films produced by precipitation in water, a low ductility was found; dodecane did not show any influence on the elongation of the films (see Figure 8). These findings are in line with the effects on strength and elasticity modulus; films produced in water remained weak and we expect this to be caused by the small contact areas between crystalline spherulites or domains (Figures 2e and f). When water/methanol mixtures were used as non-solvent, the elongation at break of these

films was close to that of water (5.5 % elongation for 60:40 methanol:water and 3.9% elongation for 30:70 methanol/water).

The elongation at break for the PDLLA films is less than 2%, which is very low compared to PLLA films (32%). Also addition of dodecane does not increase the ductility (~ 2.2%). This is due to the low flexibility and deformability of the amorphous domains in the PDLLA structure compared to the crystalline ones in PLLA. Elongation of the PDLLA films was significantly enhanced through blending with PLLA, for a 1:1 mixture the elongation at break is approximately 18%.

In the previous sections, we have shown structures in relation to observed mechanical behaviour. In summary, porous films with controlled pore size and distribution (i.e. PLLA films with dodecane prepared in air and those of methanol with a low dodecane concentration) are more flexible under tension than nonporous films (neat PLLA films prepared in air).

These effects are visualised in the morphology of fracture surfaces of the films. SEM images of cross sections of PLLA films prepared in air and with different dodecane concentration, taken directly below the fracture surface are shown in Figure 9. Typical brittle fracture was observed for the films without dodecane (see Figure 9 a), which is in line with findings in other studies [29]. The micrographs of the films prepared with dodecane (see Figure 9 b-d) show a large amount of plastically deformed materials. Figures 9 b-d show typical morphology of crazed material consisting of two phases; the continuous phase consists of fibrils, and the disperse phase consists of micro-voids. During deformation, the material can absorb more energy because of the extension of the fibrils across the micro-voids; dissipation of the energy can occur by deformation or friction of the fibrils; as they pull out from the bulk of the material [39, 41]. In literature [29], similar fracture structures have been reported in plasticized PLLA, which is more deformable than neat PLLA.
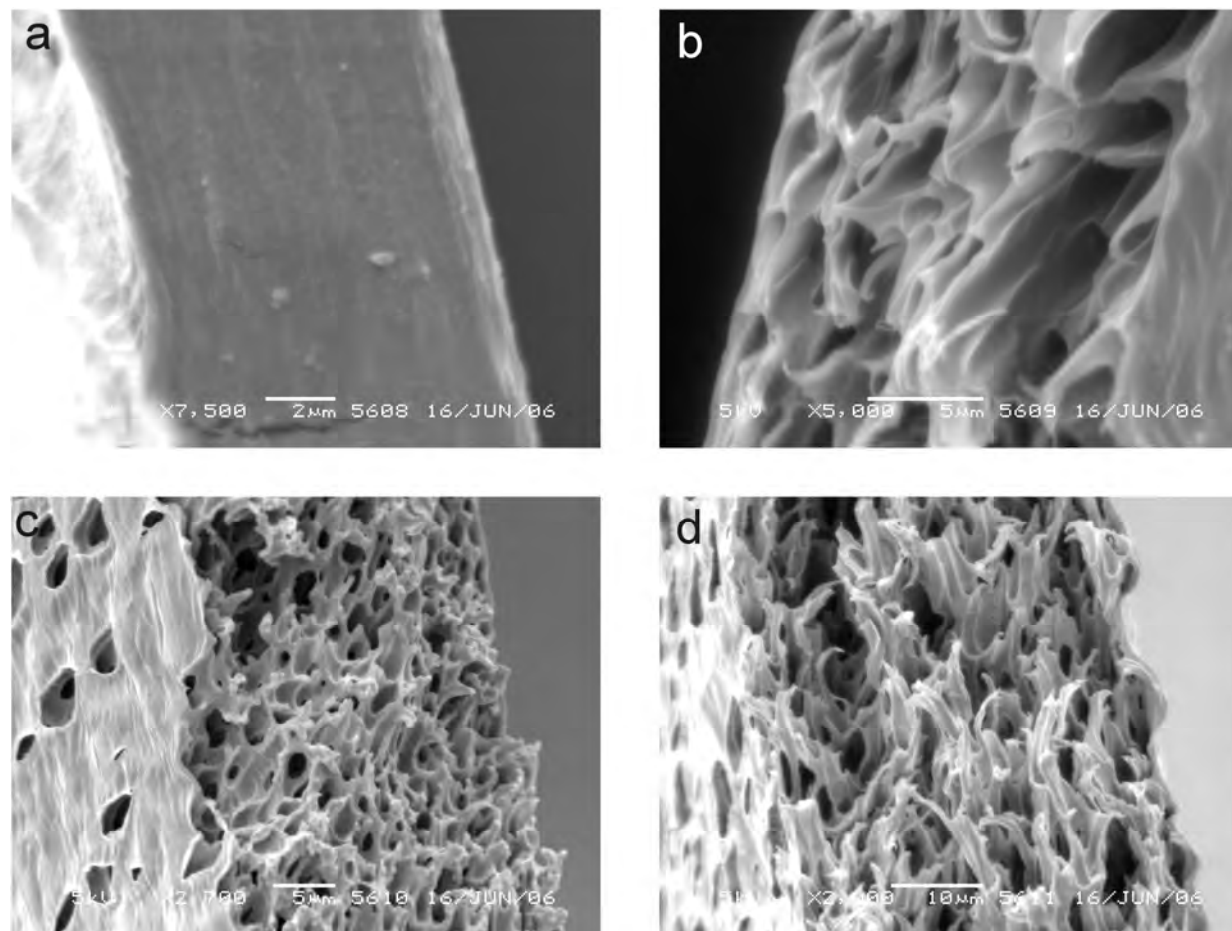
Figure 9: SEM images of cross sections of fracture surfaces of films prepared in air and with different dodecane concentration in casting solution: a) 0%, b) 5%, c) 10% and d) 15%. The initial polymer concentration in all films was 10%w/w.

DSC

Besides the structure itself, also the aggregation state (crystalline or amorphous) will influence the mechanical behaviour. Especially the effect of dodecane needs further elucidation (Figure 8); therefore, the thermal characteristics of PLLA films prepared in air were investigated using DSC. Figure 10 shows DSC thermographs of PLLA samples prepared with different dodecane concentrations. The results indicate glass transition temperatures (T_g) of approximately 53 ^{o}C and melting temperatures (T_m) from 172-177 ^{o}C, which did not differ significantly between the samples. A significant decrease in the crystallization temperature of up to 10 ^{o}C (from 93 to 83 ^{o}C) was observed when neat PLLA films and films with dodecane were compared independently of the dodecane concentration used. For plasticized PLLA, a reduction in the crystallization temperature was reported by other

researchers [26, 29] and they attributed this effect to an increase in chain mobility. When relating these finding to our DSC results, one may conclude that the dodecane phenomenologically slightly acts as a plasticizer.
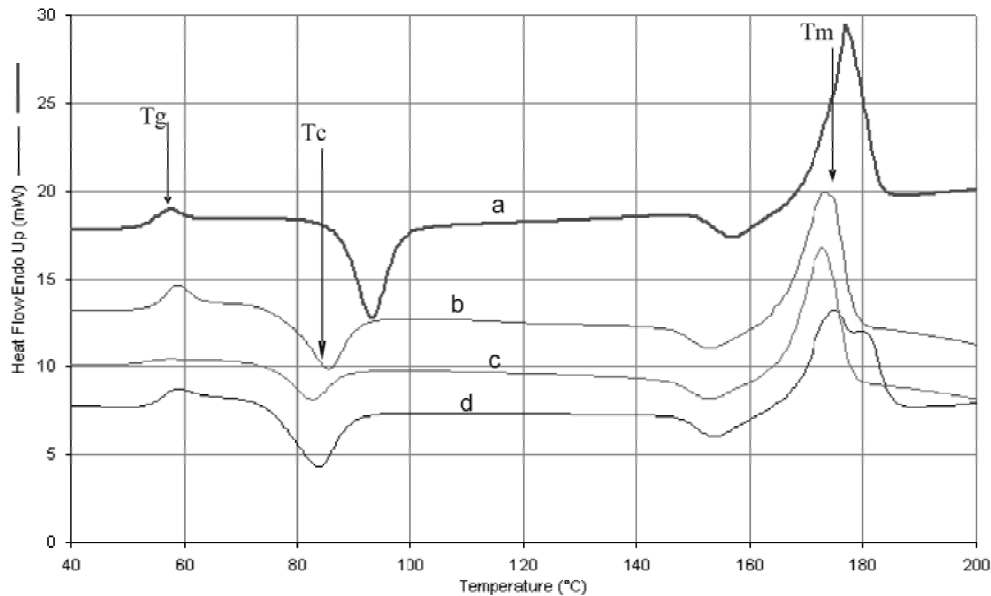
Figure 10: DSC curves (first scan) of PLLA films prepared in air with different dodecane concentrations in casting solution: a): a) 0%, b) 5%, c) 10% and d) 15%. The initial polymer concentration in all films was 10%w/w.

Options for biomedical applications

For application of PLA products in the biomedical field, specific requirements depending on the application will come into play and these will always be a combination of structural and mechanical properties. For instance; in some applications such as guided tissue regeneration, isolation of the wounded area during the healing process is required. Therefore devices with dense structures are preferred over porous ones, as the polymer implant will function as a barrier to allow the growth of specific tissue and to obstruct the migration of other tissues that disturb the healing process [9, 14]. For some other applications, devices with porous structures are preferred. One may think here of for example cell scaffolding; for transport of nutrients and oxygen to the cells, pores are required [9].

The findings in the study show how certain structures with specific properties can be produced, using the process conditions (e.g. air casting versus immersion precipitation, choice of polymer, addition of dodecane and nonsolvent) as variables. In principle this enables us to taylor for various biomedical applications by adjusting the aforementioned process conditions. In Table 1, a summary of our films is presented, with some suggestions for potential applications in the biomedical field based on their strength, ductility and porosity.

Table 1: strength, ductility and porosity of Polylactide films prepared by immersion precipitation and film casting and with different dodecane concentration for different possible applications in biomedical field.

Films specification					
Parameter	1) • PLLA • No dodecane • Film casting	1) • PLLA • No dodecane • precipitation in methanol 2) • PLLA • low dodecane • precipitation in methanol and film casting 3) • 1:1 PLLA: PDLLA • Low dodecane • Precipitation in methanol and film casting	1) • PLLA • high dodecane • Film casting	1) • PDLLA • Precipitation in methanol and Film casting	1) • PLLA • With dodecane • precipitation in water
Strength (+ strong)	+++ (70 Mpa)	++ (20-30 Mpa)	+ (4-10 Mpa)	+ (10-15 Mpa)	- (<4 Mpa)
Ductility (+ductile)	- (7% elongation)	+ (20-40% elongation)	++ (40-70% elongation)	-- (<4% elongation)	-- (<4% elongation)
Porosity(+porous)	-- (nonporous)	+ (< 30%)	++ (>60%)	- (<10%)	++ (>60%)
Potential application	• barriers against soft tissue invasion (guided tissue regeneration) [9] • Sutures [1] • Buttress for prevention of air leaks after stapled pulmonary resection [10] • fracture fixation plates and rods	• Tissue engineering [16] • drug delivery devices [13] • cell culture [9] • Nerve regeneration	• Tissue engineering and repair,[16] • drug delivery devices ,[13] • heart tissue engineering [16] • cartilage tissue engineering [15] • bone tissue regeneration • cell scaffolding and culture [9]	• guided tissue regeneration [9] • Sutures [1]	• drug delivery devices [13] • ultrasound contrast agents

Conclusions

A variety of PLA films was prepared using film casting and immersion precipitation methods. The results show that the mechanical properties, morphology, and porosity of PLA films can be fine-tuned by preparation procedure, nonsolvent quality, dodecane concentration, and PLA crystallinity.

Neat PLLA films prepared by air casting show the hard and brittle nature of the polymer, whereas films prepared by immersion precipitation in methanol show less hardness and improved ductility. The addition of dodecane was found to be an effective and straightforward method to generate porous films with a highly regular pore structure. The addition of dodecane decreased the tensile strength, and elastic modulus of films, but remarkably improved the ductility of the films prepared in air. The films prepared in water were fragile and much weaker than those prepared in methanol and air. PDLLA films had less tensile strength, lower modulus, and considerably lower ductility than PLLA films.

The diversity in the properties of the films obtained in this study opens the way for a wide range of potential applications in the field of i.e. biomaterials.

Acknowledgements

References

1.   Heino, A., Naukkarinen, A., Kulju, T., Törmälä, P., Pohjonen, T., Mäkelä, E.A., *Characteristics of poly(L-)lactic acid suture applied to fascial closure in rats.* Journal of biomedical materials research, 1996. **30**(2): p. 187.

2.   Auras, R., Harte, B., Selke, S., *An overview of polylactides as packaging materials.* Macromolecular bioscience, 2004. **4**(9): p. 835.

3.   Urayama, H., Kanamori, T., Kimura, Y., *Properties and biodegradability of polymer blends of poly(L-lactide)s with different optical purity of the lactate units.* Macromolecular materials and engineering, 2002. **287**(2): p. 116.

4.   Urayama, H., Ma, C., Kimura, Y., *Mechanical and thermal properties of poly(L-lactide) incorporating various inorganic fillers with particle and whisker shapes.* Macromolecular materials and engineering, 2003. **288**(7): p. 562.

5.   Garlotta, D., *A literature review of poly(lactic acid).* Journal of polymers and the environment, 2001. **9**(2): p. 63.

6.   Suyatma, N. E., Copinet, A., Tighzert, L., Coma, V., *Mechanical and barrier properties of biodegradable films made from chitosan and poly (lactic acid) blends.* Journal of polymers and the environment, 2004. **12**(1): p. 1.

7.   Ouchi, T., Ichimura, S., Ohya, Y., *Synthesis of branched poly(lactide) using polyglycidol and thermal, mechanical properties of its solution-cast film.* Polymer, 2006. **47**(1): p. 429.

8.   Auras, R. A., Harte, B., Selke, S., Hernandez, R., *Mechanical, physical, and barrier properties of poly(lactide) films.* Journal of plastic film & sheeting, 2003. **19**(2): p. 123.

9.   Luciano, R. M., Zavaglia, C. A. C., Duek, E. A. R., Alberto-Rincon, M. C.., *Synthesis and characterization of poly(L-lactic acid) membranes: Studies in vivo and in vitro.* Journal of materials science. Materials in medicine, 2003. **14**(1): p. 87.

10.   Itoh, E., Matsuda, S., Yamauchi, K., Oka, T., Iwata, H., Yamaoka, Y., Ikada, Y., *Synthetic absorbable film for prevention of air leaks after stapled pulmonary resection.* Journal of biomedical materials research, 2000. **53**(6): p. 640.

11.   Bleach, N. C., Nazhat, S. N., Tanner, K. E., Kellomäki, M., Törmälä, P., *Effect of filler content on mechanical and dynamic mechanical properties of particulate biphasic calcium phosphate - Polylactide composites.* Biomaterials, 2002. **23**(7): p. 1579.

12. Furukawa, T., Matsusue, Y., Yasunaga, T., Shikinami, Y., Okuno, M., Nakamura, T., *Biodegradation behavior of ultra-high-strength hydroxyapatite/poly (L-lactide) composite rods for internal fixation of bone fractures.* Biomaterials, 2000. **21**(9): p. 889.

13. Park, YJ., Nam, K. H., Ha, S. J., Pai, C.M., Chung, C. P., Lee, S. J., *Porous poly(L-lactide) membranes for guided tissue regeneration and controlled drug delivery: Membrane fabrication and characterization.* Journal of controlled release, 1997. **43**(2-3): p. 151.

14. Giardino, R., Fini, M., Aldini, N. N., Giavaresi, G., Rocca, M., *Polylactide bioabsorbable polymers for guided tissue regeneration.* Journal of trauma injury infection and critical care, 1999. **47**(2): p. 303.

15. Lee, S. H., Kim, B. S., Kim, S. H., Kang, S. W., Kim, Y. H., *Thermally produced biodegradable scaffolds for cartilage tissue engineering.* Macromolecular bioscience, 2004. **4**(8): p. 802.

16. Pêgo, A. P., Siebum, B., Van Luyn, M. J. A., Gallego y Van Seijen, X. J., Poot, A. A., Grijpma, D.W., Feijen, J., *Preparation of Degradable Porous Structures Based on 1,3-Trimethylene Carbonate and D,L-Lactide (Co)polymers for Heart Tissue Engineering.* Tissue engineering, 2003. **9**(5): p. 981.

17. Babensee, J.E., Anderson, J. M., McIntire, L. V., Mikos, A. G., *Host response to tissue engineered devices.* Advanced Drug Delivery Reviews, 1998. **33**(1-2): p. 111.

18. Lu, L., Peter, S. J., Lyman, M. D., Lai, H. L., Leite, S. M. A., Tamada, J., Vacanti, J. P., Langer, R., Mikos, A.G., *In vitro degradation of porous poly(L-lactic acid) foams.* Biomaterials, 2000. **21**(15): p. 1595.

19. Griffith, L. G., *Polymeric biomaterials.* Acta Materialia, 2000. **48**(1): p. 263.

20. Gopferich, A., *Mechanisms of polymer degradation and erosion.* Biomaterials, 1996. **17**(2): p. 103.

21. Li, H., Chang, J., *pH-compensation effect of bioactive inorganic fillers on the degradation of PLGA.* Composites Science and Technology, 2005. **65**(14): p. 2226.

22. Bleach, N. C., Tanner, K. E., Kellomäki, M., Törmälä, P., *Effect of filler type on the mechanical properties of self-reinforced polylactide-calcium phosphate composites.* Journal of Materials Science: Materials in Medicine, 2001. **12**(10-12): p. 911.

23. Pluta, M., Paul, M. A., Alexandre, M., Dubois, P., *Plasticized polylactide/clay nanocomposites. II. The effect of aging on structure and properties in relation to the filler content and the nature of its organo-modification.* Journal of Polymer Science Part B: Polymer Physics, 2006. **44**(2): p. 312.

24. Ljungberg, N., Wesslén, B., *Preparation and properties of plasticized poly(lactic acid) films.* Biomacromolecules, 2005. **6**(3): p. 1789.

25. Jacobsen, S., Fritz, H. G., *Plasticizing polylactide - the effect of different plasticizers on the mechanical properties.* Polymer engineering and science, 1999. **39**(7): p. 1303.

26. Martin, O., Avérous, L., *Poly(lactic acid): Plasticization and properties of biodegradable multiphase systems.* Polymer, 2001. **42**(14): p. 6209.

27. Perego, G., Cella, G. D., Bastioli, C., *Effect of molecular weight and crystallinity on poly(lactic acid) mechanical properties.* Journal of applied polymer science, 1996. **59**(1): p. 37.

28. Ogata, N., Jimenez, G., Kawai, H., Ogihara, T., *Structure and thermal/mechanical properties of poly(/-lactide)-clay blend.* Journal of polymer science. Part B, Polymer physics, 1997. **35**(2): p. 389.

29. Kulinski, Z., Piorkowska, E., *Crystallization, structure and properties of plasticized poly(L-lactide).* Polymer, 2005. **46**(23): p. 10290.

30. Zhang, K., Wang, Y., Hillmyer, M. A., Francis, L. F., *Processing and properties of porous poly(L-lactide)/bioactive glass composites.* Biomaterials, 2004. **25**(13): p. 2489.

31. Van De Witte, P., Esselbrugge, H., Dijkstra, P. J., Van Den Berg, J. W. A., Feijen, J., *Phase transitions during membrane formation of polylactides. I. A morphological study of membranes obtained from the system polylactide-chloroform-methanol.* Journal of membrane science, 1996. **113**(2): p. 223.

32. Sawalha, H., Schroën, K., Boom, R., *Polylactide films formed by immersion precipitation: Effects of additives, nonsolvent, and temperature.* Journal of Applied Polymer Science, 2007. **104**(2): p. 959.

33. Ma, G., Nagai, M., Omi, S., *Preparation of uniform poly(lactide) microspheres by employing the Shirasu Porous Glass (SPG) emulsification technique.* Colloids and surfaces. A, Physicochemical and engineering aspects, 1999. **153**(1-3): p. 383.

34. Hu, Y., Grainger, D. W., Winn, S. R., Hollinger, J. O., *Fabrication of poly(α-hydroxy acid) foam scaffolds using multiple solvent systems.* Journal of biomedical materials research, 2002. **59**(3): p. 563.

35.	Tasselli, F., Jansen, J. C., Sidari, F., Drioli, E., *Morphology and transport property control of modified poly(ether ether ketone) (PEEKWC) hollow fiber membranes prepared from PEEKWC/PVP blends: Influence of the relative humidity in the air gap.* Journal of membrane science, 2005. **255**(1-2): p. 13.

36.	Zhang, K., Ma, Y., Francis, L. F., *Porous polymer/bioactive glass composites for soft-to-hard tissue interfaces.* Journal of biomedical materials research, 2002. **61**(4): p. 551.

37.	Jiang, L., Wolcott, M. P., Zhang, J., *Study of biodegradable polylactide/poly(butylene adipate-co-terephthalate) blends.* Biomacromolecules, 2006. **7**(1): p. 199.

38.	Hiljanen-Vainio, M., Karjalainen, T., Seppälä, J., *Biodegradable lactone copolymers. I. Characterization and mechanical behavior of ε-caprolactone and lactide copolymers.* Journal of applied polymer science, 1996. **59**(8): p. 1281.

39.	Kinloch, A. J., Young, R. J., *Fracture behaviour of polymers.* Applied science publisheres: London and Ney York, 1983.

40.	Gibson, J. G., Michael, F. A., *Cellular solids : structure and properties.* Pergamon Press: Oxford, 1988.

41.	Liu, W., Shen, J., Wang, Z., Lu, F., Xu, M., *The deformation mechanism of polyphenylquinoxaline films.* Polymer, 2001. **42**(17): p. 7461.

Chapter 4

Polylactide microspheres prepared by pre-mix membrane emulsification - effects of solvent removal rate*

Abstract

Polylactide microspheres were prepared by pre-mix membrane emulsification and subsequent extraction of solvent in a coagulation bath, and ultimately to the gas phase. The polymer was dissolved in dichloromethane and emulsified with water or water-methanol mixtures by repeated passage through a glass membrane. During and after emulsification, the droplets are exposed to a bath consisting of a mixture of water and methanol. Transfer of dichloromethane takes place into the bath and (subsequently) to the gas phase. Compared to water, the solubility of dichloromethane is increased when using water-methanol mixtures; the continuous phase can quickly dissolve a significant amount of the solvent, while transfer to the gas phase is strongly enhanced as well. This was observed experimentally and by computer simulation, using a combined model based on the Maxwell-Stefan theory for non-ideal, multi-component mass transfer.

With increasing methanol concentration, the size and span of the microspheres became smaller, and was approximately 1 µm at 30% methanol. The surface morphology of these particles was solid and smooth, whereas holes were observed in those prepared in pure water. At methanol concentrations higher than 30%, the size of the microspheres increased again. This is probably due to the swelling of the particles because of the high in-diffusion of methanol which increases the porosity of the particles. Our main conclusion is that particles of defined size and size distribution can be produced by simply adjusting the non-solvent composition of the pre-mix.

Introduction

In the last few decades, microspheres have been extensively prepared and used for different purposes including, chromatography column packings, sensors, coatings, and controlled drug delivery systems [1]. Besides as solid microspheres, also hollow microspheres such as ultrasound contrast agents (UCAs) are of interest. In this paper, the preparation of solid microspheres is investigated as a model system for UCAs. UCAs, used in ultrasound imaging, are gas microbubbles stabilized by a thin (biodegradable) polymer or protein shell [2], that can resonate with ultrasound and reflect the signal, thus yielding much better resolution. The size of UCAs is typically a few micrometers (1-7 µm), comparable to the size of the red blood cells, which allows passage through the fine capillaries and veins in the body [3]. The efficiency of the UCAs is expected to be dependent on their size, size distribution, shell strength and elasticity, *in vivo* persistence, and colloidal stability [4-6]. Amongst others, the conditions of preparation are expected to influence these properties, and how they do so is investigated in this paper. Using non-hollow microspheres as model system allows us to distinguish effects of the primary preparation process from effects caused by post-processing to form the cavity inside the spheres.

Both UCAs and microspheres are produced by emulsification of a solution that contains the biodegradable polymer (e.g., polylactide), in a nonsolvent phase that, optionally, contains a stabilizer. The emulsification is currently done using standard techniques such as sonicators, high-pressure homogenizers, and colloid mills[7, 8]; a few studies report on the use of newer techniques as membrane emulsification [9-11]. In contrast to the standard techniques, membrane emulsification gives much better control over the primary droplet size and hence over the microsphere size [11, 12]. After emulsification, the solvent, which is usually poorly miscible with the nonsolvent, diffuses slowly from the droplets to the nonsolvent, and subsequently, to the nonsolvent bath surface where it evaporates into a gas phase (usually air). Due to the resulting loss of solvent, the polymer solution becomes more concentrated and solidifies into a polymeric particle.

The particle formation process is complicated by coalescence and other disproportionation processes, such as Ostwald ripening. Thus, for control of the size and size distribution of microspheres, factors such as solvent removal time need to be controlled, because it influences the precipitation process of the polymer [13-15]. This is also expected to be a key factor for the properties of UCAs, together with thickness, and mechanical properties of the polymer shell.

In this study, we aim to produce polymer particles with better uniformity in size and shape, by using one of the membrane emulsification techniques, called pre-mix membrane emulsification. The model system investigated here is poly(L)lactic acid, dissolved in dichloromethane (DCM), which is emulsified into a nonsolvent bath, containing a mixture of water and optionally methanol. By varying the ratio between water and methanol, one can vary the extraction rate of DCM, and the microsphere formation time. The relevant time scales during microsphere processing are investigated and optimized in relation to the size and morphology of the microspheres.

Theory (Modelling)

Static system

The solvent extraction rates are important for understanding the particle formation process. We therefore use a model for the mass transfer processes taking place. Although the system comprises four components, we simplify this system to one with three components; DCM, water, and methanol because the initial polymer concentration is very low (around 1% w/w) and its effect on DCM removal is expected to be negligible in the important initial stages of the process.

The process is assumed to be isothermal at 25 $^\circ$C and takes place through three phases (see Figure 1):, the organic phase (modelled as pure DCM), the nonsolvent phase (water or water-methanol mixture), and the gas phase. DCM and methanol are assumed to be the only components that are transported and evaporated during the removal process. Water has a high boiling point compared to the other components, DCM (40 $^\circ$C) and methanol (64.7 $^\circ$C). In addition, it is present in excess, which means that its molar velocity (m·s^{-1}) is very low, even when some

water would evaporate. Its velocity will have no influence on the other velocities in the system and can thus be neglected. The DCM concentration at the organic-nonsolvent interface is assumed equivalent to its saturation concentration in the respective nonsolvent. Further, it is assumed that the diffusion coefficients are independent of the concentration, and the activity coefficients are assumed constant (but not equal to one) during the removal process.

The Maxwell-Stefan (MS) approach is used to describe the diffusive mass transfer during the solvent removal process. The general form of the MS diffusion equation is as follows:

$$\frac{x_j}{D_{ij}}\left(u_i - u_j\right) + \frac{x_k}{D_{ik}}\left(u_i - u_k\right) = -\frac{d\ln a_i}{dz} \tag{1}$$

where x_i is the mole fraction of component i (mol·mol^{-1}), D_{ij} is the Maxwell-Stefan diffusion coefficient between components i and j (m^2·s^{-1}), u is the velocity (ms^{-1}), a is the activity of the component (-), and z is the relevant spatial coordinate (m).
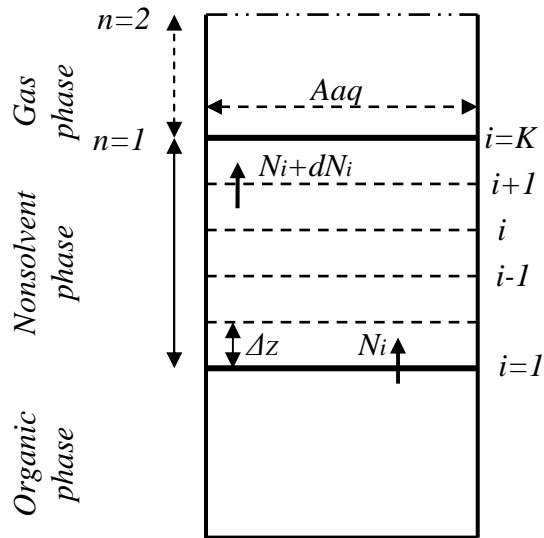
Figure 1: Schematic layout of the model of the solvent removal process. The system is divided into three phases: organic, nonsolvent, and gas phase. Index i represents the number of the layer in the nonsolvent phase (from $i=1$ at the organic-nonsolvent interface to $i=K$ at the nonsolvent-gas interface). Index n represents the number of the layer in the gas phase ($n=1$ at the gas-nonsolvent interface and $n=2$ is ambient air).

Equation 1 can be rewritten such that the mass transfer is expressed in terms of fluxes instead of velocities of the components, as shown in the following equations:

$$N_1 = -\frac{c_t D_{13}}{A}\left((D_{23}x_1 + D_{12}x_3)\frac{dx_1}{dz} + (D_{23}x_1)\cdot\frac{dx_2}{dz} \right) \tag{2}$$

$$N_2 = -\frac{c_t D_{23}}{A}\left(D_{13}x_2\frac{dx_1}{dz} + (D_{13}x_2 + D_{12}x_3)\frac{dx_2}{dz} \right) \tag{3}$$

with $A = x_1 x_3 D_{23} + x_2 x_3 D_{13} + x_3^2 D_{12}$

with N_1 and N_2 the fluxes of components *1* (DCM) and 2 (methanol) in the nonsolvent phase (mol·m^2 ·s^{-1}), and c_t the initial total concentration of nonsolvent phase (mol·m^{-3}) (the detailed derivation of the equations can be found in the appendix). The diffusion equations of the components in the gas phase were derived using the same procedure followed for the nonsolvent phase.

Mass balances

Two mass balance equations were derived for the system; equation 4 is the mass balance for the total organic phase, while equation 5 is the balance for the nonsolvent phase.

$$\frac{dM_{o,i}}{dt} = -N_{o,i}A_o \tag{4}$$

$$\frac{dM_i}{dt} = N_{o,i}A_o - N_{i,evp}A_{aq} \tag{5}$$

In this equation, $M_{o,i}$ is the total amount of component i in the organic phase (M_0) (mol), and M_i is the total amount of component i in the nonsolvent phase (M_i) in time (mol·s^{-1}). $N_{i,evp}$ is the molar flux of i, evaporating from the nonsolvent phase (mol·m^{-2}·s^{-1}) into the air, $N_{o,i}$ is the molar flux of component i from the organic to the nonsolvent phase (mol·m^{-2}·s^{-1}), A_o is the surface area of the organic phase (m^2), and A_{aq} is the surface area of the nonsolvent phase (m^2).

The system is non-stationary, and as the nonsolvent phase is not mixed, there are gradients in the concentrations of DCM and methanol. Thus, we need to solve the continuity equations in space and time:

$$c_t \frac{\partial x_i}{\partial t} = -\frac{\partial N_i}{\partial z} \qquad (6)$$

A standard forward-in-time / centred-in-space (FTCS) differencing scheme is used for solving the partial differential equations. The boundary conditions can be found in the appendix.

Dynamic stirred system

In order to evaluate the mass transfer phenomena in more detail than the static system allows, also a dynamic system is set-up. The system described here consists of DCM droplets of uniform size that are homogenously distributed in a well-mixed nonsolvent, which closely resembles the system during production of the microspheres. Here, we only focus on the extraction of the solvent from the droplets into the nonsolvent bulk, as it is the most important stage in the process that determines the solidification of the polymer. The general mass transfer and mass balance equations that govern this system are the same as the ones described for the static system, and only two parameters should be adjusted. The first one is the exchange area available for mass transfer; i.e. the interfacial area of the droplets, while the second one is the thickness of the boundary layer around the droplets in the well-mixed bulk. The boundary layer can be calculated as follows:

$$\delta = d/Sh \qquad (7)$$

where δ is the thickness of the boundary layer around the droplet (m) d is the diameter of the droplet (m) and Sh is the Sherwood number (-), which is in this case equal to 2 (for small droplets having negligible velocity relative to the surrounding fluid) [16].

Parameters

The parameters required for the model, such as diffusion coefficients, saturation concentrations (maximum solubility), and activity coefficients of the components were taken or calculated from literature, or measured experimentally. All the diffusion coefficients are summarized in Table 1.

Table 1: Reported and calculated diffusion coefficients of components in the system ($m^2 \cdot s^{-1}$)

Diffusivity ($m^2 \cdot s^{-1}$)	DCM in water	methanol in water	DCM in methanol
Literature	$1.57 \cdot 10^{-9}$ [17] [a]	$(1.62-2.1) \cdot 10^{-9}$ [18] [b]	*ND*
Calculated at 25°C, Eq (8)	$1.285 \cdot 10^{-9}$	$1.887 \cdot 10^{-9}$	$2.1 \cdot 10^{-9}$

	DCM in air	methanol in air	DCM in methanol vapour
Literature	$1.04 \cdot 10^{-5}$ [19]	$1.67 \cdot 10^{-5}$ [19]	*ND*
Calculated at 25°C, Eq (10)	$1.227 \cdot 10^{-5}$	$1.73 \cdot 10^{-5}$	$1.045 \cdot 10^{-5}$

[a] *reported at 30 ° C,* [b] *reported at the range of 30-40 ^{0}C.*

Diffusion coefficients

To calculate the binary Maxwell-Stefan diffusivity in a multi-component mixture, the following equation from Taylor and Krishna was used [20]:

$$D_{ij} = D_{ij}^{0\frac{1+x_j-x_i}{2}} D_{ji}^{0\frac{1+x_i-x_j}{2}} \tag{8}$$

where D_{ij} is the Maxwell-Stefan diffusivity ($m^2 \cdot s^{-1}$) and D^o_{ij} is the diffusivity at infinite dilution ($m^2 \cdot s^{-1}$), which can be calculated with the Stokes-Einstein equation:

$$D_{ij}^0 = \frac{k_b T}{6\pi\mu_j r_j} \tag{9}$$

where k_b is Boltzmann's constant ($J \cdot K^{-1}$), T is the temperature (K), μ_j is the viscosity of the nonsolvent (Pa·s), and r_i is the radius of the diffusing component (m). The radii of the diffusing components were estimated by using a reverse calculation of known diffusivity values using equation (9).

For diffusion coefficients of components in the gas phase, the equation from Wesselingh and Krishna was used [21]:

$$D_{ij} = K_x \cdot \frac{T^{1.75}}{P\left(v_i^{1/3} + v_j^{1/3}\right)^2} \left(\frac{1}{M_i} + \frac{1}{M_j}\right)^{1/2}$$

(10)

K_x is a constant with a value of ($3.16 \cdot 10^{-8}$ $K^{-1.75} \cdot kg^{1.5} \cdot m^3 \cdot s^{-3} \cdot mol^{-7/6}$), T is the temperature (K), P is the pressure (Pa), v is the molar (diffusion) volume of a component in the gas phase ($m^3 \cdot mol^{-1}$), and M is the molecular weight of the component ($kg \cdot mol^{-1}$).

Activity coefficients

For the calculation of the activity coefficients of components in our system, the following ternary Bonham equations were used [22]:

$$T \ln \gamma_k = \frac{\left[\sum x_i A_{ij} B_{ki}^{0.5}\right]^2}{\left[\sum (x_i A_{ij})\right]^2} \quad \text{with} \quad A_{12} = \frac{b_1}{b_2}, \quad A_{21} = \frac{b_2}{b_1}$$

(11)

$$\sqrt{B_{12}} = \sqrt{\frac{b_1}{R}}\left(\frac{\sqrt{c_1}}{b_1} - \frac{\sqrt{c_2}}{b_2}\right), \quad \sqrt{B_{21}} = \sqrt{\frac{b_2}{R}}\left(\frac{\sqrt{c_2}}{b_2} - \frac{\sqrt{c_1}}{b_1}\right)$$

(12)

$$c = \frac{27 R^2 T_c^2}{64 P_c}, \quad b = \frac{R T_c}{8 P_c}$$

(13)

where k indicates the investigated component, index i represents components 1 to n, j is the reference component, A & B are derived from van der Waals constants, T_c is the critical temperature (K), and P_c is the critical pressure of the corresponding component (Pa).

Saturation concentration

The data available in the literature about the saturation concentration (maximum solubility) of DCM in water-methanol mixtures is very limited; therefore theses values were measured experimentally using Gas Chromatography (GC: see materials and methods section).

Experimental

Materials

In this study, poly (L-lactide) (PLLA) with an intrinsic viscosity of 1.21 dl·g^{-1} from PURAC (Biochem B.V., Gorinchem, the Netherlands) was used. As a solvent for the polymer, Dichloromethane (DCM), (HPLC, gradient grade) from Merck was taken. As a nonsolvent, Milli-Q water with Methanol (HPLC, gradient grade, ≥99.9%) (Aldrich) was applied. As a stabiliser, poly-(vinylalcohol) (PVA 23/88) from Ter Hell, Hamburg, Germany was used. All chemicals were used as received.

Methods

Gas Chromatography (GC)

To measure the concentration of DCM in different water-methanol mixtures, a Hewlett Packard 6890 Series gas chromatograph equipped with a 30-m x 0.32-mm x 1 µm capillary column, Chrompac 8762 CP Sil 19CB, with back injector (split ratio of 200:1) and flame ionization detector was used. The temperature program was initially set to 100 $^{\circ}$C and increased linearly to 160 $^{\circ}$C in seven min. Helium was used as carrier gas at a flow rate of 367.6 mL·min^{-1}. To obtain the actual concentration of the components, calibration curves were used.

Saturation concentration (solubility) measurement

The saturation concentration of DCM (solvent) was measured using the liquid-liquid equilibrium method, adapted from the method described by Peschke *et al* [23]. Mixtures of DCM and nonsolvent phase, which consists of different water-methanol mixtures, were prepared in equilibration cells. The DCM-nonsolvent phase mixtures were shaken well, and then placed in a water bath that was maintained at a temperature of 25 $^{\circ}$C for about 24 hours. Samples from the nonsolvent phase (top), and the DCM phase (bottom) were collected and analysed by GC. The DCM-nonsolvent ratio was kept constant at 1:1 (v/v) at a total volume of 15 ml. The following water-methanol mixtures were used: 1:0, 2:1, 1:1, and, 1:2 (v/v).

Validation experiment

For validation of the model, mixtures of DCM-nonsolvent phase (at constant ratio of 1:1 (v/v)) were prepared in 10 mL (± 0.1 mL) graduated cylinders. As

nonsolvent phase, water, and 1:1 (v/v) water-methanol were used (in triplicate). The cylinders were placed in a water bath at constant temperature of 25 °C. The total weight and volume of each sample were measured at different times and the concentration of the components in each phase was measured by GC. To validate the assumptions used in the model, weight and volume of control samples that consisted only of the continuous phase i.e. pure water, pure methanol, and water-methanol mixtures were also measured.

Preparation of PLA microspheres

PLLA was first dissolved in DCM to prepare a stock solution of 10% (w/w). An aqueous solution of PVA (1%) was used as another stock solution. To prepare a pre-emulsion, 0.5 g of the polymer solution, and 1.15 g DCM were added to 11 g of nonsolvent that consisted of 8 g of different methanol-water mixtures and 3 g of the PVA solution. In the nonsolvent phase, the following concentrations of methanol were used: 10%, 20%, 30%, 40%, 45%, and 50% w/w (nonsolvent). The polymer and nonsolvent solutions were mixed for about 1 min in a closed vessel, using a magnetic stirrer at approximately 1000 rpm. This emulsion will be called the premix from now on. This premix was homogenized (in an open system) by passing it through a 1-µm glass filter (Acrodisc GF syringe filter, glass fibre, Sigma-Aldrich) manually. This process was repeated 11 times to ensure droplet monodispersity as much as possible. The emulsion with the microspheres was then left for about 1 h under gentle stirring in order to evaporate DCM, after which PLLA microspheres were obtained. The microspheres were subsequently repeatedly washed and centrifuged three times at a centrifugation speed of 3000 RCF. Each of the three centrifugation-steps was for 20 min; in between, the spheres were washed with water in order to remove PVA. After that, the microspheres were freeze-dried using a Christ Epsilon 2-6D freeze dryer (Salm and Kipp, the Netherlands). The freeze drying program was initially set at -20 °C and 1.03 mbar for about 4hr and then 9 hr at -5 °C and the final drying step was conducted at 20 °C and 0.001 mbar for 12 hr.

Characterization of PLA microspheres

The size and size distribution of the microspheres were measured after evaporation of the solvent using laser light scattering (Malvern Mastersizer 2000, Malvern

Instruments Ltd., Worcestershire, United Kingdom) which allows detection of particles in a diameter range of 0.01-1000 µm. The average particle size was expressed as the volume-weighted mean diameter, $d_{4,3}$. The morphology of the freeze-dried microspheres was visualized by scanning electron microscopy (SEM) (JEOL 6300F, Tokyo, Japan).

Results and discussion

Solubility of DCM

The solubility of DCM in the nonsolvent bath is an important parameter, since it determines the initial rate of extraction of DCM. Its values in the methanol-water mixtures are unfortunately unknown. Therefore, the solubility was measured by GC; the results are shown in Figure 2a. Concentrations of methanol > 70% were not considered because it is known from experimental studies that no microspheres can be obtained at these concentrations.

The solubility of DCM increases with increasing methanol concentration. DCM is only slightly miscible with pure water, and this capacity increases rapidly by addition of methanol to the water, as DCM is fully miscible with methanol. From Figure 2b, it is clear that the concentration of methanol in the aqueous phase was always higher than that in the DCM phase.

Validation of the model

Evaporation of water was not included in the model; therefore, this effect had to be compensated for. Evaporation fluxes from water and water methanol mixtures were measured experimentally and calculated with a simple model (see appendix). The calculated water fluxes agreed well with the measured values ($5.1 \cdot 10^{-7}$ g·s^{-1} for the simulation and $5.7 \cdot 10^{-7}$ g·s^{-1} for the experiment). The actual model was validated by measuring the total mass reduction in systems consisting of DCM and water or DCM and a 1:1 (v/v) methanol water mixture, and comparing those values with the model predictions. Without taking the water evaporation flux into account the model underestimates the measured values, however with the measured water evaporation flux, the model predictions are adequate (see Figures 3a and b).
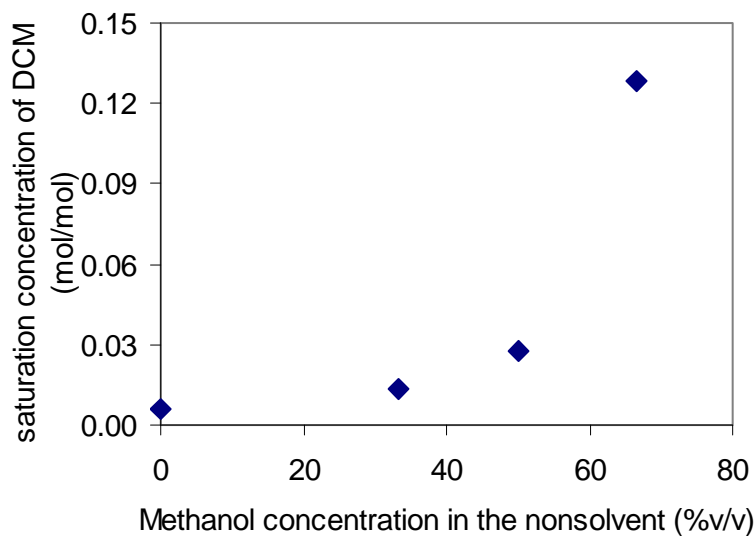
Figure 2a: Saturation concentration of DCM in different water-methanol mixtures.
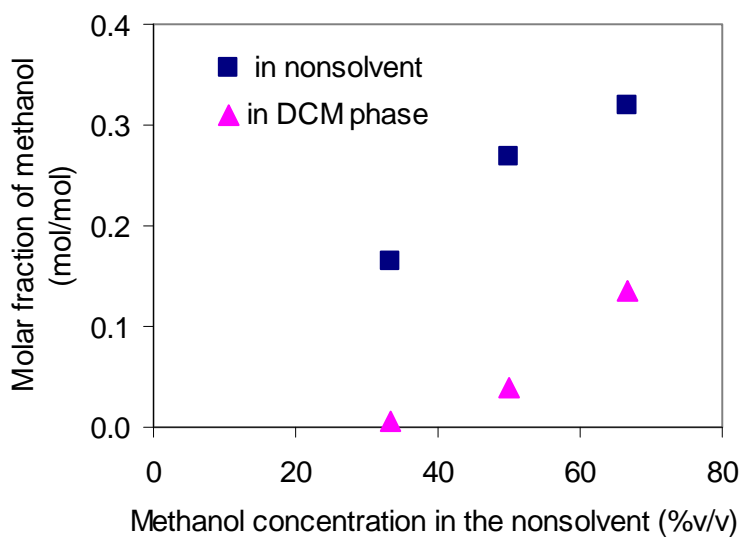
Figure 2b: Equilibrium concentration of methanol in the nonsolvent and DCM phases for different methanol-water mixtures.
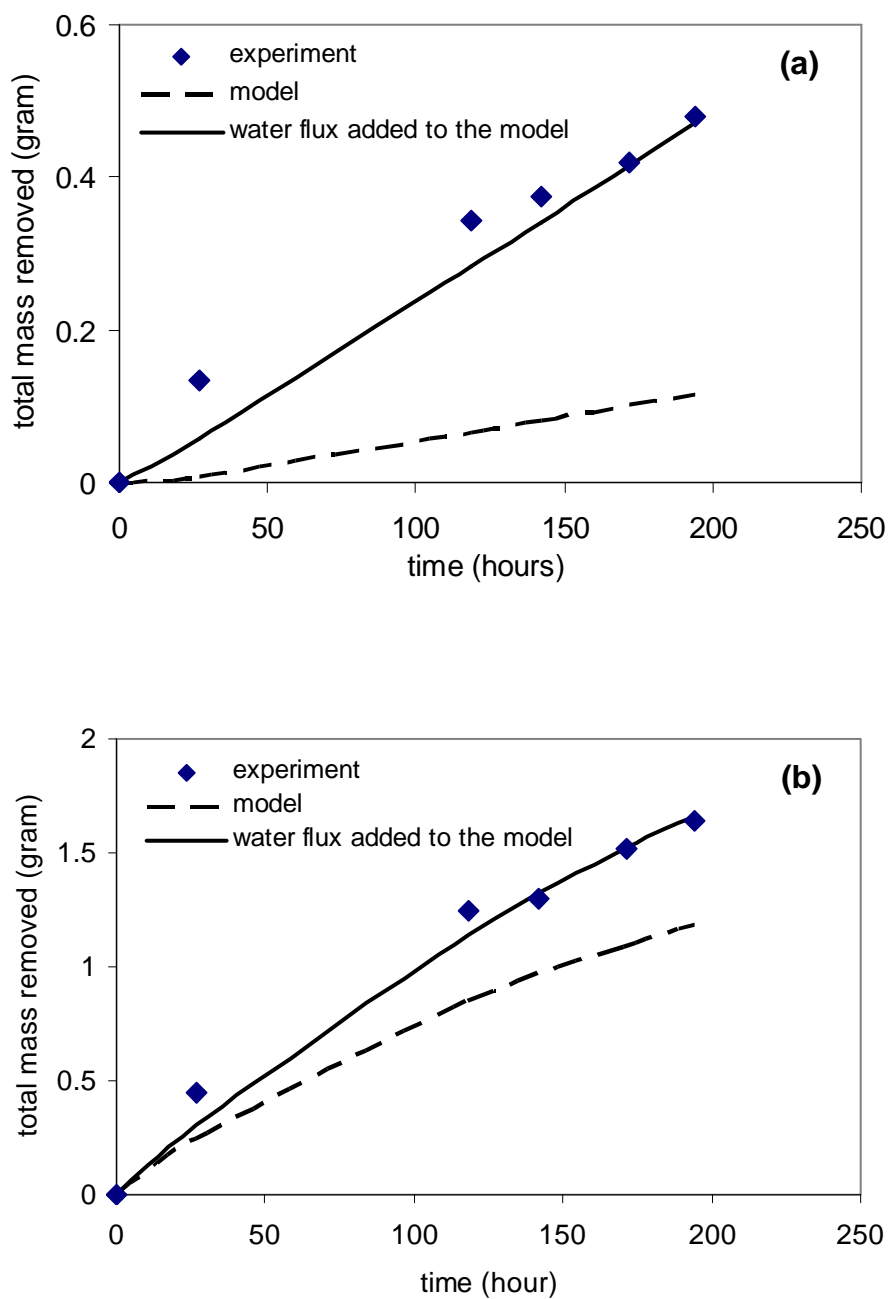
Figure 3: Total mass of components removed using: a) water, b) 1:1 (v:v) methanol:water as nonsolvent. The initial volume of the components in the experiments and simulations was: 3.1 ml DCM and 3 ml of different methanol-water mixtures.

Simulation results-static system

To investigate the overall removal rate of DCM, simulations were performed with the static model system for different water-methanol mixtures. Both the total amount of DCM extracted to the nonsolvent (amount lost from the DCM phase), and the amount evaporated to the gas phase were calculated for different methanol compositions in the nonsolvent; the results are shown in figure 4. When water was used as nonsolvent, only small amounts of DCM were extracted, whereas these amounts strongly increased with increasing methanol concentration in the nonsolvent: the total rate of removal of DCM is increased by a factor of about 15, when going from 0 to 67 % methanol. This is ascribed to the solubility increase of DCM in water methanol mixtures as described previously in Figure 2ab. As a result of the higher DCM concentrations in water methanol mixtures, the driving force for evaporation of DCM to the gas phase also increases as is reflected in the amount of evaporated DCM after 194 hours (see Figure 4; the time is the same as in the validation experiment).
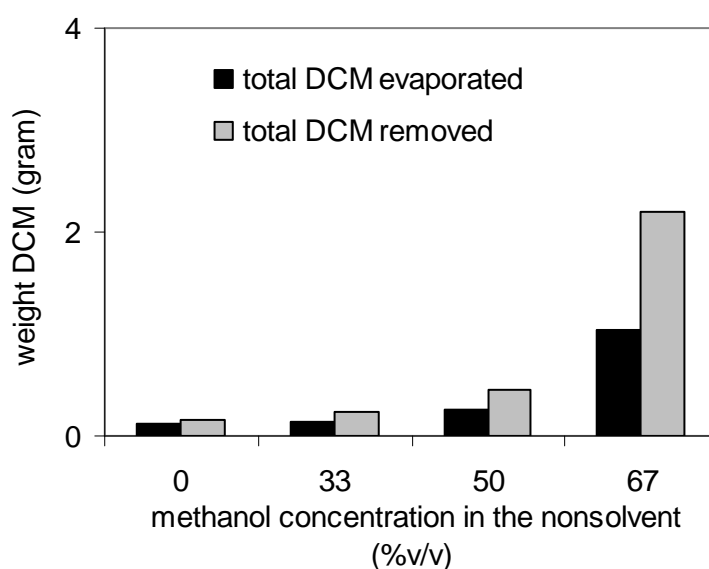
Figure 4: Total DCM weight dissolved in the nonsolvent phase (lost from DCM phase) and total amount evaporated in 194 hours using various methanol concentrations. The initial volume of the components in the simulation was: 3.1 ml DCM and 3 ml of different methanol-water mixtures.

To investigate the DCM removal process in more detail, concentration profiles of DCM as a function of the position in the nonsolvent phase were evaluated. Figure 5 shows that the highest concentration, which was equivalent to the saturation concentration in the nonsolvent used, was obviously found in the DCM-continuous interface (layer *1* in Figure 1) and the concentration gradually decreases with increasing distance away from the DCM interface to reach a minimum at the nonsolvent bath – gas phase interface (layer *k*). These differences in concentration indicate that the evaporation of DCM to the gas phase is considerably faster than its diffusion across the nonsolvent.
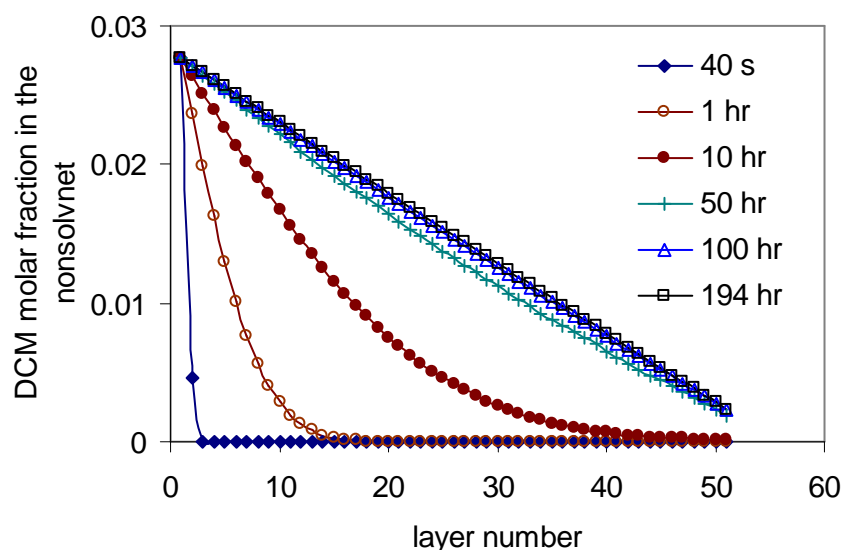
Figure 5: Concentration profiles of DCM at different times as a function of layer position across the nonsolvent phase (simulation data of 1:1 (v:v) methanol:water system). The nonsolvent was divided into 51 layers, where layer 1 is the DCM-continuous phase interface (layer *1* in Figure 1), and layer 51 is the continuous-gas phase interface (layer *k* in Figure 1).

Mass transfer resistance analysis

The mass transfer resistances in the system were analysed. In Table 2, a comparison of mass transfer resistances in the nonsolvent and the gas phase are presented for two nonsolvents: pure water and 1:1 (v/v) methanol-water. The transfer resistance in the nonsolvent phase is the dominant resistance in the system; it is inversely proportional to the diffusion coefficient of the component which is in general lower in liquids than in gases (see Table 1). The results show also that the

resistance in the liquid phase was similar for both nonsolvent baths, whereas in the gas phase, the resistance for 1:1 (v/v) methanol-water is markedly higher than for water. This can be explained as follows. The transfer resistance in the gas phase is inversely proportional to the partition coefficient (ratio of concentration in gas and in liquid), and since the DCM concentration in 1:1 (v/v) methanol-water is higher than in water, the partition coefficient of DCM in water methanol mixture is lower than in water, and consequently the transfer resistance is higher.

Table 2: Transfer resistance values ($s·m^{-1}$) in the nonsolvent and gas phase for water and 1:1 (v/v) methanol:water

Transfer resistance ($s.m^{-1}$)	Liquid	Gas
water	$2.3·10^7$	$0.1·10^6$
1:1 (v/v) methanol-water	$2.3·10^7$	$3.8·10^6$

From the previous analysis, it is clear that improving mass transfer in the liquid phase is the main issue when faster production of microspheres is required. In practice, this can be achieved by inducing convection (i.e., stirring), which was investigated with experiments and simulations.

Simulation results-stirred system

The extraction rate of DCM from uniform DCM droplets in a well-mixed nonsolvent bulk was investigated (without including evaporation to the gas phase in the analysis). Figure 6 shows the simulation results of the total mass of DCM extracted to the different nonsolvent baths as a function of time, and it is obvious that the extraction of DCM proceeds very fast compared to the system without stirring; saturation was reached in a few seconds. This can be attributed to the huge interfacial area between the droplets and the well-mixed nonsolvent bulk. In addition to that, the boundary layer around droplets is very small compared to the system without stirring, which also leads to faster extraction. The high extraction rate of the solvent in this system compared to the static system might suggest that the mass transfer resistance at the droplets nonsolvent bulk interface is not the

dominant resistance in the system, and the resistance at the gas-liquid interface could become the rate limiting one. The removal profile is therewith changed into a very fast primary extraction, and slower secondary evaporation. The evaporation is much faster than without stirring, since the rate-limiting step (diffusion through the nonsolvent bath) has been removed.

From the previous sections we can conclude that addition of methanol can facilitate the initial removal of DCM from the droplets, and this could be an interesting lead for the production of particles. The production process can be speeded up considerably, and perhaps more importantly, the particles are expected to become firmer earlier in the process, therewith making them less susceptible to deformation, coalescence, and other disproportionation processes later.
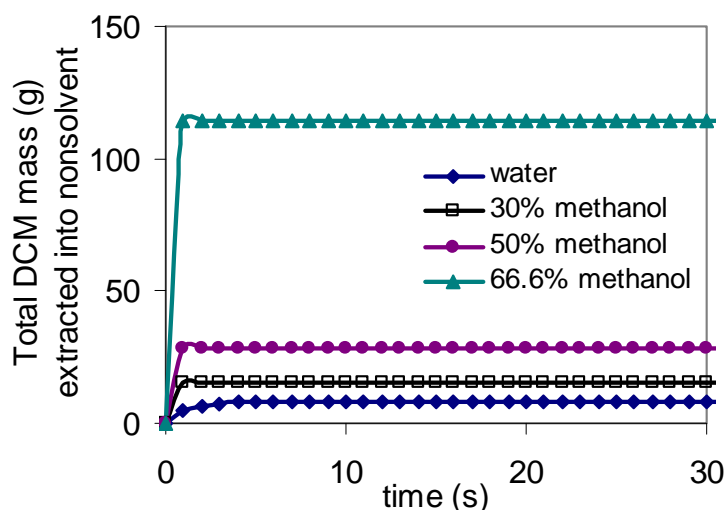
Figure 6: Total DCM weight extracted from DCM droplets into the nonsolvent phase (without evaporation) as a function of time for different methanol-water mixtures (v/v) as nonsolvent. The initial volume of the components in the simulation was: 150 ml DCM and 300 ml of different methanol-water mixtures.

Effect of nonsolvent on properties of PLA microspheres

The effect of the nonsolvent composition on the properties of the final PLLA microspheres (i.e. size, size distribution, and morphology) was investigated. The microspheres were prepared in different methanol/water mixtures; the obtained size distributions are shown in Figure 7. The type of nonsolvent used has a strong effect

on the size and size distribution of the microspheres. With increasing methanol concentration, the size of the microspheres decreases and the size distribution gets sharper. However, at 30% methanol, a minimum of 1 µm is reached. Increasing the methanol concentration further (i.e. > 30%) leads to an increase in the size of the microspheres. At a methanol concentration of 50% and higher, no microspheres could be formed anymore.

These results are explained as follows: the presence of methanol lowers the interfacial tension and, consequently, the droplets are more easily broken down to smaller ones [24, 25] as is demonstrated for particles prepared with 5-30% methanol. Together with this, the presence of methanol leads to faster precipitation of the polymer, which preserves the size and size distribution of droplets better. In water, the precipitation process takes longer, since the DCM evaporation takes a considerable time, therewith possibly allowing undesired effects, such as Ostwald ripening and coalescence of the droplets. However, when the methanol concentration exceeds a certain limit (i.e. > 30%), the droplets become bigger again. Possibly, at these concentrations, a significant amount of methanol diffuses into the spheres, swelling them, and perhaps leading to particles with higher porosity and thus bigger size. For methanol concentrations >50%, a film-like material is formed instead of microspheres. It might be that the methanol/water/DCM becomes completely miscible, and PLLA simply precipitates out, being incompatible with the new single-phase bath. Another explanation could be that the interfacial tension of the systems becomes very low at a certain methanol concentration, therewith preventing PVA stabilisation of the particles.

SEM images of the microspheres prepared in 30% methanol and water are shown in Figure 8. The SEM images confirmed the size distribution results; microspheres prepared in water were bigger and had a broader size distribution compared to those prepared with 30% methanol. Further, the surface morphology of the microspheres was influenced by the nonsolvent. A solid and smooth surface was obtained when the microspheres were prepared in 30% methanol (Figure 8a), whereas holes were observed in the surface of the microsphere prepared in water (Figure 8b). The optimum concentration of methanol seems to be 30%. The

interfacial tension is low enough to allow production of small and monodisperse particles, while DCM removal is fast enough to conserve the shape of the particles.
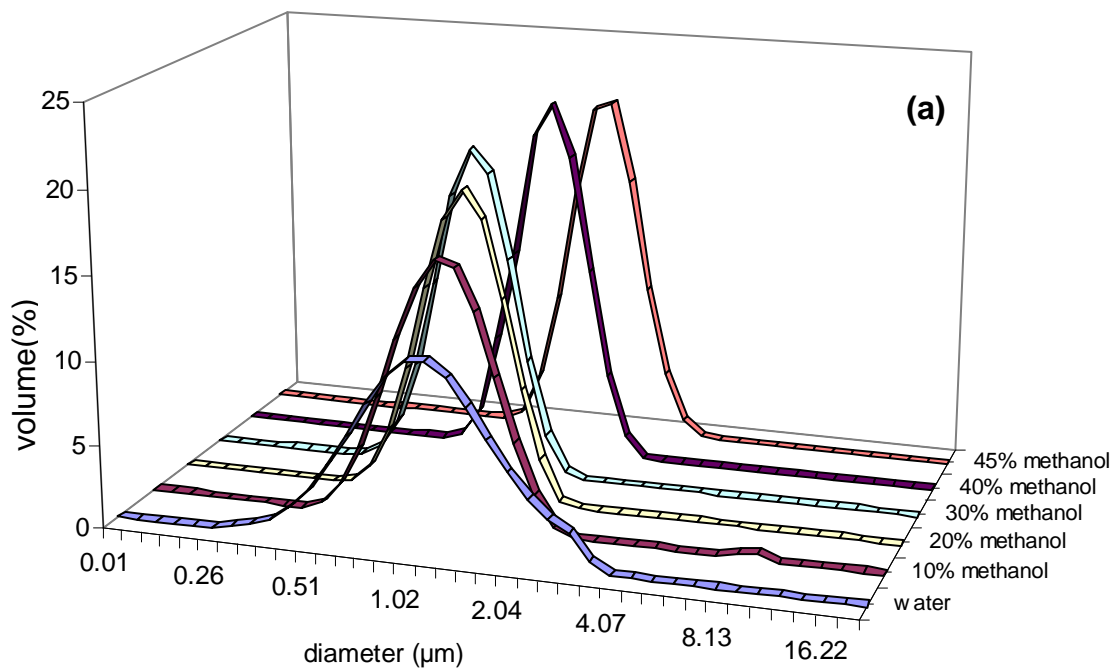
Figure 7a: Particle size distribution of PLLA microspheres prepared with water-methanol mixtures as nonsolvents.
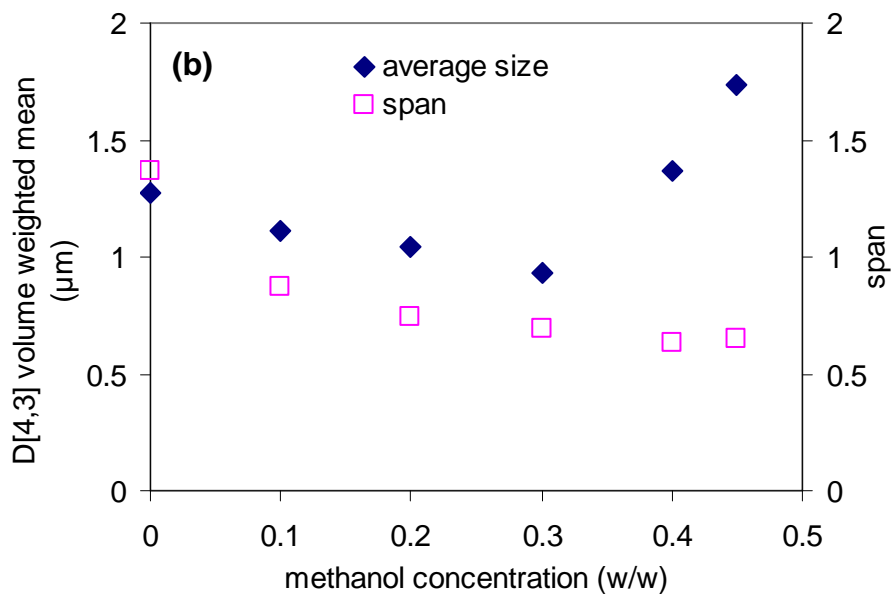
Figure 7b: Average particle size and span of PLLA microspheres prepared with different water-methanol mixtures as nonsolvents.
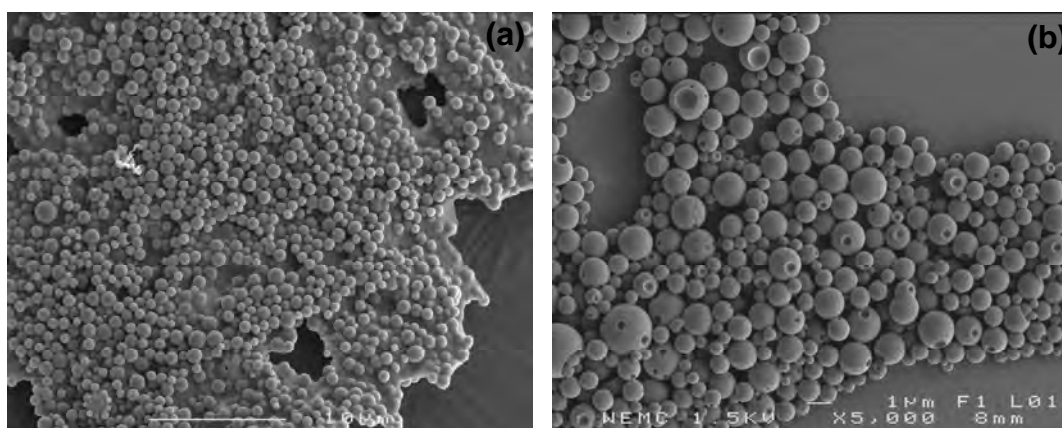
Figure 8: SEM images of PLLA microspheres prepared in different nonsolvents: a) 30% (w/w) methanol, b) water.

Conclusions

Poly(L)lactic acid (PLLA) microspheres were successfully prepared by premix membrane emulsification of a PLA/dichloromethane solution in baths with varying ratios of water and methanol. Addition of methanol to the bath gave smaller, more monodisperse microspheres; at 30% methanol the microsphere size was around 1 µm with a span of 0.7. At higher methanol concentrations, the microsphere size increased again.

This effect is due to an acceleration of solvent removal, by much stronger extraction into the nonsolvent bath when methanol is present, as could be illustrated with the help of a model for multi-component mass transfer. In addition, emulsification was easier (less force was needed to push the emulsion through the membrane) at intermediate methanol concentrations due to lower interfacial tension. When the methanol concentration is too high, the in-diffusion of methanol into the spheres increases, which probably increases the swelling and the porosity of the spheres; thus the particle size increased for methanol concentrations > 30%.

Our main conclusion is that small particles of defined size and size distribution can be produced by adjusting the nonsolvent bath composition of the pre-mix used for membrane emulsification. This finding is relevant for the preparation of solid microspheres and of ultrasound contrast agents (hollow microspheres).

Acknowledgements

List of Symbols

x : mole fraction [mol·mol^{-1}]

D : Maxwell-Stefan diffusion coefficient [m^2·s^{-1}]

u : velocity [ms^{-1}]

a : activity [-]

z : relevant spatial coordinate [m]

N : molar flux [mol·m^2 ·s^{-1}]

c_t : initial total concentration of nonsolvent phase [mol·m^{-3}]

M_o : total amount of organic phase [mol]

M_i : total amount of nonsolvent phase in time [mol·s^{-1}]

A_o : surface area [m^2]

δ : thickness of the boundary layer around the droplet [m]

d : diameter of the droplet [m]

Sh : Sherwood number [-]

D^o : diffusivity at infinite dilution [m^2·s^{-1}]

k_b : Boltzmann's constant [J·K^{-1}]

T : temperature [K]

μ : viscosity [Pa·s^{-1}]

r : radius of diffusing component [m]

K_x : constant [3.16·10^{-8} K$^{-1.75}$·kg$^{1.5}$·m^3·s^{-3}·mol$^{-7/6}$]

P : pressure [Pa]

ν : molar (diffusion) volume of a component in the gas phase [$m^3 \cdot mol^{-1}$]

M : molecular weight of the component [$kg \cdot mol^{-1}$]

A : constant

B : constant

T_c : critical temperature [K]

P_c : critical pressure [Pa].

References

1.   Ravi Kumar, M. N., *Nano and microparticles as controlled drug delivery devices.* Journal of pharmacy & pharmaceutical sciences, 2000. **3**(2): p. 234.

2.   Dayton, P.A., Chomas, J.E., Lum, A.F.H., Allen, J.S., Lindner, J.R., Simon, S.I., Ferrara, K.W., *Optical and acoustical dynamics of microbubble contrast agents inside neutrophils.* Biophysical journal, 2001. **80**(3): p. 1547.

3.   Schutt, E.G., Klein, D.H., Mattrey, R.M., Riess, J.G., *Injectable microbubbles as contrast agents for diagnostic ultrasound imaging: The key role of perfluorochemicals.* Angewandte Chemie (International ed.), 2003. **42**(28): p. 3218.

4.   Bloch, S.H., Short, R.E., Ferrara, K.W., Wisner, E.R., *The effect of size on the acoustic response of polymer-shelled contrast agents.* Ultrasound in medicine & biology, 2005. **31**(3): p. 439.

5.   De Jong, N., Bouakaz, A., Frinking, P., *Basic acoustic properties of microbubbles.* Echocardiography, 2002. **19**(3): p. 229.

6.   Wang, S.H., Chang, P.H., Shung, K.K., Levene, H.B., *Some considerations on the measurements of mean frequency shift and integrated backscatter following administration of Albunex®.* Ultrasound in medicine & biology, 1996. **22**(4): p. 441.

7.   Feinstein, S.B., Keller, M.W., Kerber, R.E., Vandenberg, B., Hoyte, J., Kutruff, C., Bingle, J., Welsh, A.H., *Sonicated echocardiographic contrast agents: reproducibility studies.* Journal of the American Society of Echocardiography, 1989. **2**(2): p. 125.

8.   Winkelmann, J.W., Kenner, M.D., Dave, R., Chandwaney, R.H., Feinstein, S.B., *Contrast echocardiography.* Ultrasound in Medicine & Biology, 1994. **20**(6): p. 507.

9.   Ma, G., Nagai, M., Omi, S., *Preparation of uniform poly(lactide) microspheres by employing the Shirasu Porous Glass (SPG) emulsification technique.* Colloids and surfaces. A, Physicochemical and engineering aspects, 1999. **153**(1-3): p. 383.

10.   Sabhapondit, A., Sarmah, A., Borthakur, A., Haque, I., *Study of the preparation and mechanism of formation of hollow monodisperse polystyrene microspheres by SPG (Shirasu Porous Glass) emulsification technique.* Journal of applied polymer science, 2002. **85**(7): p. 1530.

11. Vladisavljević, G.T., Williams, R.A., *Recent developments in manufacturing emulsions and particulate products using membranes.* Advances in colloid and interface science, 2005. **113**(1): p. 1.

12. Liu, R., Ma, G., Meng, F.-T., Su, Z.-G., *Preparation of uniform-sized PLA microcapsules by combining Shirasu Porous Glass membrane emulsification technique and multiple emulsion-solvent evaporation method.* Journal of Controlled Release, 2005. **103**(1): p. 31.

13. Van de Witte, P., Dijkstra, P. J., Van den Berg, J. W. A., Feijen, J., *Phase separation processes in polymer solutions in relation to membrane formation.* Journal of Membrane Science, 1996. **117**(1-2): p. 1.

14. Sawalha, H., Schroën, K., Boom, R., *Polylactide films formed by immersion precipitation: Effects of additives, nonsolvent, and temperature.* Journal of Applied Polymer Science, 2007. **104**(2): p. 959.

15. Sawalha, H., Schroën, K., Boom, R., *mechanical properties and porosity of polylactide for biomedical applications.* Journal of applied polymer science, 2008. **107**(1): p. 82.

16. Perry, R.H., Green, D.W. *Perry's chemical engineers' handbook*, McGraw-Hill 1999, New York, USA 1997 pp. 5-65.

17. Hartmans, S., Tramper, J., *Dichloromethane removal from waste gases with a trickle-bed bioreactor.* Bioprocess engineering, 1991. **6**(3): p. 83.

18. Lee, Y.E., Li, S.F.Y., *Binary diffusion coefficients of the methanol/water system in the temperature range 30-40 °C.* Journal of chemical and engineering data, 1991. **36**(2): p. 240.

19. Reid, R.C., Prausnitz J.M., Poling B.E., *The properties of gases and liquids*, McGraw-Hill, Inc., New York, 1987.

20. Taylor, R., Khrisna,R. *Multicomponent Mass Transfer*, John Wiley & Sons, Inc., New York, 1993.

21. Wesselingh, J.A., Khrisna, R., *Mass Transfer in Multicomponent Mixtures*, Delft University Press, Delft, 2000.

22. Van Winkle, M.Y.E., *Distillation*, McGraw-Hill, Inc., New York, 1967.

23. Peschke, N., Sandler, S.I., *Liquid-liquid equilibria of fuel oxygenate + water + hydrocarbon mixtures. 1.* Journal of chemical and engineering data, 1995. **40**(1): p. 315.

24.   Vladisavljević, G.T., Shimizu, M., Nakashima, T. , *Production of multiple emulsions for drug delivery systems by repeated SPG membrane homogenization: Influence of mean pore size, interfacial tension and continuous phase viscosity.* Journal of membrane science, 2006. **284**(1-2): p. 373.

25.   Van Der Graaf, S., Steegmans, M.L.J., Van Der Sman, R.G.M., Schroën, C.G.P.H., Boom, R.M., *Droplet formation in a T-shaped microchannel junction: A model system for membrane emulsification.* Colloids and Surfaces A: Physicochemical and Engineering Aspects, 2005. **266**(1-3): p. 106.

Appendices

Derivation of the diffusion equations using Maxwell Stefan relationships

The general Maxwell Stefan equations for DCM (1) and Methanol (2) relative to water (3) are given by:

$$\begin{cases} \dfrac{x_2}{D_{12}}(u_1 - u_2) + \dfrac{x_3}{D_{13}}(u_1 - u_3) = -\dfrac{d\ln a_1}{dz} \\[3mm] \dfrac{x_1}{D_{12}}(u_2 - u_1) + \dfrac{x_3}{D_{23}}(u_2 - u_3) = -\dfrac{d\ln a_2}{dz} \end{cases} \tag{1a}$$

By taking γ_i constant, one can see that

$$\frac{d\ln a_i}{dz} = \frac{d\ln \gamma_i x_i}{dz} = \frac{1}{\gamma_i x_i}\frac{d\gamma_i x_i}{dz} = \frac{1}{x_i}\frac{dx_i}{dz} \tag{2a}$$

The bootstrap relation used here is $u_3 = 0$, enabling us to obtain the velocities compared to the laboratory fixed frame of reference. Equations (1a) and (2a) can be combined in:

$$\begin{cases} \left(\dfrac{x_2}{D_{12}} + \dfrac{x_3}{D_{13}}\right)u_1 - \dfrac{x_2}{D_{12}}u_2 = -\dfrac{1}{x_1}\dfrac{dx_1}{dz} \\[3mm] \left(\dfrac{x_1}{D_{12}} + \dfrac{x_3}{D_{23}}\right)u_2 - \dfrac{x_1}{D_{12}}u_1 = -\dfrac{1}{x_2}\dfrac{dx_2}{dz} \end{cases} \text{ or } \begin{cases} \left(\dfrac{x_2}{D_{12}} + \dfrac{x_3}{D_{13}}\right)x_1 u_1 - \dfrac{x_1 x_2}{D_{12}}u_2 = -\dfrac{dx_1}{dz} \\[3mm] \left(\dfrac{x_1}{D_{12}} + \dfrac{x_3}{D_{23}}\right)x_2 u_2 - \dfrac{x_1 x_2}{D_{12}}u_1 = -\dfrac{dx_2}{dz} \end{cases} \tag{3a}$$

This can be expressed as

$$\bar{B}\bar{u} = \bar{X} \text{ with } \bar{B} = \begin{bmatrix} \dfrac{x_1 x_2}{D_{12}} + \dfrac{x_1 x_3}{D_{13}} & -\dfrac{x_1 x_2}{D_{12}} \\[3mm] -\dfrac{x_1 x_2}{D_{12}} & \dfrac{x_1 x_2}{D_{12}} + \dfrac{x_2 x_3}{D_{23}} \end{bmatrix}; \quad \bar{u} = \begin{pmatrix} u_1 \\ u_2 \end{pmatrix}; \quad \bar{X} = \begin{pmatrix} -\dfrac{dx_1}{dz} \\[3mm] -\dfrac{dx_2}{dz} \end{pmatrix} \tag{4a}$$

By inversion of matrix B we can obtain the relations that are explicit in the velocities:

$$\bar{u} = \bar{L}\bar{X} = \bar{B}^{-1}\bar{X} \text{ with } \bar{L} = \bar{B}^{-1} = \frac{1}{A}\begin{bmatrix} \dfrac{D_{13}}{x_1}(x_1 D_{23} + x_3 D_{12}) & \dfrac{D_{13}}{x_1}x_2 D_{23} \\[3mm] \dfrac{D_{23}}{x_2}x_1 D_{23} & \dfrac{D_{23}}{x_2}(x_2 D_{13} + x_3 D_{12}) \end{bmatrix} \tag{5a}$$

With A $= x_2 x_3 D_{13} + x_1 x_3 D_{23} + x_3{}^2 D_{12}$. This ultimately yields as equations for the fluxes N_i (with $N_i = x_i \, c_t \, u_i$):

$$N_1 = -\frac{c_t D_{13}}{A}\left(\left(D_{23} x_1 + D_{12} x_3 \right)\frac{dx_1}{dz} + \left(D_{23} x_1 \right)\cdot\frac{dx_2}{dz} \right) \qquad \text{(2, model)}$$

$$N_2 = -\frac{c_t D_{23}}{A}\left(D_{13} x_2 \frac{dx_1}{dz} + \left(D_{13} x_2 + D_{12} x_3 \right)\frac{dx_2}{dz} \right) \qquad \text{(3, model)}$$

The equations are solved using a simple forward time / centered space (FTCS) scheme.

Boundary conditions

The concentrations of the components are assumed to be constant in time at the organic-nonsolvent interface. To calculate the driving force for DCM at this boundary, the difference in molar fraction between interface and two layers above is approximated by Taylor series approach with second order accuracy as follows:

$$\frac{dx_i}{dz} = \frac{4x_i(t,i+1) - x_i(t,i+1) - 3x_i(t,i)}{2\Delta z} \qquad \text{(6a)}$$

At the nonsolvent-gas phase boundary, the fluxes of the components in the liquid phase are equal to those in the gas phase at the interface ($N_{iL} = N_{iG}$). The driving forces for fluxes of the component in the liquid and gas phase through this boundary are approximated by Taylor series approach with second order accuracy using an additional gridline (the concentrations of DCM and methanol in the bulk of the air are assumed to be zero):

$$\frac{dx_i}{dz} = \frac{x_i(t,k+1) - x_i(t,k-1)}{2\Delta z}$$
$$\frac{dy_i}{dz} = \frac{y_i(t)}{\delta_G} \qquad \text{(7a)}$$

where $y_i(t)$ is the composition at the gas-liquid interface, given by:

$$y_i(t) = \frac{\gamma_i x_i(t) p_{sat,i}(T)}{p_T} \qquad \text{(8a)}$$

$P_{sat,i}$ is the saturation pressure of i at the interface, and P_T is the total pressure of the components.

Calculation of the evaporation flux of pure water

The evaporation flux of pure water to the ambient air was calculated using the following expression:

$$N_w(t) = \frac{D_{wG}}{\delta_G}\left(\frac{p_{sat,w}}{RT} - \frac{p_{b,w}}{RT}\right) \tag{9a}$$

where N_w is the evaporation flux of water, D_{wG} is the diffusion coefficient of water vapor in air (calculated using equation 10), δ_G is the thickness of the gas phase boundary layer, $p_{sat,w}$ is the saturation concentration of water and $p_{b,w}$ is the partial pressure of water in the air bulk phase:

$$p_{w,b} = RH\, p_w \tag{10a}$$

RH is the relative humidity and p_w is the vapour pressure of water, calculated using the Antoine equation:

$$\log p_w = A_w - \frac{B_w}{T + C_w} \tag{11a}$$

A_w(10.06), *B_w(1650.27)*, and *C_w(-46.81)* are the Antoine constants for water.

Chapter 5

Preparation of hollow polylactide microcapsules through premix membrane emulsification - effects of nonsolvent properties*

Abstract

Hollow polylactide microcapsules that can be used as ultrasound contrast agents were prepared using premix membrane emulsification. Polylactide/dichloromethane and dodecane solutions were emulsified together with a nonsolvent phase (water or a water-alcohol mixture) by repeated passage through a glass fibre membrane. The solvent, dichloromethane, diffuses out of the droplets and the polylactide solidifies around a droplet of dodecane. To investigate the effect of the nonsolvent properties on the size and span of the microcapsules, different methanol-water, ethanol-water and 2-propanol-water mixtures were used as nonsolvents.

The alcohol lowers the interfacial tension and increases the viscosity of the nonsolvent, and therewith it decreases the size and the span of the microcapsules. It was remarkable that 2-propanol yields the smallest size (0.35 µm) followed by ethanol (0.8 µm) and methanol (1.5µm). In contrast, the smallest span was obtained with methanol (0.7), whereas 2-propanol gave the largest span (1.5). The results further show that the size and the span of the microcapsules decreases with increasing number of emulsification passes and transmembrane flux. The presence of alcohol in the nonsolvent phase increases the efficiency of the emulsification process and decreases the optimum number of passes required to obtain the minimum average size of the droplets. A three-parameter correlation was defined that could quantitatively describe the effects of all the aforementioned parameters on the size of the microcapsules.

Introduction

Microcapsules or microspheres have become increasingly important because of their widespread application in various fields ranging form cosmetics, coatings, inks, pesticides, electronic photocopying, catalysis, chromatography column packings, and calibration standards for biomedical and pharmaceutical products [1-6]. Microcapsules prepared out of biodegradable polymer such as polylactide, poly(glycolide), poly(ε-caprolactone), poly(saccharides), or albumin have been frequently used to deliver several types of drugs in the body (e.g. antibiotics, anticancer, antimicrobial drugs, vaccines, and proteins) [7-11]. Another important application for biodegradable microspheres is hollow microcapsules as ultrasound contrast agents (UCA's), which are gas microbubbles encapsulated in a thin polymer or protein shell [12]. The gas core of these microcapsules enables them to oscillate in an acoustic field and effectively reflect the ultrasound signal [13].

The size of the microcapsules is important for *in-vivo* applications [14-17]. Small particles can easily pass through the fine capillary blood vessels and the lymphatic endothelium, therefore, they have longer circulation times in the blood before being drained to the liver [18, 19]. Further, they have higher binding capability and accumulation at the target sites, and give less inflammatory and immune response from the tissues and cells of the body than big particles [18, 20].

Apart from the average size, a narrow size distribution gives better control over the dose and release behavior of the encapsulated drug, yields higher drug encapsulation efficiency, and better biocompatibility with cells and tissues of the body than polydisperse particles [18, 21]. Specifically, monodisperse UCA's are expected to lead to a more specific and uniform acoustic response. Therefore, preparation of microcapsules or UCA's of small and uniform size is of a great importance. However, preparation of these capsules with controlled size and size distribution is still a challenge.

Biodegradable polymeric microcapsules and UCA's are usually prepared by emulsification. A homogenous solution that consists of polymer, solvent, and a poor solvent is emulsified in a nonsolvent phase (continuous phase) that also may contain a proper surfactant. The solvent is slightly miscible with the nonsolvent, and therefore diffuses slowly from the droplets towards the nonsolvent-air surface,

and evaporates there. Due to the resulting loss of solvent, the droplets become smaller. The poor solvent inside the droplets (which is insoluble in the nonsolvent bath) becomes supersaturated and forms a droplet in the core of the emulsion droplet. The polymeric solution surrounding the droplet becomes more and more concentrated and solidifies into a polymeric shell. Subsequent removal of the particles from the solution and freeze-drying to remove the alkane, results in the required microbubbles [22].

Conventional emulsification techniques such as mechanical stirring, homogenization, or ultrasonication are frequently used to prepare hollow and solid microcapsules [23, 24]. However, none of these techniques gives a good control over the size and size distribution of the microcapsules. Relatively newer emulsification techniques such as membrane emulsification were proposed in literature for preparation of monodisperse emulsions and microspheres [25-27]. Several types of membrane emulsification can be distinguished such as cross-flow membrane emulsification, microchannel emulsification, and premix membrane emulsification [27]. The method of choice in this paper is premix emulsification, which starts with coarse polydisperse droplets that are pushed through a membrane. Passing the emulsion through the pores of the membrane breaks the coarse droplets up into smaller ones, and repeating this process results in an emulsion with small droplets with a more uniform size distribution than the original emulsion. In earlier work, we showed that premix membrane emulsification could lead to very narrowly dispersed emulsions, however these emulsions were used to prepare solid polylactide particles [28].

Based on the aforementioned considerations, the objective of this study was to prepare hollow microcapsules of controlled size and size distribution (ultimately aimed at use as UCA's) by premix membrane emulsification. For preparation of the microcapsules, polylactide is dissolved in dichloromethane (the solvent). This solution together with dodecane (the poor solvent) was then emulsified with a nonsolvent containing a mixture of water and different alcohols. Dichloromethane is better soluble in a nonsolvent that contains an alcohol, and therefore addition of alcohol will speed up the solidification process. At the same time, addition of an alcohol increases the viscosity of the nonsolvent phase and it will reduce the interfacial tension of the droplets. It was expected that smaller droplets could be

obtained at higher viscosity of the continuous phase, and at a lower interfacial tension. Therefore, the nonsolvent phase was systematically varied. The effects on the microcapsules were evaluated in terms of size, monodispersity, and morphology. A quantitative correlation was developed to relate the particle size with the interfacial tension and viscosity of the nonsolvent, the transmembrane flux, and the number of emulsification cycles.

Materials and methods

Materials

Poly(L-lactide) (PLLA), (intrinsic viscosity of 1.21 $dl \cdot g^{-1}$) was provided by PURAC Biochem B.V. (Gorinchem, the Netherlands). Dichloromethane (DCM) (HPLC, gradient grade) was supplied by Merck (Amsterdam, the Netherlands) and used as a solvent for the polymer. Dodecane ($\geq$99%) was obtained from Sigma-Aldrich (Zwijndrecht, the Netherlands) and used as poor solvent for the polymer. Milli-Q water with Methanol, 2-propanol (HPLC, gradient grade, $\geq$99.9%) from Aldrich (Zwijndrecht, the Netherlands), and ethanol (HPLC, gradient grade) from Merck (Amsterdam, the Netherlands) were applied as nonsolvents. Poly-(vinylalcohol) (PVA 23/88) provided by Ter Hell (Hamburg, Germany) was used as a stabilizer.

Methods

Preparation of microcapsules

In this study, premix membrane emulsification was used to prepare microcapsules. Certain amounts of PLLA were dissolved in DCM to prepare a 2% (w/w) stock solution. To 0.5 g of this solution, 1 g DCM and 0.15 g dodecane were added, and this mixture was added to 11 g of nonsolvent solution. The nonsolvent consisted of 3 g of 1% (w/w) PVA/water solution and 8 g of water-alcohol mixture. All ingredients were mixed for 1 min with a magnetic stirrer at approximately 900 rpm to form the coarse premix emulsion. To prevent solidification of the polymer, especially in the presence of alcohols, the alcohols were added to the mixture immediately after the start of premixing. The premix emulsion was then manually

passed through a 1-µm glass fiber syringe membrane (Acrodisc GF syringe filter, Pall) between 1 and 15 times using the same membrane, to form the polymer emulsion with smaller droplets. DCM was subsequently removed by stirring at 900 rpm on a magnetic stirrer for 1 hr, leaving behind oil-filled microcapsules. These microcapsules were collected by centrifugation at 3000 RCF for 20min, and washed with Milli-Q water to remove the PVA. The same collection/washing step was repeated three times. The oil core of the microcapsules was removed by freeze drying using a Christ Epsilon 2-6D freeze dryer (Osterode, Germany) to obtain the hollow microcapsules. The freeze drying step was conducted under the following conditions: -20 $^\circ$C and 103 Pa for about 4hr, and then for 9 hr at -5°C and the final drying stage was at gradually decreased pressure from 103 to 0.1 Pa at a constant temperature of 20°C for 12 hr.

Control of transmembrane flux and reproducibility

A certain volume of the premix emulsion was manually pushed through the membrane within a certain time. With increasing experience of the person who carried out the experiments the syringe could be emptied during the time that was needed for specific conditions, and reproducible experiments could be carried out. We tried to control the applied manual force to keep passing time as constant as possible through all emulsification passes.

Size and size distribution measurements

To determine the average size and size distribution profiles, laser light scattering (Malvern Mastersizer 2000, Malvern Instruments Ltd., Worcestershire, United Kingdom) was used. The same sample was measured in triplicate and each size distribution was calculated by the instrument software. From this an average size distribution was constructed which was subsequently used to calculate the average volume median diameter d_{50}. This procedure was used for all samples prepared with alcohols. For water samples, the first measurement was taken since solvent removal was taking place, therewith influencing the droplet size during measurement.

Scanning electron microscope

The morphology of the microcapsules was observed by scanning electron microscopy (SEM) (JEOL 6300F, Tokyo, Japan). The samples were prepared as follows: a suspension of oil-filled microcapsules was filtered with a filter paper to remove PVA solution. After that, the capsules are dried and visualized together with the filter in the CryoSEM; the background structure is the filter. The CryoSEM was operated at the freezing temperature of liquid nitrogen ($-196\,^{\circ}$C); to prevent evaporation of dodecane.

In order to show the hollow core of the microcapsules, the microcapsules were fractured before viewing with SEM. To do that, a droplet of hollow microcapsules suspension was trapped in between two glass plates coated with a thin layer of polylysine and dried in air. Microcapsules were then fractured by splitting the glass plates.

Interfacial tension measurements

The interfacial tension between DCM and different nonsolvents was measured using dynamic drop shape tensiometery. A drop of DCM was generated at the tip of a needle that was submerged in a nonsolvent bath and the interfacial tension between the DCM-nonsolvent interfaces was then measured in time. Based on the shape of the DCM drop, the interfacial tension was calculated by the tensiometer software using the Laplace equation.

Viscosity and density measurements

The density of different nonsolvents was determined from the mass/volume ratio using a graduated cylinder. For the viscosity measurements of the nonsolvents, a Ubbelohde viscometer was used. Before samples were measured, the instrument was carefully cleaned and calibrated by determining the flow time of de-ionized water. All the measurements were carried out in triplicate at a constant temperature of (approximately) 25 $^{\circ}$C.

Results and discussion

Effect of nonsolvent properties on size and size distribution

To investigate the effect of the nonsolvent on the size and size distribution, a PLLA-DCM and dodecane solution was emulsified with different alcohol-water mixtures. Figures 1a-c show the average size, and span of the microcapsules obtained after emulsification with methanol-water (Figure 1a), ethanol-water (Figure 1b), and 2-propanol-water (Figure 1c), respectively. Both size and span decrease with increasing alcohol concentration in the nonsolvent, up to a certain alcohol concentration at which a minimum size is obtained (30% for methanol and ethanol, and 25% for 2-propanol). At higher alcohol concentrations, the size and span increase again, and above a certain concentration (50% for methanol, 45% for ethanol and 35% (w/w) for 2-propanol), no droplets were formed anymore.

2-Propanol gives the smallest average size (0.4 µm) followed by ethanol (0.8 µm) and methanol (1.5µm) (see Figure 2 for size distributions); however the smallest span was obtained with methanol (0.7), while 2-propanol had the largest span of (1.5). These effects can be attributed to the combined effects of alcohols on interfacial tension and viscosity of the nonsolvent, and on the removal rate of the solvent. Several researchers have reported that the size of the droplets obtained with premix membrane emulsification is directly proportional to the interfacial tension and inversely proportional to the viscosity of the nonsolvent [29, 30].
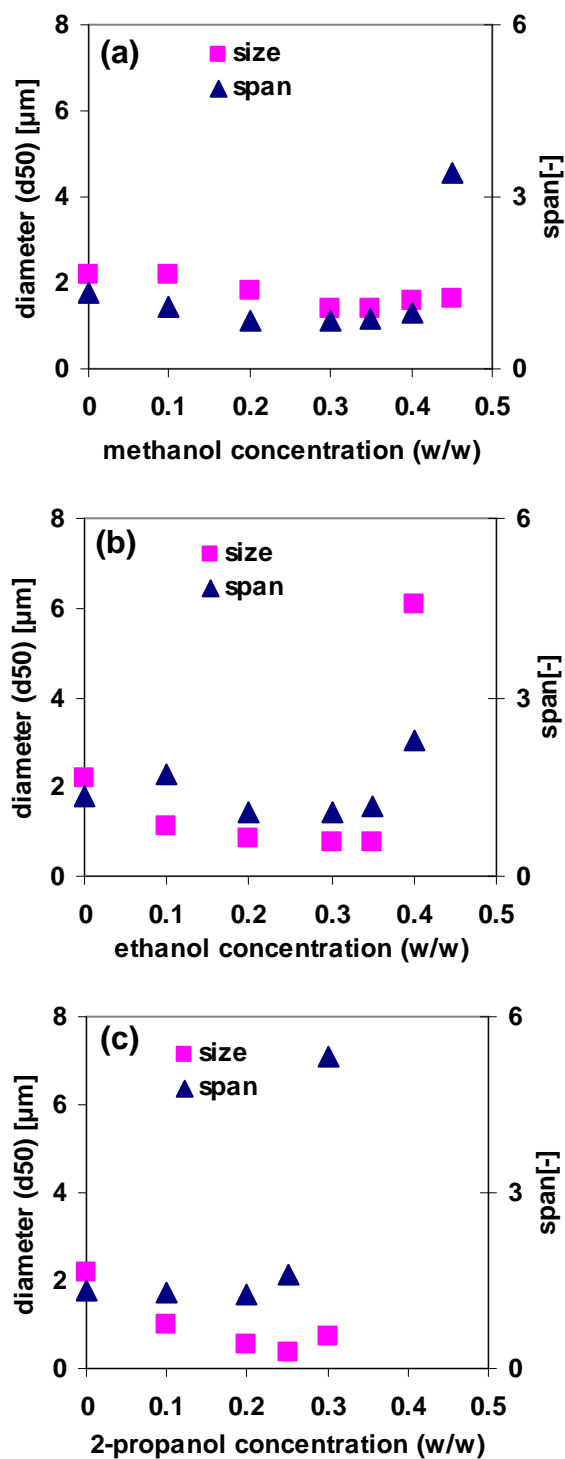
Figure 1: Average size and span of UCA's particles prepared with different water-alcohols mixtures as nonsolvents: methanol-water (a), ethanol-water (b), 2-propanol-water (c). The size distribution was measured after evaporation of the solvent. The measurements were done at a transmembrane flux of 97 $m^3 m^{-2} h^{-1}$.
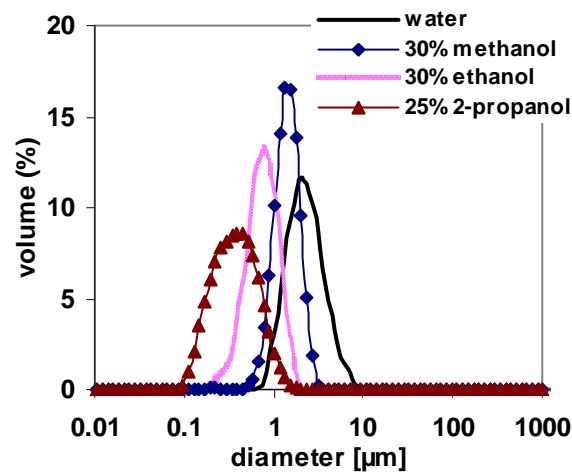
Figure 2: Particle size distribution of PLLA microcapsules prepared with different alcohol-water mixtures as nonsolvents. The size distribution was measured after evaporation of the solvent. The measurements were done at a transmembrane flux of 97 $m^3 m^{-2} h^{-1}$.

Table 1: Interfacial tension and dynamic viscosity of water alcohols mixtures.

Nonsolvent	Interfacial tension (σ) [mN·m^{-1}]	Viscosity (η) [mPa·s]
Water	28.2	0.92
30% (w/w) methanol-water	8.4	1.54
30% (w/w) ethanol-water	2.4	2.17
25% (w/w) 2-propanol-water	below measuring limit	2.27

Addition of alcohol to the nonsolvent not only lowers the interfacial tension but also remarkably increases the viscosity of the nonsolvent (Table 1), and it was found indeed that the droplet sizes were influenced. The fact that the span is largest with the use of 2-propanol might be related to the stability: a very low interfacial

tension and a relatively high solubility of DCM in the nonsolvent phase could well result in coalescence and significant Oswalt ripening.

The presence of alcohols in the nonsolvent increases the solvent removal rate from the droplets, as DCM is fully miscible with the pure alcohols [28]. As a result, the polymer solidifies relatively quickly (compared with water), and the droplet size and size distribution are better preserved. With water, DCM removal is very slow, because DCM is only slightly miscible with water, therefore the solidification of the polymer takes much longer, which allows the still liquid droplets to aggregate, ripen and coalesce, leading to larger droplets and wider distributions [28]. High alcohol concentrations in the nonsolvent phase not only increase the out-diffusion rate of the solvent from the droplets, but also increase the in-diffusion of the alcohol into the droplets. This may cause the particles to swell, and may result in an increase of the porosity of the final microcapsules. At even higher alcohol concentrations (>50% for methanol, >45% for ethanol, or >35% for 2-propanol), it is expected that DCM/dodecane will dissolve in the alcohol water mixture, forming a single phase. PLLA becomes supersaturated in this phase, and precipitates in the form of much smaller (solid) spheres, or a film on the bottom. This phenomenon occurs for all alcohols, albeit at different concentrations, which indicates that the interaction of nonsolvent solution with PLLA and DCM depends on the alcohol used.

SEM micrographs of the prepared microcapsules are shown in Figures 3 and 4. Figure 3 shows the non-freeze dried microcapsules and the capsules are filled with dodecane; Figure 4 shows the hollow microcapsules obtained after freeze-drying. The majority of the particles are spherical and have a smooth surface. The sizes in the micrographs are in agreement with the values in Figures 1 and 2.

Effect of nonsolvent properties on emulsification efficiency

Figure 5 shows the effect of the number of emulsification cycles on the size and size distribution of emulsion droplets prepared with water and 30% (w/w) methanol as nonsolvent. With 30% methanol, the size of the droplets decreases already after a single pass, and does not change anymore after three passes. With water, the homogenization process is less effective. The average size decreases gradually, and a minimum size was only approached after about 10 passes. Figure 5b shows that

while the use of methanol always results in narrow size distributions, this is not the case with water, even after 11 passes (figure 5c). In addition, the droplets made with methanol are more stable.
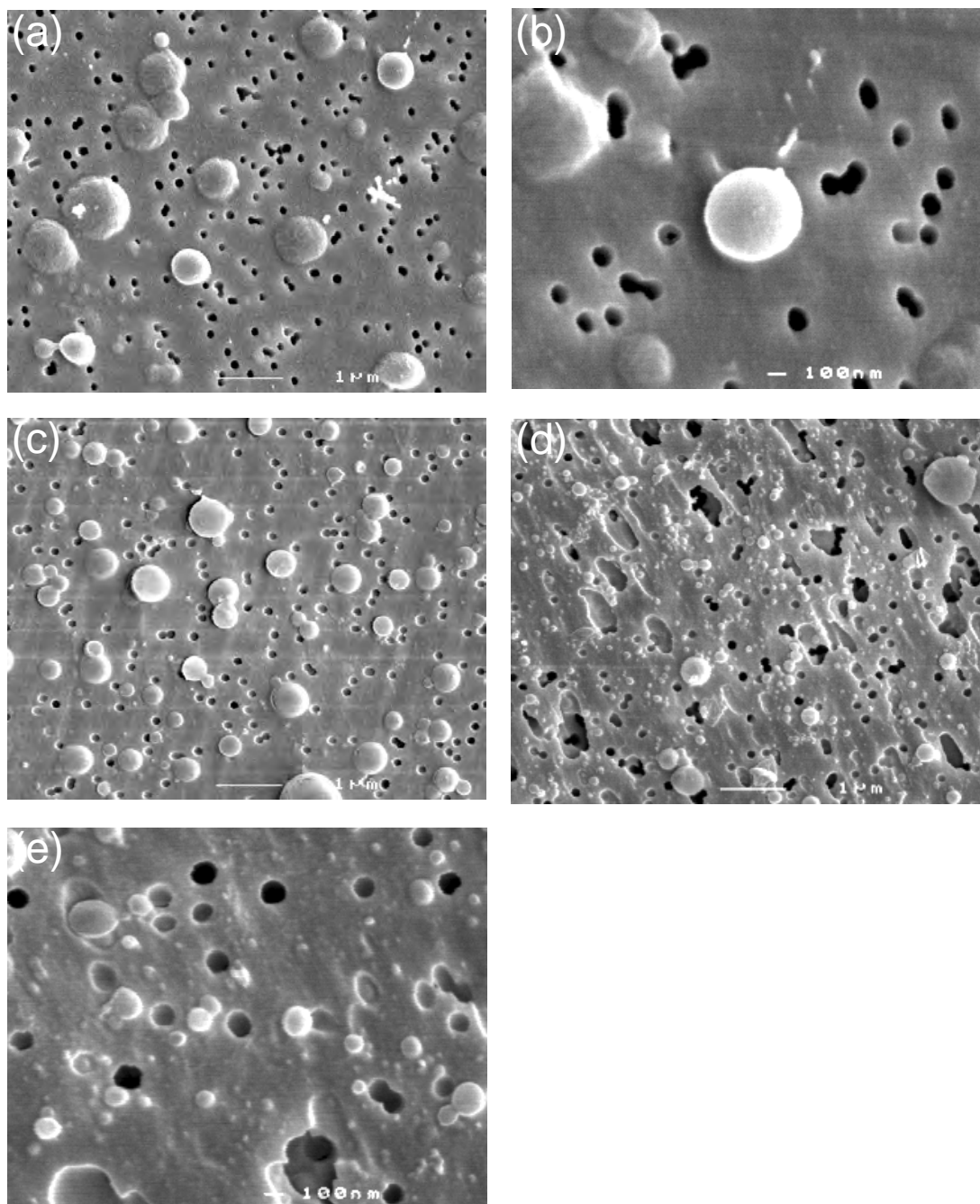
Figure 3: SEM micrographs of dodecane-filled PLLA microcapsules prepared with different alcohol-water mixtures as nonsolvents: 30% methanol (a), magnification of a (b), 30% ethanol (c), 25% 2-propanol (d), magnification of d (e).
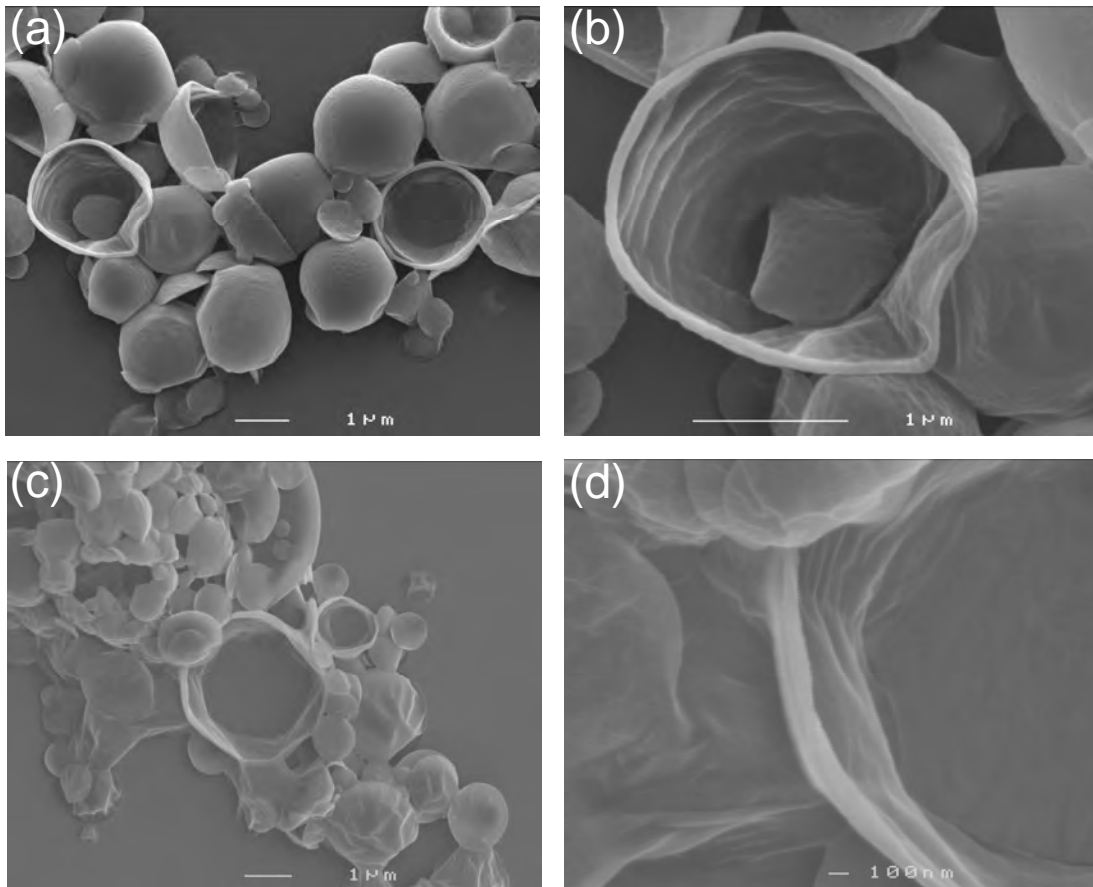
Figure 4: SEM micrographs of hollow PLLA microcapsules prepared with different nonsolvents: 30% methanol (a), magnification of a (b), water (c), magnification of c (d).

Hunter and Frisken suggested that during passage through the hydrophilic pores of the membrane, the emulsion droplet deforms into a cylinder. The oil droplets are separated from the wall of the pore by a lubrication layer of nonsolvent [31]. At low interfacial tension and/or high viscosity of the nonsolvent, the thickness of the lubrication layer increases, and the radius of the oil cylinders decreases, resulting in smaller droplets [29, 31]. Besides this, solidification proceeds faster with 30% methanol, and therefore there is less chance of coalescence or ripening.
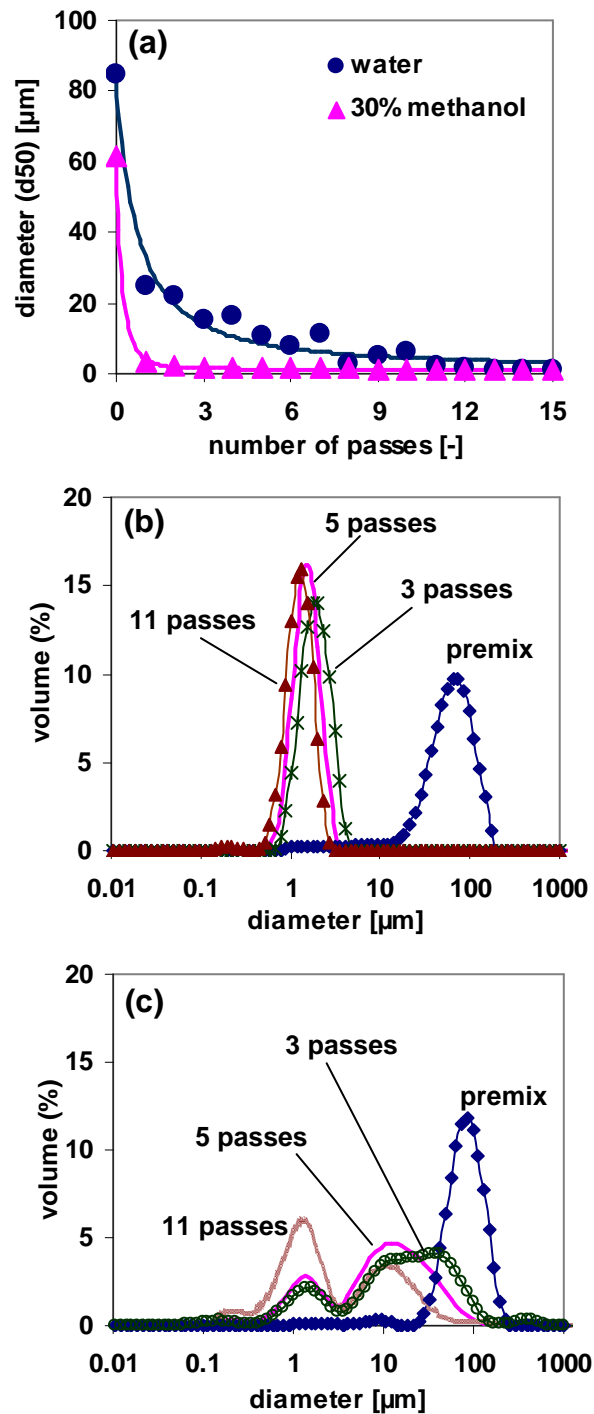
Figure 5 : Effect of number of number of emulsification passes on: average diameter of microcapsules droplets prepared with water and 30 % methanol-water mixture as nonsolvents (a), size distribution profiles of microcapsules droplets prepared with 30% methanol (b) and water (c). The size was measured immediately after emulsification.

Effect of transmembrane flux

The transmembrane flux J [$m^3 \cdot m^{-2} \cdot s^{-1}$] through the membrane is defined as:

$$J = \frac{Q_v}{A \cdot \varepsilon} \qquad (1)$$

In which Q_v is the volumetric flow rate [$m^3 \cdot h^{-1}$], A is the cross sectional area of the membrane [m^2] and ε is the porosity of the membrane [-]. The transmembrane flux defined in this way is equal to the average velocity of the emulsion in the membrane. Figure 6 shows that high transmembrane fluxes result in smaller droplets. This is in line with our expectations: the shear stress inside the pores of the membrane increases (as was the case at high viscosity), and that facilitates droplet break-up [29].
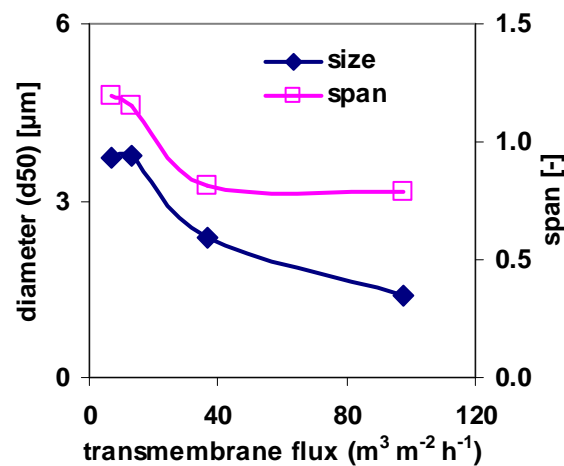
Figure 6: Effect of transmembrane flux on average size and span of microcapsules particles prepared with 30 % methanol-water mixture as nonsolvent. The size distribution was measured after evaporation of the solvent.

Development of a correlation

We expect that the droplet size, relative to the pore size of the membrane, depends on the viscosity of the nonsolvent and the interfacial tension via the capillary number [29, 32]:

With $Ca = \dfrac{\sigma}{\eta \cdot J}$ (2)

in which σ is the interfacial tension of the nonsolvent [mN·m⁻¹] and η is the dynamic viscosity of the nonsolvent [mPa·s]. In addition, the obtained droplet size will depend on the number of passes N. This results in a correlation of the form:

$$\frac{d_{50}}{d_{pore}} = \alpha \cdot Ca^{\beta} \cdot N^{\gamma}$$ (3)

Where, d_{50} is the average diameter of the droplets, and d_{pore} is the average diameter of the pores in the membrane.

Because the droplets shrink after emulsification, due to extraction of the solvent, the original droplet size was calculated from the measured average diameter of the final solidified droplets, assuming that the total reduction in volume of the microcapsules is equivalent to the total volume of solvent lost.

Equation 3 was fitted to all data with alcohols using the least sum of squares method, which led to an acceptable fit (see Figure 7), and parameter values $\alpha = 0.481$, $\beta = 0.422$ and $\gamma = -0.249$. The standard deviation of these parameters (α, β, γ) was typically less than 10%, which indicates a good reliability for the investigated system. The correlation could not adequately describe the data obtained with only water. This may be caused by the much slower removal rates of the solvent that possibly also allows the liquid droplets to coalesce. In that case, it is also not expected that the correlation would cover these data points.
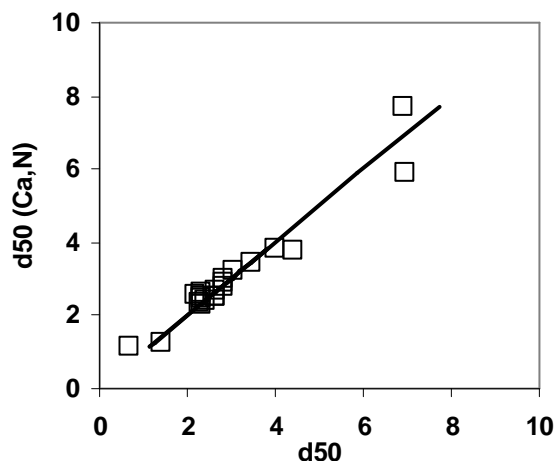
Figure 7: Measured values of the median diameter (d50) (squares) fitted to equation 3 (solid line).

Conclusions

Narrowly-dispersed polylactide hollow microcapsules with sizes 0.35 – 5 µm were successfully prepared by premix membrane emulsification of a polylactide/dichloromethane/ dodecane solution in alcohol-water mixtures. We found that the size and the span of the microcapsules could be precisely controlled by choosing the appropriate type and concentration of alcohol in the nonsolvent. Addition of alcohol to the nonsolvent strongly decreases the size of the microcapsules: the alcohol lowers the interfacial tension and increases the viscosity of the nonsolvent resulting in more effective emulsification. The minimum size of about 0.35 µm was obtained with 25% 2-propanol-water as nonsolvent followed by 0.8 µm for 30% ethanol-water and 1.4 µm for 30% methanol-water. The size distribution of the particles obtained with 30% methanol was sharper than the ones obtained with 30% ethanol-water, and 25%propanol-water. The composition of the nonsolvent is an important parameter, which can be used to adjust both the average size and the span of the microcapsules, while at the same time speeding up the preparation process through faster solidification.

Acknowledgements

References

1. Perugini, P., Genta, I., Pavanetto, F., Conti, B., Scalia, S., Baruffini, A., *Study on glycolic acid delivery by liposomes and microspheres.* International Journal of Pharmaceutics, 2000. **196**(1): p. 51.

2. Guo, H. L., Zhao, X. P., *Preparation of a kind of red encapsulated electrophoretic ink.* Optical Materials, 2004. **26**(3): p. 297.

3. Shukla, P. G., Kalidhass, B., Shah, A., Palaskar, D.V., *Preparation and characterization of microcapsules of water-soluble pesticide monocrotophos using polyurethane as carrier material.* Journal of microencapsulation, 2002. **19**(3): p. 293.

4. Wu, H., Liu, Z., Wang, X., Zhao, B., Zhang, J., Li, C., *Preparation of hollow capsule-stabilized gold nanoparticles through the encapsulation of the dendrimer.* Journal of Colloid and Interface Science, 2006. **302**(1): p. 142.

5. Maciejewska, M. M., Osypiuk, J., Gawdzik, B., *Preparation and characterization of the chromatographic properties of ethylene glycol dimethacrylate/divinylbenzene polymeric microspheres.* Journal of polymer science. Part A, Polymer chemistry, 2005. **43**(14): p. 3049.

6. Freiberg, S., Zhu, X. X., *Polymer microspheres for controlled drug release.* International Journal of Pharmaceutics, 2004. **282**(1-2): p. 1.

7. Prior, S., Gamazo, C., Irache, J. M., Merkle, H. P., Gander, B., *Gentamicin encapsulation in PLA/PLGA microspheres in view of treating Brucella infections.* International Journal of Pharmaceutics, 2000. **196**(1): p. 115.

8. Chen, H., Langer, R., *Oral particulate delivery: status and future trends.* Advanced Drug Delivery Reviews, 1998. **34**(2-3): p. 339-350.

9. Hanes, J., Cleland, J. L., Langer, R., *New advances in microsphere-based single-dose vaccines.* Advanced Drug Delivery Reviews, 1997. **28**(1): p. 97.

10. Perez, M. H., Zinutti, C., Lamprecht, A., Ubrich, N., Astier, A., Hoffman, M., Bodmeier, R., Maincent, P., *The preparation and evaluation of poly([epsilon]-caprolactone) microparticles containing both a lipophilic and a hydrophilic drug.* Journal of Controlled Release, 2000. **65**(3): p. 429.

11. Chen, Y., McCulloch, R. K., Gray, B. N., *Synthesis of albumin-dextran sulfate microspheres possessing favourable loading and release characteristics for the anticancer drug doxorubicin.* Journal of Controlled Release, 1994. **31**(1): p. 49.

12. Lathia, J. D., Leodore, L., Wheatley, M. A., *Polymeric contrast agent with targeting potential.* Ultrasonics, 2004. **42**(1-9): p. 763.

13. Dayton, P. A., Chomas, J. E., Lum, A. F. H., Allen, J. S., Lindner, J. R., Simon, S. I., Ferrara, K. W., *Optical and acoustical dynamics of microbubble contrast agents inside neutrophils.* Biophysical journal, 2001. **80**(3): p. 1547.

14. De Jong, N., Bouakaz, A., Frinking, P., *Basic acoustic properties of microbubbles.* Echocardiography, 2002. **19**(3): p. 229.

15. Bloch, S. H., Short, R. E., Ferrara, K. W., Wisner, E. R., *The effect of size on the acoustic response of polymer-shelled contrast agents.* Ultrasound in medicine & biology, 2005. **31**(3): p. 439.

16. Grizzi, I., Garreau, H., Li, S., Vert, M., *Hydrolytic degradation of devices based on poly(-lactic acid) size-dependence.* Biomaterials, 1995. **16**(4): p. 305.

17. Wang, S. H., Chang, P. H., Shung, K. K., Levene, H. B., *Some considerations on the measurements of mean frequency shift and integrated backscatter following administration of Albunex®.* Ultrasound in medicine & biology, 1996. **22**(4): p. 441.

18. Chu, L. Y., Park, S. H., Yamaguchi, T., Nakao, S. I., *Preparation of Micron-Sized Monodispersed Thermoresponsive Core-Shell Microcapsules.* Langmuir, 2002. **18**(5): p. 1856.

19. Gref, R. R., Minamitake, Y., Peracchia, M. T., Trubetskoy,V., Torchilin,V., Langer, R., *Biodegradable long-circulating polymeric nanospheres.* Science, 1994. **263**(5153): p. 1600.

20. Anderson, J. M., Shive, M. S., *Biodegradation and biocompatibility of PLA and PLGA microspheres.* Advanced Drug Delivery Reviews, 1997. **28**(1): p. 5.

21. Liu, R., Huang, S.-S., Wan, Y.-H., Ma, G.-H., Su, Z.-G., *Preparation of insulin-loaded PLA/PLGA microcapsules by a novel membrane emulsification method and its release in vitro.* Colloids and Surfaces B: Biointerfaces, 2006. **51**(1): p. 30.

22. Böhmer, M. R., Schroeders, R., Steenbakkers, J. A. M., de Winter, S. H. P. M., Duineveld, P. A., Lub, J., Nijssen, W. P. M., Pikkemaat, J. A., Stapert, H. R., *Preparation of monodisperse polymer particles and capsules by ink-jet printing.* Colloids and surfaces. A, Physicochemical and engineering aspects, 2006. **289**(1-3): p. 96.

23. Feinstein, S. B., Keller, M. W., Kerber, R. E., Vandenberg, B., Hoyte, J., Kutruff, C., Bingle, J., Welsh, A. H., *Sonicated echocardiographic contrast*

agents: reproducibility studies. Journal of the American Society of Echocardiography, 1989. **2**(2): p. 125.

24. Winkelmann, J. W., Kenner, M. D., Dave, R., Chandwaney, R. H., Feinstein, S. B., *Contrast echocardiography.* Ultrasound in Medicine & Biology, 1994. **20**(6): p. 507.

25. Liu, R., Ma, G., Meng, F.-T., Su, Z.-G., *Preparation of uniform-sized PLA microcapsules by combining Shirasu Porous Glass membrane emulsification technique and multiple emulsion-solvent evaporation method.* Journal of Controlled Release, 2005. **103**(1): p. 31.

26. Ma, G. H., Omi, S., Dimonie, V. L., Sudol, E. D., El-Aasser M. S., *Study of the preparation and mechanism of formation of hollow monodisperse polystyrene microspheres by SPG (Shirasu Porous Glass) emulsification technique.* Journal of applied polymer science, 2002. **85**(7): p. 1530.

27. Vladisavljević, G. T., Williams, R. A., *Recent developments in manufacturing emulsions and particulate products using membranes.* Advances in colloid and interface science, 2005. **113**(1): p. 1.

28. Sawalha, H., Purwanti, N., Rinzema, A., Schroën, K., Boom, R., *Polylactide microspheres prepared by premix membrane emulsification-Effects of solvent removal rate.* Journal of membrane science, 2008. **310**(1-2): p. 484.

29. Vladisavljević, G. T., Shimizu, M., Nakashima, T., *Production of multiple emulsions for drug delivery systems by repeated SPG membrane homogenization: Influence of mean pore size, interfacial tension and continuous phase viscosity.* Journal of membrane science, 2006. **284**(1-2): p. 373.

30. Vladisavljević, G. T., Surh, J., McClements, J. D., *Effect of emulsifier type on droplet disruption in repeated Shirasu porous glass membrane homogenization.* Langmuir, 2006. **22**(10): p. 4526.

31. Hunter, D. G., Frisken, B. J., *Effect of extrusion pressure and lipid properties on the size and polydispersity of lipid vesicles.* Biophysical journal, 1998. **74**(6): p. 2996.

32. Xu, J. H., Luo, G. S., Chen, G. G., Wang, J. D., *Experimental and theoretical approaches on droplet formation from a micrometer screen hole.* Journal of membrane science, 2005. **266**(1-2): p. 121.

Chapter 6

Addition of oils to polylactide casting solutions as a tool to tune film morphology and mechanical properties*

Abstract

PLLA films exhibit toughening by addition of oils to the polymer casting. This was investigated by casting films from solution and evaporation in air; the investigated oils were linear alkanes, cyclic alkanes, and two terpenes (limonene and eugenol). The addition of the oils greatly influenced the morphology and thermal and mechanical properties of the films. Most oils rendered porous films; a variety of morphologies was obtained. Films prepared with hexane and eugenol showed a solid, nonporous structure similar to neat PLLA films, with similar mechanical properties. The thermal transition temperatures of the films decreased through addition of oil, depending on the oil used, the decrease could be up to 30 °C (glass transition), 45 °C (cold crystallization), and 15 °C (melting temperature). The films prepared without oil were stiff and brittle. Upon addition of most of the oils, the maximum strength and elastic moduli decreased, but their ductility improved considerably. Limonene, the most extreme case, gave a very ductile film with an elongation at break up to 200%. The main conclusion of this study is that various oils can be used to tune and improve the properties of PLLA films.

Introduction

Polylactide (PLA) is a biodegradable polymer that is produced through polymerization of lactide, the cyclic dimers of lactic acid, which can be derived by fermentation of renewable resources such as corn or sugarcane [1]. Lactide is generally available in two different isomers, (L-lactide) and (D-lactide) with different properties. Optically pure poly(L-lactide) (PLLA) and poly(D-lactide) (PDLA) are semicrystalline polymers, while poly(DL-lactide) (PDLLA), a random copolymer that can be prepared from a racemic mixture of D and L isomers, is completely amorphous [1, 2].

PLA is well biodegradable, biocompatible, and has high mechanical strength [3], which makes it an attractive polymer for biomaterials such as scaffolds [4], films [5], and microparticles [6-8]. However, the inherent brittleness and low toughness of PLA remain limitations for large-scale application in medical devices and packaging materials [1, 9, 10].

Much effort has been put into improving the flexibility of PLA through several approaches including copolymerization, blending, and plasticization. Various types of polymers have been used for toughening PLA by blending, such as: polycaprolactone [11], poly(ethylene succinate) [12], poly[(butylenes-adipate)-*co*-terephthalate] [13], poly(propylene glycol) [14], poly(ethylene glycol) [15], and starch [16]. The miscibility and compatibility between PLA and these polymers are key factors for successful toughening of the blends [17, 18]. Poor miscibility or compatibility can induce phase separation in the blend, resulting in different mechanical properties [18-20].

Low molecular weight plasticizers like glucose monoester [21], citrate esters [22], partial fatty acid ester [21], ethylene oxide [23], tributyl citrate [24] and oligomeric lactic acid [10] have also been reported to increase the flexibility of PLA. Addition of these plasticizers improved the ductility to (up to 200% elongation at break) and efficiently reduced the glass transition temperature of the polymer from around 60 °C to 30 °C [10, 24]. However, migration of the plasticizers out of the bulk of the polymer may weaken the stability of the blend [24, 25].

Toughening PLA materials is an important research objective that has attracted much attention in the last decade. In a previous study [26], PLLA films were prepared through the film casting method; dodecane was added to the casting solution to induce extra porosity in the films. The dodecane did not only increase the porosity but it also increased the elongation at break and reduced the crystallization temperature of the films. This has motivated us to investigate the effects of other alkanes and oils on the properties PLLA films.

We report here on the use of alkanes (hexane, decane, dodecane, and hexadecane), cyclic alkanes (cyclohexane and cyclodecane), and two terpenes (limonene and eugenol). PLLA films are prepared through film casting in air, and the resulting films were evaluated on their thermal properties (glass transition temperature, cold crystallization temperature, melting temperature, and enthalpies of crystallization and melting), and mechanical properties (maximum strength, and elongation at break). Besides, the morphology of the films was observed with SEM and related to the observed thermal and mechanical properties.

Materials and Methods
Materials
The PLLA used in this study was purchased from PURAC (Biochem B.V., Gorinchem, the Netherlands) with an intrinsic viscosity of 1.21 dl·g^{-1}. The solvent dichloromethane (DCM) (HPLC, gradient grade) was obtained from Merck. The oils added to the polymer casting solution were hexane (HPLC, gradient grade, (≥99.9%)) from Aldrich, dodecane (≥99%) from Sigma-Aldrich, hexadecane (>99%), and cyclohexane (≥99.5%) from Merck, and decane (95%), cyclodecane (95%), eugenol, and limonene (≥96%) from Fluka.

Methods
Preparation of the PLLA films
Specific amounts of PLLA were dissolved in DCM. The oil was then added to the polymer solution to prepare casting solutions with concentrations of 10:90 (w/w) PLLA/DCM and 10/10/80 (w/w) PLLA/oil/DCM. The casting solutions were stirred for 1-2 days. To prepare the films, the film casting method was used. First,

the casting solution was cast on a mould with an initial layer thickness of 100 µm, and was then left in a fume-cupboard under ambient conditions to evaporate the DCM. After evaporation, the films were collected and freeze-dried to remove the residual oil using a Christ Epsilon 2-6D freeze dryer (Salm and Kipp, the Netherlands). The freeze dryer was initially run for about 4 hr at -20 °C and 1.03 mbar and then for 9 hr at -5°C and 1.03 mbar, and finally at 20°C and 0.001 mbar for about 12 hr. After freeze-drying, the films were ready for characterization.

Characterization of the films

Thermal properties

The thermal properties of the films were studied using differential scanning calorimetry (DSC). Pieces of the films were cut, placed in stainless steel pans and then placed in Perkin Elmer Diamond DSC (Perkin-Elmer Co., Norwalk, CT). Two samples of each film were heated in the DSC from 0°C to 200 °C at heating rate of 10°C /min. The glass transition temperature, cold crystallization temperature, melting temperature, and enthalpies of cold crystallization, pre-melt crystallization, and melting of the samples were then determined from the DSC curves.

Mechanical properties

The tensile strength, the elongation at break, and Young's modulus of the films were measured using the Texture Analyzer T2 (Stable Micro Systems Ltd., Surrey, UK). Samples were cut from the films in a dog-bone shape with a total length of 37 mm, gauge length of about 15 mm (±1), and width of 13 mm at the top and 7.2 mm (narrowest) at the middle to induce the fracture in the middle of the sample. The tensile tests were performed with three to seven samples of each film at constant crosshead speed of 0.1 mm/second until break.

Morphology

The morphology of the films was visually observed with scanning electron microscope (SEM) (JEOL, JSM-5600 LV). Cross-sections of the films were fractured in liquid nitrogen and then coated with a thin platinum layer (~5 nm) using a sputter-coater (JEOL, JFC-1300) before viewing with SEM.

Results and discussion

Morphology

The effect of the oil on the morphology of PLLA films was investigated using SEM. Figure 1 shows the SEM images of PLLA films prepared with different oils in the casting solution. For the neat PLLA film prepared from a solution of (10:90 PLLA:DCM), a solid, dense and nonporous structure was obtained (see Figure 1a). As soon as the film is exposed to the air after casting, evaporation of the DCM takes place and consequently, the polymer solidifies. It is expected here that the polymer solidified into a dense and nonporous film; however, the thickness of the film is around 22 µm, which is about a factor 2 higher than would be expected on the basis of the fraction of the polymer in the solution (10% in a film with 100 µm initial thickness). The film therefore seems to contain some mesoscopic porosity.

The structure of the films is different with oil added to the casting solution. For linear alkanes, either a solid or a porous film was obtained, depending on the alkane used. With hexane, a solid and nonporous structure similar to that of neat PLLA was obtained (see Figure 1 b), most probably because the hexane evaporated before it could have any strong effect on the structure (even though the film seems to be somewhat thinner). With higher linear alkanes, porous structures were formed. With decane, an asymmetric morphology consisting of a thin solid top layer and a fairly uniform porous sub-layer was observed (Figure 1c), whereas with dodecane and hexadecane, the top solid layer was not present anymore. The structure became more open and showed bigger pores (Figures 1d and 1e). The asymmetricity in the film made with decane may be due to some evaporation of the decane in conjunction with DCM, leading to a lower concentration of decane near the surface, and hence a lower porosity in the film near the surface. As dodecane and higher alkanes are less volatile, they will not evaporate to the same extent during film formation, and the asymmetric structure will not be created. Clearly, there is a relation between the type of alkane, and the film structure obtained.
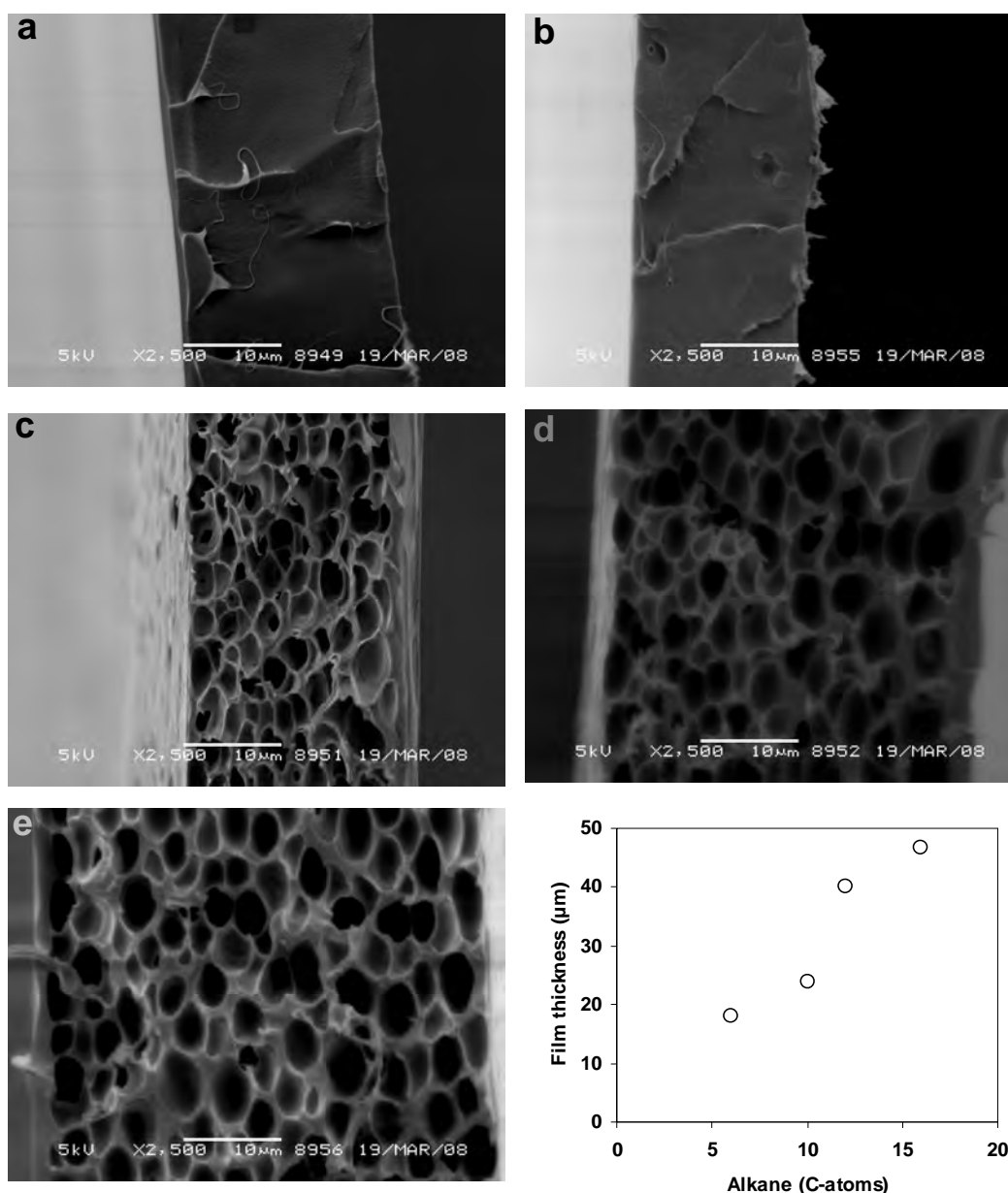
Figure 1: SEM images of cross sections of PLLA films prepared with different alkanes in the casting solution: a) neat PLLA (no oil), b) hexane, c) decane, d) dodecane, e) hexadecane and f) thickness of the films as a function of alkane C-atoms. The initial polymer and oil concentrations in all films were 10%w/w.

To investigate this further, cyclic alkanes were used. Comparison of cyclohexane (figure 2b) and cyclodecane (figure 2a) yields the same trend as with linear alkanes: the higher the alkane, the thicker and more symmetric the film. Comparison of the film prepared with cyclodecane (Figure 2a) to that with linear decane (Figure 1c) shows a symmetric morphology with more open structure and bigger pores. With

cyclohexane, some semicircular closed cells were formed in the film prepared with cyclohexane (Figure 2b), which is differed from the nonporous film obtained with its linear counterpart. Other oils (limonene and eugenol) yielded different morphologies. With limonene, an asymmetric, open cellular morphology with relatively small pores was obtained (Figure 2c), whereas eugenol gave a rough, dense, and nonporous structure (see Figure 2d), with some evidence of a non-brittle fracture in the sample preparation (even though carried out in liquid nitrogen). This indicates that the interaction between the eugenol and the polymer is sufficiently strong to avoid phase separation between the oil and the polymer during evaporation of the solvent. In other words: in contrast to limonene, eugenol seems to be almost a good solvent for the polymer.
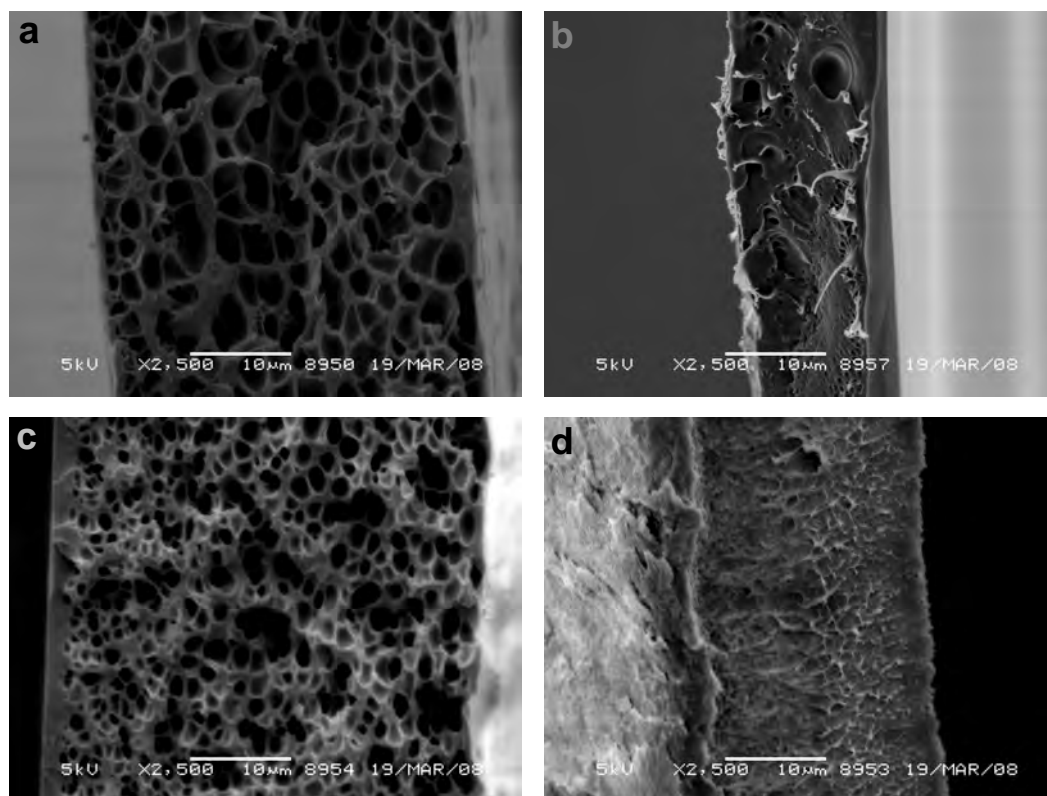
Figure 2: SEM images of cross sections of PLLA films prepared with different oils in the casting solution: a) cyclodecane, b) cyclohexane, c) limonene, and d) eugenol. The initial polymer and oil concentrations in all films were 10%w/w.

The difference in the physicochemical properties of the oils i.e. boiling point, chemical structure, and interaction with the polymer and solvent are expected to cause the differences in film morphology. During formation of the film, DCM evaporates, which slowly increases the concentrations of the polymer and oil in the film until a certain limit is reached at which the solution in the film will de-mix into a polymer rich matrix phase and a dispersed polymer poor, oil rich phase [26]. Upon further removal of DCM, the polymer around the oil droplets solidifies forming the wall of the pores, and the trapped oil droplets are the precursors of the pores observed in the structure [27].

Besides DCM, also evaporation or out-diffusion of the oil can take place during film formation depending on the oil used. This reduces the oil concentration in the film, and subsequently, the porosity. When the boiling point of the oil is sufficiently low (as with hexane), large amounts of the oil evaporate from the film before a significant amount of the solvent has evaporated. No porosity will be formed, and the film will be dense. All other oils have higher boiling points, therefore no evaporation occurs and porous films were obtained. For eugenol, a nonporous film was obtained in spite of the high boiling point of the oil (> 250 °C). Most probably, the polymer is more compatible with eugenol than the other oils due to its hydroxyl group. Thus after the solvent was evaporated, the polymer was highly swollen with the remaining eugenol and probably still somewhat fluid. Therefore, slow out-diffusion of the eugenol after the film was supposed to have formed, ultimately led to the formation of a dense film.

One can therefore conclude that porosity in PLA films can be induced and tailored through the type of the oil. In the following section, we will discuss the effect of the oils on the thermal characteristics of the polymer such as glass transition (T_g), cold crystallization (T_c), and melting temperature (T_m).

Thermal properties

Figure 3 shows some examples of DSC heat-up thermographs of the films. As illustrated in the figure, the neat PLLA film exhibited a glass transition at 59 °C, two exothermic peaks for cold crystallization at 103 °C and pre-melt crystallization at 161 °C, respectively, and an endothermic melting peak at 179 °C. The thermal characteristics of all films are summarized in Table 1.

The addition of most of the oils decreased the thermal transition temperatures (T_g, T_c, and T_m) of the films. Depending on the oil used, the decrease can be as much as 30 °C in T_g, 45 °C in T_c and 15 °C in T_m (see Table 1). The films prepared with cyclic alkanes showed lower T_g, T_c and T_m than those prepared with linear alkanes, and therefore the interaction between cyclic alkanes and PLA seems to be stronger than the interaction with linear alkanes. With limonene, the lowest thermal transition temperatures were observed (T_g = 30 °C, T_c = 58 °C and T_m = 163 °C), which supports the previous conclusion of strong interaction between this oil and PLA.
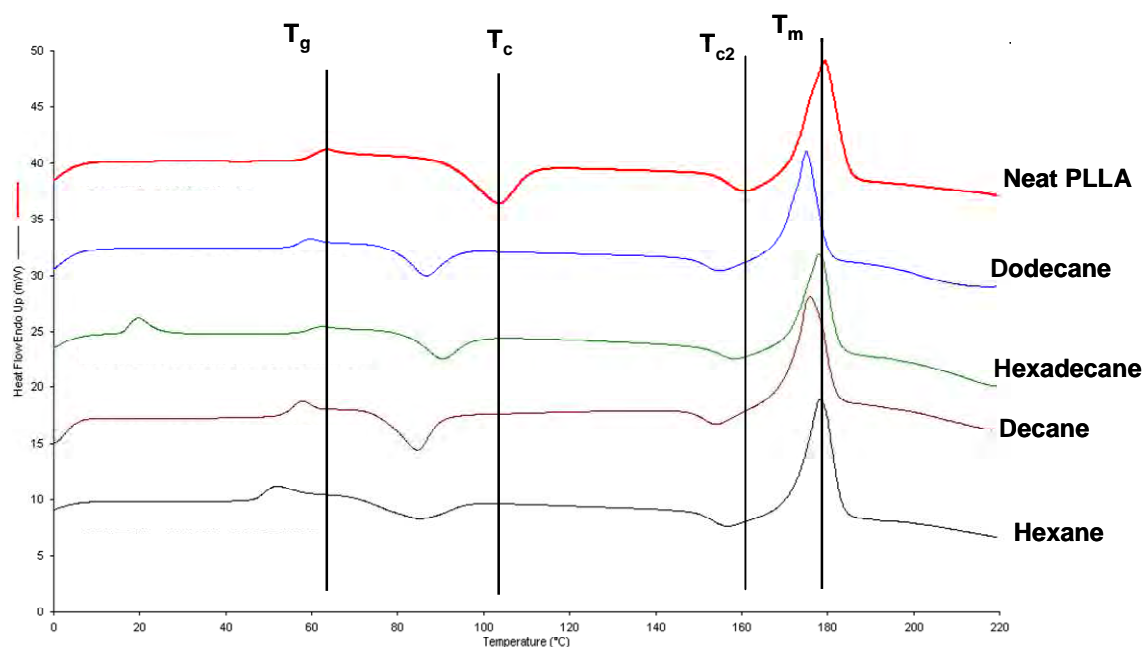
Figure 3: DSC curves of PLLA films prepared with different oils in the casting solution. First line (left), glass transition temperature, second line cold crystallisation temperature, third line pre-melt crystallisation, fourth line, melting temperature.

The degree of crystallinity (X_c) of the films was derived from the heat of fusion of the film (ΔH_f) and heat of fusion of 100% crystalline PLLA (ΔH_f^0) as shown in equation 1a. The heat of fusion of the films was calculated by subtracting the melting enthalpy (ΔH_m) from the enthalpies of cold crystallization (ΔH_c) and pre-

melt crystallization (ΔH_{c2}) (equation 1b) [24]. The heat of fusion of 100% crystalline PLLA was taken from literature (93 J/g) [24].

$$X_c = \frac{\Delta H_f}{\Delta H_f^0} * 100\% \tag{1a}$$

With $\Delta H_f = \Delta H_m - \Delta H_c - \Delta H_{c2}$ (1b)

Table 1: Thermal characteristics of PLLA films prepared with different oils.

Oil	T_g	T_c	T_m	ΔH_c	ΔH_{c2}	ΔH_m	X_c
	°C	°C	°C	J/g	J/g	J/g	%
Neat PLLA	59	103	179	28	8	56	22
Hexadecane	59	90	178	21	7	58	32
Dodecane	56	87	175	19	8	55	30
Decane	54	85	176	23	9	56	26
Hexane	48	85	178	19	8	56	31
Cyclodecane	54	79	164	17	6	38	16
Cyclohexane	39	67	168	22	4	43	18
Eugenol	34	87	170	2	1	48	48
Limonene	30	58	163	26	1	40	14

The results show that the crystallinity of the films strongly depends on the oil used. The maximum degree of crystallinity (48%) was found in the film prepared with eugenol (see Table 1). In general, the films prepared with linear alkanes were more crystalline than those prepared with cyclic alkanes. The lowest X_c (14%) was found for the film prepared with limonene (see Table 1).

The variation in the thermal behavior is in line with the observed structures (Figures 1 and 2). The thermodynamic interactions largely determine the solidification mechanism of the polymer during the preparation process, which affects the morphology and mobility of the created structures. The effects of the

oils on the thermal behavior of the film are similar to those reported for plasticized PLLA, which may suggest that the addition of oils increased the segmental mobility of the PLLA chains in the structure [14, 24]. This is manifested in the decrease in T_g and T_c, which allows the polymer to crystallize at lower temperatures. Therefore, it is expected that this will influence the mechanical properties of the films as described in the next section.

The high crystallinity obtained with eugenol can be explained by the film formation process: the eugenol remained inside the film after evaporation of the solvent, and remains there for some time (while slowly diffusing outwards). The high mobility in the film, due to the high swelling then gives ample time crystallization to take place. Thus, the final film will have higher crystallinity than those films in which the chain mobility was reduced more quickly.

Mechanical properties

Figure 4 shows typical stress-strain dependency curves of the films. The maximum strength, elastic moduli, and elongation values at break are shown in figures 5, 6 and 7, respectively. Neat PLLA film were brittle with a high maximum strength of approximately 60 MPa, elastic modulus of around 2 GPa, and very low elongation at break of < 8%.
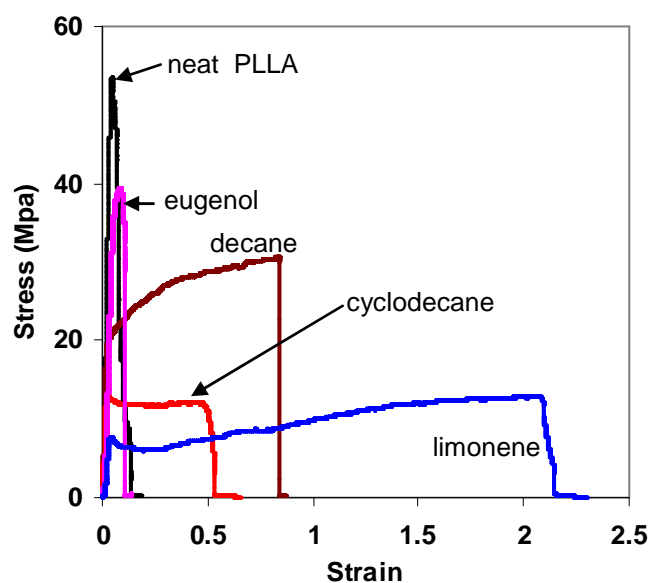
Figure 4: Stress-strain diagrams of PLLA films prepared with different oils in the casting solution. The initial polymer and oil concentrations in all films were 10%w/w.
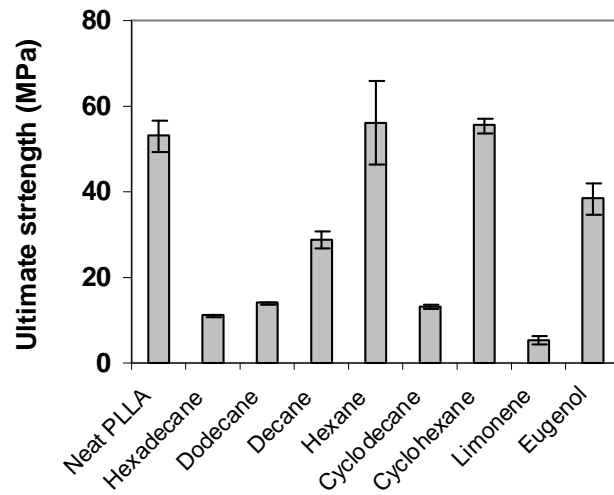
Figure 5: Ultimate strength of PLLA films prepared with different oils in the casting solution. The initial polymer and oil concentrations in all films were 10%w/w.
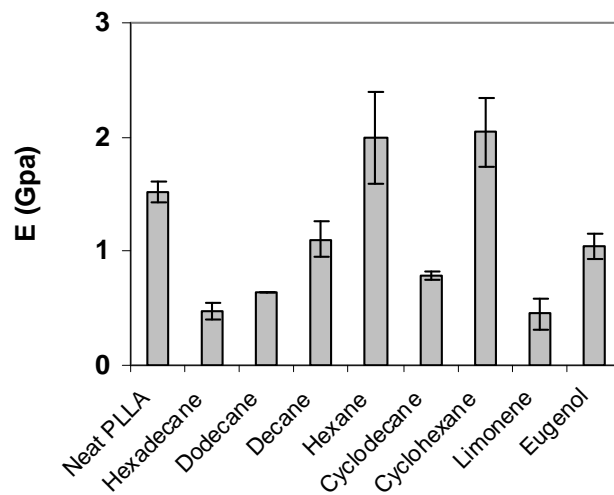
Figure 6: Elasticity modulus of PLLA films prepared with different oils in the casting solution. The initial polymer and oil concentrations in all films were 10%w/w.
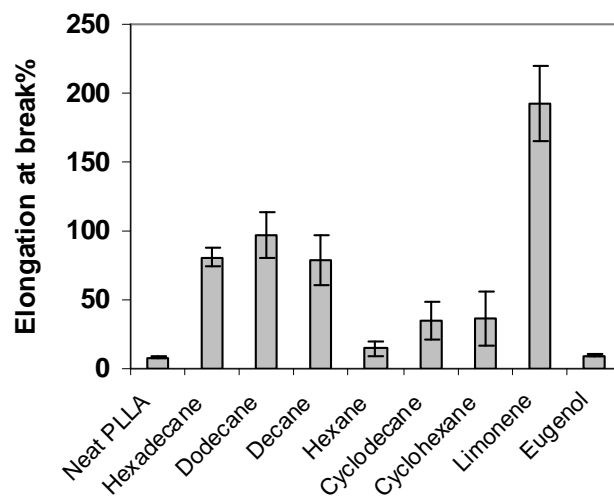
Figure 7: Elongation at break of PLLA films prepared with different oils in the casting solution. The initial polymer and oil concentrations in all films were 10%w/w.

As was the case for the film morphology and their thermal properties, the mechanical properties were highly dependent on the oil used as well (see Figures 4-7). In general, the addition of oils led to reduced tensile strength and elastic moduli whereas the ductility was enhanced. The films prepared with hexane, cyclohexane and eugenol showed similar behavior to neat PLLA film with a relatively high maximum strength and elasticity, and a low elongation at break. With higher linear alkanes (decane, dodecane, and hexadecane), the films were weaker, but the ductility of the films was considerably improved and their elongation at break could be up to 90%. The most remarkable effect was found for limonene, which yielded a very ductile film with an elongation at break of more than 200%. This high ductility is similar to that reported for plasticized PLLA and can be attributed to the fact that the film prepared with limonene has the lowest thermal transitions temperatures, evidence of high segmental mobility of the polymer chains in the film [10, 24]. The increase in the segmental mobility was obvious from the strain hardening of the film (stretching behaviour) during tensile testing as shown in Figure 4.

Summarizing, for porous films, addition of the oils reduces the thermal transitions temperatures of the films and accordingly increases their flexibility and decreases their stiffness. For the solid films formed with hexane and eugenol, we see different behaviour: hexane has very limited influence, while eugenol shows evidence of long-term plasticization, slow formation of a dense film and hence high crystallinity.

Porous films show lower strength and elasticity but higher plastic deformability compared to nonporous films. The presence of the pores in the structure allows dissipation of the fracture energy through the interfaces, which increases the ability of material to absorb more energy during deformation, thus final rupture of the films is delayed [26, 28].

The nature of the porous structure, i.e. the size and size distribution of the pores, seems to influence the mechanical properties. Films with large pores and open structures (i.e cyclodecane or hexadecane) were weaker compared to other films with less open structures (e.g. decane). During stretching of the film, fracture can propagate easily and grow through the porous areas, and this growth is easer and

faster in large pores, which reduces the maximum stress that the film can bear during tension [26, 28].

From these results, it is obvious that addition of oils to PLLA films gives a variety of effects on their properties. PLLA films can be given a range of properties, and therewith, the field of application for PLLA may be extended considerably due to the flexibility of the preparation method.

Conclusions

The properties of PLLA films prepared through air casting can be influenced through addition of oil to the casting solution. The morphology, thermal and mechanical properties of films could be tailored.

In general, addition of oils leads to porosity and lowers the glass transition temperature, therewith allowing the polymer to crystallize at lower temperatures. As a result, the toughness the films improves, and the stiffness is reduced.

Linear alkanes show higher porosities and more symmetric films with increasing alkane chain length, which is due to their volatility. Cyclic alkanes show the same trend, but show higher porosity. This shows that interaction with solvent or polymer is important as well.

Eugenol yielded a dense film with high crystallinity, due to its strong interaction with the polymer; the eugenol remains in the film after evaporation of the solvent and plasticizes the matrix, facilitating crystallization.

The main conclusion of this study is that PLLA films with more desirable properties can be obtained through addition of oils to the casting solution and subsequent removal by freeze-drying. The technique that was used is flexible, and the differences in properties are very pronounced, e.g. up to 200% deformation at break.

Acknowledgements

for preparing the SEM images, and ing. Herman de Beukelaer, A&F-BP Sustainable Chemistry and Technology, Wageningen University, for his help in the DSC analysis.

References

1.   Jacobsen, S., Degée, Ph., Fritz, H.G., Dubois, Ph., Jérôme, R., *Polylactide (PLA) - a new way of production.* Polymer engineering and science, 1999. **39**(7): p. 1311.

2.   Maillard, D., Prud'homme, R.E., *Chirality Information Transfer in Polylactides: From Main-Chain Chirality to Lamella Curvature.* Macromolecules, 2006. **39**(13): p. 4272.

3.   Drumright, R.E., Gruber, P.R., Henton, D.E., *Polylactic acid technology.* Advanced materials, 2000. **12**(23): p. 1841.

4.   Karageorgiou, V., Kaplan, D., *Porosity of 3D biomaterial scaffolds and osteogenesis.* Biomaterials, 2005. **26**(27): p. 5474.

5.   Luciano, R. M., Zavaglia, C. A. C., Duek, E. A. R., Alberto-Rincon, M. C., *Synthesis and characterization of poly(L-lactic acid) membranes: Studies in vivo and in vitro.* Journal of materials science. Materials in medicine, 2003. **14**(1): p. 87.

6.   Mohamed, F., Van Der Walle, C.F., *Engineering biodegradable polyester particles with specific drug targeting and drug release properties.* Journal of Pharmaceutical Sciences, 2008. **97**(1): p. 71.

7.   Sawalha, H., Purwanti, N., Rinzema, A., Schroën, K., Boom, R., *Polylactide microspheres prepared by premix membrane emulsification-Effects of solvent removal rate.* Journal of membrane science, 2008. **310**(1-2): p. 484.

8.   Sawalha, H., Fan, Y., Schroën, K., Boom, R.,*Preparation of hollow polylactide microcapsules through premix membrane emulsification-Effects of nonsolvent properties.* Journal of membrane science, 2008. **325**(2): p. 665.

9.   Ljungberg, N., Wesslén, B., *The effects of plasticizers on the dynamic mechanical and thermal properties of poly(lactic acid).* Journal of Applied Polymer Science, 2002. **86**(5): p. 1227.

10.   Martin, O., Avérous, L., *Poly(lactic acid): plasticization and properties of biodegradable multiphase systems.* Polymer, 2001. **42**(14): p. 6209.

11.   Broström, J., Boss, A., Chronakis, I.S., *Biodegradable films of partly branched poly(L-lactide)-co-poly(ε-caprolactone) copolymer: Modulation of phase morphology, plasticization properties and thermal depolymerization.* Biomacromolecules, 2004. **5**(3): p. 1124.

12. Lu, J., Qiu, Z., Yang, W., *Fully biodegradable blends of poly(l-lactide) and poly(ethylene succinate): Miscibility, crystallization, and mechanical properties.* Polymer, 2007. **48**(14): p. 4196.

13. Jiang, L., Wolcott, M.P., Zhang, J., *Study of biodegradable polylactide/poly(butylene adipate-co-terephthalate) blends.* Biomacromolecules, 2006. **7**(1): p. 199.

14. Kulinski, Z., Piorkowska, E., Gadzinowska, K., Stasiak, M., *Plasticization of poly(L-lactide) with poly(propylene glycol).* Biomacromolecules, 2006. **7**(7): p. 2128.

15. Sheth, M., Kumar, R.A., Davé, V., Gross, R.A., Mccarthy, S.P., *Biodegradable polymer blends of poly(lactic acid) and poly(ethylene glycol).* Journal of applied polymer science, 1997. **66**(8): p. 1495.

16. Ke, T., Sun, S.X., Seib, P., *Blending of poly(lactic acid) and starches containing varying amylose content.* Journal of applied polymer science, 2003. **89**(13): p. 3639.

17. Younes, H., Cohn, D., *Phase separation in poly(ethylene glycol)/poly(lactic acid) blends.* European polymer journal, 1988. **24**(8): p. 765.

18. Pillin, I., Montrelay, N., Grohens, Y., *Thermo-mechanical characterization of plasticized PLA: Is the miscibility the only significant factor?* Polymer, 2006. **47**(13): p. 4676.

19. Hu, Y., Hu, Y.S., Topolkaraev, V., Hiltner, A., Baer, E., *Aging of poly(lactide)/poly(ethylene glycol) blends. Part 2. Poly(lactide) with high stereoregularity.* Polymer, 2003. **44**(19): p. 5711.

20. Park, J.W., Im, S.S., *Phase behavior and morphology in blends of poly(L-lactic acid) and poly(butylene succinate).* Journal of Applied Polymer Science, 2002. **86**(3): p. 647.

21. Jacobsen, S., Fritz, H.G., *Plasticizing polylactide - the effect of different plasticizers on the mechanical properties.* Polymer engineering and science, 1999. **39**(7): p. 1303.

22. Labrecque, L.V., Kumar, R.A., Davé, V., Gross, R.A., Mccarthy, S.P., *Citrate esters as plasticizers for poly(lactic acid).* Journal of applied polymer science, 1997. **66**(8): p. 1507.

23. Chen, C.-C., Chueh, J.-Y., Tseng, H., Huang, H.-M., Lee, S.-Y., *Preparation and characterization of biodegradable PLA polymeric blends.* Biomaterials, 2003. **24**(7): p. 1167.

24. Ljungberg, N., Wesslén, B., *Preparation and properties of plasticized poly(lactic acid) films.* Biomacromolecules, 2005. **6**(3): p. 1789.

25. Shibata, M., Teramoto, N., Inoue, Y., *Mechanical properties, morphologies, and crystallization behavior of plasticized poly(l-lactide)/poly(butylene succinate-co-l-lactate) blends.* Polymer, 2007. **48**(9): p. 2768.

26. Sawalha, H., Schroën, K., Boom, R., *mechanical properties and porosity of polylactide for biomedical applications.* Journal of applied polymer science, 2008. **107**(1): p. 82.

27. Sawalha, H., Schroën, K., Boom, R., *Polylactide films formed by immersion precipitation: Effects of additives, nonsolvent, and temperature.* Journal of Applied Polymer Science, 2007. **104**(2): p. 959.

28. Kinloch, A. J., Young, R. J., *Fracture Behaviour of Polymers*. Applied science publisheres: London and Ney York, 1983.

Chapter 7

Hollow polylactide microcapsules with controlled morphology and thermal and mechanical properties*

Abstract

Hollow polylactide microcapsules were prepared by multistage premix membrane emulsification of polylactide/dichloromethane/oil solutions in water (nonsolvent). Through extraction and evaporation of dichloromethane, a polymer shell was formed around the oil droplet, which was subsequently removed by freeze drying to obtain hollow microcapsules.

The effects of the different oils on the morphology, thermal and mechanical properties of the hollow microcapsules were investigated. All oils resulted in hollow microcapsules with controlled shell thickness of ~ 50 nm except for eugenol, in which irregular, massive capsules were obtained. The properties of the microcapsules were strongly dependent on the oil used, e.g. the thermal transition temperatures found for hollow capsules were lower than for solid particles prepared without any oil. The crystallinity and transition temperatures of the capsules prepared with linear alkanes were higher than for cyclic alkanes; terpenes gave the lowest transition temperatures. The shell stiffness, measured with AFM, was highly dependent on the oil used. Capsules prepared with dodecane showed higher stiffness (3.3 Nm^{-1}) than with limonene (2 Nm^{-1}) or cyclohexane (1.4 Nm^{-1}).

Introduction

Biopolymer polylactide (PLA) is used for biomedical materials because it is nontoxic, biocompatible, and biodegradable in the human body and has a high mechanical strength [1, 2]. Various types of biomaterials have been prepared from PLA, e.g. scaffolds for tissue engineering, implants, sutures, and films [3-5]. PLA is also used in drug delivery systems [6-8]. Encapsulation of drugs and other bioactive compounds within microcapsules may control the release of the encapsulated compounds or may protect them from fast degradation in the body [7]. Hollow PLA microcapsules can serve as ultrasound contrast agents (UCA's) [9-11]. During imaging of the body with ultrasound, the gas core of these hollow capsules allows them to resonate in the acoustic field, which reflects the ultrasound and enhances the image contrast [10]. Moreover, hybrid UCA's that also encapsulate drugs have been developed. In this case the ultrasound can be used for imaging and to trigger the release of the encapsulated drug [9].

PLA microcapsules or UCA's are usually prepared through emulsification [11, 12]. The polymer is dissolved in a proper solvent (e.g. dichloromethane) plus a poor solvent (often called oil). This solution is then emulsified in a continuous phase which consists of a nonsolvent (i.e. water) and a proper stabilizer. After emulsification, the solvent diffuses through the nonsolvent bath and evaporates at the surface of the bath. The droplets slowly become more and more concentrated in both polymer and oil, and at a certain moment these two become incompatible, and phase separation inside the droplet takes place. An internal droplet of mainly oil is created, surrounded by a polymeric solution, which solidifies and forms a skin around the oil droplet. To obtain hollow microcapsules, the oil is removed by freeze-drying [13].

The properties of the polymer shells of microcapsules and UCA's are important for the final application. Factors like crystallinity, glass transition temperature (T_g), morphology, porosity, mechanical strength, and elasticity of the polymer shell will influence the drug release properties and acoustic activity of the microcapsules [14-18]. Some studies have reported that the release rate of a drug can be fine-tuned by controlling the T_g and crystallinity degree of particles [14]; drug release increases

153

with decreasing T_g and degree of crystallinity [14]. Moreover, the biodegradation behaviour and biocompatibility of the microcapsules in the human body are influenced by the thermo-mechanical state of the particles. Crystalline regions within the polymer matrix degrade at a slower rate compared to amorphous ones [19]. Good control may therefore improve and broaden the field of application of hollow PLA capsules.

In a previous work, we have shown that the thermal and mechanical properties of PLA films prepared through film casting can be optimised by addition of different oils to PLA casting solutions [20]. The objective of this study is to investigate these effects for PLA microcapsules. For this purpose, semi-crystalline poly(L-lactide) (PLLA) was used to produce microcapsules by premix membrane emulsification. Different types of oils were used to prepare the microcapsules and the morphology and thermal properties of the capsules were determined and compared. In addition, the mechanical properties of the capsules were probed with atomic force microscopy technique and compared to those obtained for films.

Materials and methods

Materials

PLLA with an intrinsic viscosity of 1.21 dl·g^{-1} was obtained from PURAC (Biochem B.V., Gorinchem, the Netherlands). Dichloromethane (DCM) (HPLC, gradient grade) was purchased from Merck and used as solvent. The oils used for preparation of the capsules were decane (95%), cyclodecane (95%), eugenol, and limonene (≥96%) from Fluka, hexadecane (>99%), and cyclohexane (≥99.5%) from Merck, hexane (HPLC, gradient grade, (≥99.9%)) from Aldrich and dodecane (≥99%) from Sigma-Aldrich. As nonsolvent, Milli-Q water was used with poly-(vinylalcohol) (PVA 23/88) from Ter Hell (Hamburg, Germany) as a stabilizer.

Methods

Preparation of PLLA microcapsules

The nonsolvent used consisted of 3 g of a 1% w/w PVA aqueous solution and 8 g of pure water. The polymer solution was 2% w/w PLLA in DCM. To 11 g of nonsolvent, 0.5 g of polymer solution, 1 g DCM and 0.15 g oil were added. The

premix emulsion was prepared by mixing these solutions in a closed vessel for 1 min at 900 rpm using a magnetic stirrer. The formed emulsion was then homogenized by pushing the emulsion manually through a 1 µm glass-fiber syringe membrane (Acrodisc GF syringe filter, Pall). To evaporate the solvent, the homogenized emulsion was then stirred in an open vessel for 1 h by a magnetic stirrer. Due to out-diffusion and evaporation of the solvent, the polymer solidified around the oil droplets and oil-filled PLLA microcapsules were formed. The microcapsules were then collected by centrifugation, washed with pure water, and subsequently centrifuged again to remove the PVA. After centrifugation, the microcapsules were freeze-dried with Christ Epsilon 2-6D freeze-dryer (Osterode, Germany) to remove the oil core and form hollow capsules. The freeze-drying step was conducted using the same program as was earlier applied for the films [13, 20].

Differential scanning calorimetry (DSC)

The thermal characteristics of the freeze-dried microcapsules including glass transition temperature (T_g), cold crystallization temperature (T_c), melting temperature (T_m) and enthalpies of cold crystallization (ΔH_c), pre-melt crystallization (ΔH_{c2}) and melting (ΔH_m) were measured using DSC. A specific amount of capsules was placed in stainless steel pans and then scanned using Perkin Elmer Diamond DSC (Perkin-Elmer Co., Norwalk, CT) from -60°C to 200°C at a heating rate of 10°C /min.

Mostly, no peaks for the oils were found, but in some preparations, the microcapsules contained traces of oil.

Scanning electron microscope (SEM)

The morphology of the microcapsules was visualized using SEM (JEOL, JSM-5600 LV). A droplet of freeze-dried microcapsules, re-suspended in water was dried on a glass plate and then coated with 10 nm platinum in a dedicated preparation chamber (CT 1500 HF, Oxford Instruments, Oxford UK) before viewing with SEM. To view the inner core of the capsules and to estimate the shell thickness, some of the capsules were fractured before observation with SEM. To break microcapsules, the powder was put on the sticky side of transparent "household" single side sticky tape. The capsules were pushed firmly on the sticky layer with pressed airflow. The transparent tape with the microcapsules was then

put onto double-sided sticky carbon tape (EMS, Washington, U.S.A.). The transparent tape was peeled off from the carbon tape, to fracture the capsules.

Atomic force microscopy (AFM)

Force-distance curves of PLLA microcapsules were obtained using a NanoScope IIIa multimode scanning probe microscope (SPM) with a PicoForce extension (Veeco Instruments Inc, Plainview, NY) equipped with piezoelectric scanner "E" (*x*, *y* range 12.5 µm × 12.5 µm). The force measurements were carried out using standard V-shaped contact mode cantilever (Veeco Instruments Inc, Plainview, NY) with a nominal spring constant of 0.57 N·m^{-1} and tip radius of ~10 nm. The deflection sensitivity of the photo-detector of the AFM was calibrated using a hard substrate (silica chip, which was cleaned in plasma oven).

To immobilize the microcapsules, a droplet of the capsule suspension was dripped onto a silica chip after which the sample was frozen at -80 °C for 1h. The frozen silica chip with microcapsules was subsequently freeze-dried to firmly immobilize the hollow capsules on the chip. To measure the force curves, the chip with microcapsules was located onto the piezoelectric scanner. The sample was then placed under the AFM-tip and the immobilized capsule was compressed between the AFM-tip and silica chip. The vertical position of the tip and the deflection of the cantilever were recorded by instrument software and converted later into force-distance curve. All measurements were performed under ambient conditions (~20 °C and 40% relative humidity) on at least five randomly selected microcapsules per sample. Topographic images of the microcapsules before and after measurements were taken by AFM.

Results and discussion

Effects of oil on thermal properties

Figure 1 shows the DSC thermographs of PLLA microcapsules prepared with different oils. The thermal transition temperatures (T_g, T_c and T_m) and enthalpies (ΔH_m, ΔH_c and ΔH_{c2}) are presented in Table 1. The oils have a big effect on the thermal characteristics of the capsules. Neat PLLA particles (solid particles prepared without oil) showed T_g at 58 °C, T_c at 90 °C and T_m at 177 °C. The thermal transition temperatures of the hollow capsules prepared with oils were

lower than those of solid particles made out of neat PLLA. Table 1 illustrates that depending on the type of oil used, the T_g of the capsules could be reduced up to 30 °C. The same trend was found for T_c and T_m, in which a maximum reduction of about 20 °C, and 15 °C was observed, respectively. The T_g, T_c and T_m of the capsules papered with cyclic alkanes were lower than those prepared with normal alkanes (see Table 1). The terpenes showed the biggest effect on the thermal behaviour of the capsules in which eugenol gave the lowest thermal transition temperatures ($T_g = 30$ °C, $T_c = 71$ °C and $T_m = 163$ °C).

The type of oil did not only influence the thermal transition temperatures, but also the crystallinity of the capsules. The degree of crystallinity is defined as the ratio between the heat of fusion of the capsules and the heat of fusion of 100% crystalline PLLA as described in the following equations.

$$X_c = \frac{\Delta H_f}{\Delta H_f^0} * 100\% \qquad (1a)$$

$$\text{with } \Delta H_f = \Delta H_m - \Delta H_c - \Delta H_{c2} \qquad (1b)$$

Where X_c is the degree of crystallinity, ΔH_f is the heat of fusion of capsules, ΔH_f^0 is the heat of fusion of 100% crystalline PLLA which was given in the literature as 93 J/g [22], and ΔH_c ΔH_{c2}, and ΔH_m are enthalpies of cold crystallization, pre-melt crystallization, and melting respectively.

As can be seen in Table 1, the neat PLLA particles had an X_c of approximately 20%. The X_c of the capsules prepared with oils varied with the type of oil used from around 0% to 45%. The minimum X_c of 0% was obtained with cyclodecane, whereas limonene gave the maximum X_c of 44%. Cyclic alkanes produced capsules with lower crystallinity as compared to the normal alkanes (see Table 1).
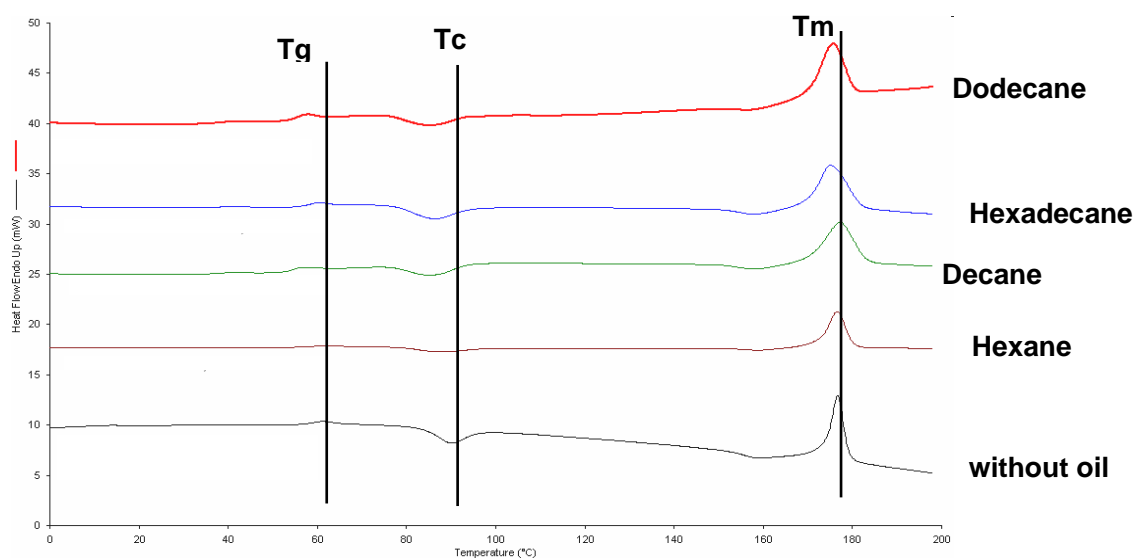
Figure 1: DSC curves of PLLA microparticles prepared with different oils. The measurements were conducted at a heating rate of 10°C /min.

Table 1: Thermal properties of PLLA microcapsules prepared with different oils.

Oil	T_g	T_c	T_m	ΔH_c	ΔH_{c2}	ΔH_m	X_c
	°C	°C	°C	J/g	J/g	J/g	%
Neat PLLA	58	90	177	17	8	43	19
Hexadecane	56	86	175	15	4	35	18
Dodecane	53	85	176	11	3	35	23
Decane	53	86	177	10	4	33	20
Hexane	55	87	177	11	3	45	33
Cyclodecane	45	78	165	15	21	24	~0
Cyclohexane	46	80	173	15	3	41	25
Eugenol	30	71	163	9	0	34	27
Limonene	41	-	174	0	0	41	44

The effects of the oils on the thermal properties of the capsules are related to the effects of the oils on the solidification process of the polymer during the formation of the capsules [20, 23, 24]. Removal of the solvent from the emulsion droplets after emulsification increases the concentrations of the polymer and the oil in the droplets. After some time, the polymer and oil in the droplet reach saturation, and phase separation will take place after which the polymer will solidify around the oil

droplets. The solidification process of the polymer greatly determines the eventual properties of the resulting capsules. The low thermal transition temperatures of the capsules prepared with eugenol suggests that PLLA has better interaction with eugenol than with other oils, which makes the polymer chains more mobile during capsule formation. Correspondingly, the high crystallinity of the capsules prepared with limonene indicates strong interaction of PLLA with limonene which slows down the phase separation and gives mobility and time for crystallization to occur before complete solidification of the polymer. The polymer seems to be less compatible with alkanes as compared to the other oils, consequently, the phase separation takes place more quickly while the mobility of the polymer is reduced faster. Therefore, the thermal transition temperatures with alkanes are higher than for other oils.

When comparing the thermal behaviour of the capsules with that of air-cast films, one can see that most of oils give similar trends in which the thermal transition temperatures were the highest with normal alkanes and the lowest with terpenes, although it should be noted that the preparation method of films is different [20]. The films were prepared by casting and evaporation to the air, while capsules were submersed in a nonsolvent. This indicates that the interactions between the polymer and most of the oils are rather important for the solidification of the polymer. Besides this, solvent interactions are expected to play are role, since the crystallinity in the films was different than in capsules. For example, the crystallinity of the films prepared with limonene was lowest (~15%) [20], whereas it was highest for the capsules with limonene (~ 45%). This may be ascribed to the slower removal rate of the DCM from the capsules into the nonsolvent (DCM and water are poorly miscible) which gives more time for crystallization to take place. The results obtained so far clearly demonstrate that the oils can be effectively used to influence the thermal properties of the capsules. The next section focuses on the effects of the oils on the morphology of the capsules.

Effects of oil on morphology
Figures 2 and 3 show SEM micrographs of hollow PLLA microcapsules prepared with different oils. The majority of the capsules are spherical and have average sizes between 1-2 µm. With all oils hollow capsules could be produced except for

eugenol, in which irregular,, massive particles were formed (see Figure 3d). The formation of hollow capsules is thus influenced by the physical properties of the oil (i.e. mutual solubility and interaction with polymer, solubility in the nonsolvent and boiling point). The oil must be insoluble in the polymer and nonsolvent (otherwise it will not form a separate droplet inside the droplet of polymer solution), and its boiling point should be high enough to stay inside the polymer shell during out-diffusion and evaporation of the solvent. For instance, when the capsules were prepared with volatile oils (i.e. hexane and cyclohexane), some of the oil evaporated during capsules formation which yielded solid particles. The fact that with eugenol no hollow particles were formed may be ascribed to the good interaction of this oil with PLLA which implies that the oil did not create a single droplet of oil and leaves the polymer highly swollen with the oil. The solidification of the polymer slows down, therewith allowing enough time for the oil to diffuse out to the external nonsolvent phase (the solubility in water is higher than for other oils).
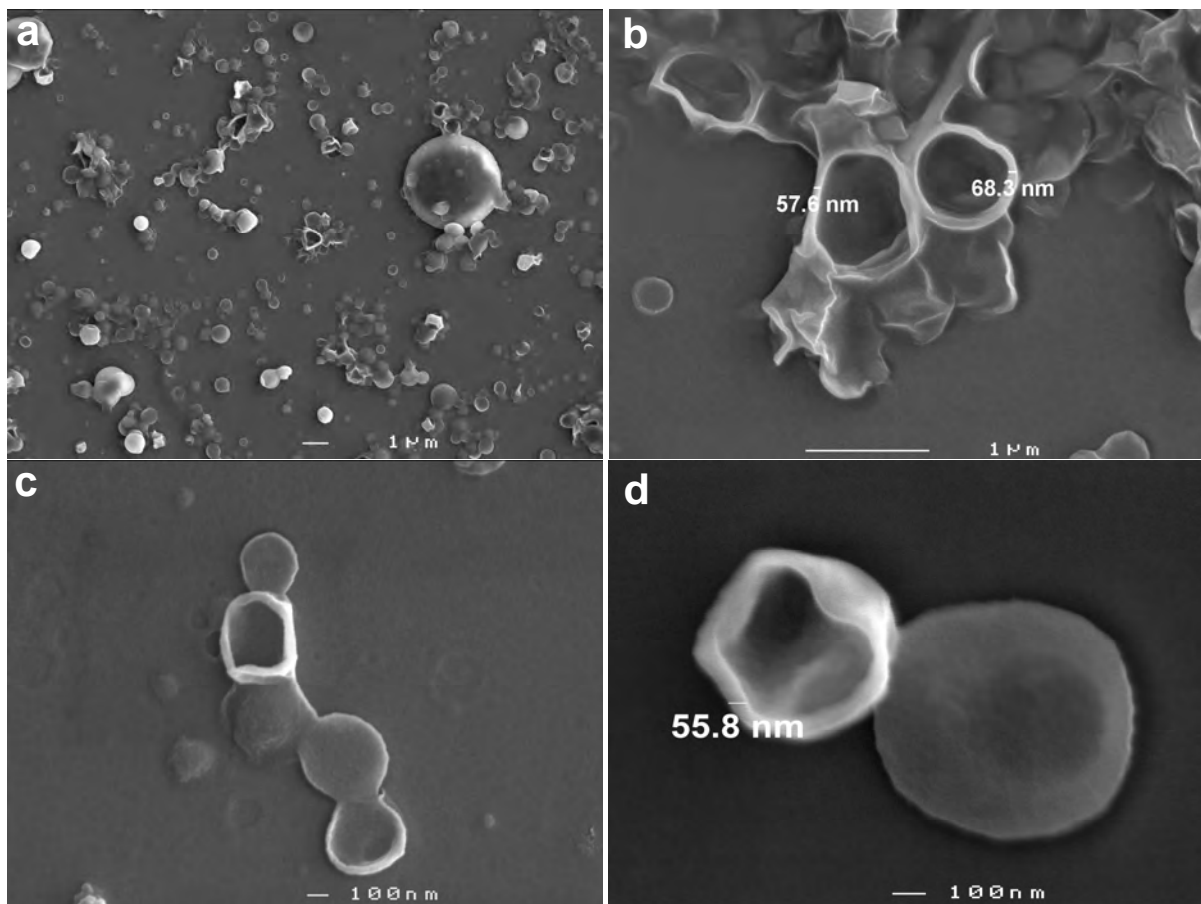
Figure 2: SEM micrographs of PLLA microparticles prepared with different alkanes: (a) and (b) hexadecane, (c) decane, and (d) hexane.

The effects of the oils on the morphology of the air-cast films and capsules prepared in this study are comparable. The oils that produced hollow capsules were the same ones that produced porous films. With eugenol, a dense and nonporous film was obtained which supports the conclusion of strong interaction of the oil with the polymer such that phase separation was avoided and the structure collapsed into a dense film [20].

The shell thickness is another important property of the capsules. Figures 2 and 3 show that most of the oils yielded capsules with relatively homogeneous and controlled shell thicknesses of approximately 50-70 nm. The concentration of the oil is one of the factors that is expected to influence the thickness and morphology of the shell. Figure 4 shows SEM pictures of PLLA capsules prepared from a 10% w/w polymer stock solution and with two different dodecane concentrations. The pictures showed that with increasing the oil concentration from 9% (normal recipe) (Figure 4a) up to 24% w/w (Figure 4b), the shell thickness was reduced and more defects appeared in the shell. In addition, the capsules buckled and crumbled when more oil was used; and this indicates that the shell became much weaker, and could not withstand the generated capillary forces during removal of dodecane. This illustrates that the polymer/oil ratio is an important parameter that can be used to fine-tune the shell thickness and consequently the strength of the capsules.

To investigate the mechanical shell properties in detail, AFM was used, as is described in the next section.

Effects of oil on mechanical properties of capsules
The force-distance curves of hollow PLLA microcapsules prepared with different oils were obtained through AFM. The AFM images of all measured capsules showed that the sizes of these capsules were comparable (between 1-2 µm). In addition, no changes in the topography of capsules before and after experiments were observed, which indicates that the applied load did not cause any irreversible deformation in the capsules, and that the measurements were performed in the elastic regime. Figure 5 shows the typical cantilever deflection (*d*) versus the piezo
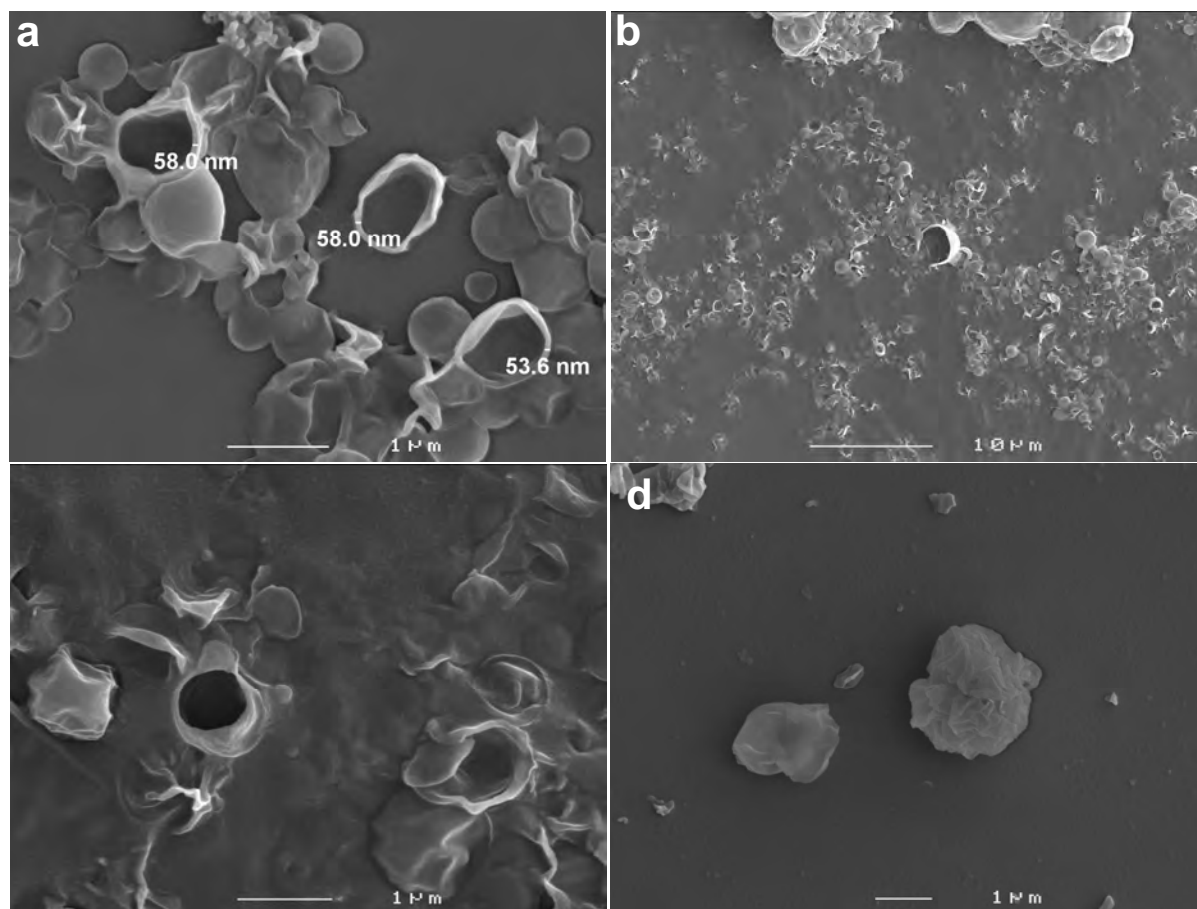
Figure 3: SEM micrographs of PLLA microparticles prepared with different oils: (a) cyclodecane, (b) and (c) limonene, and (d) eugenol.
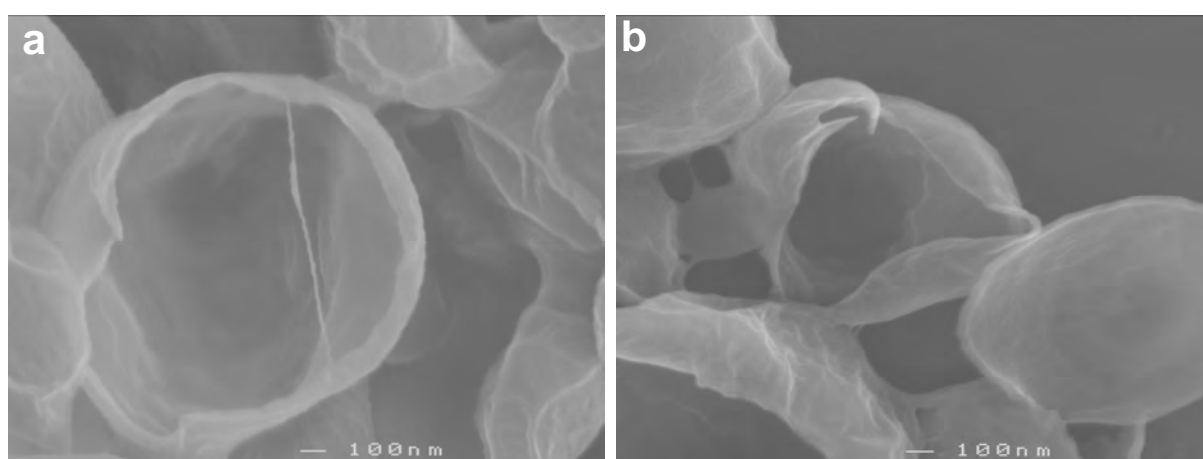
Figure 4: SEM micrographs of PLLA microparticles prepared with different dodecane concentrations: (a) 9% w/w, and (b) 24% w/w. The polymer concentration was 10% w/w PLLA/DCM.

displacement (*z*) curve together with a schematic description of the experiment. The solid curve in the figure corresponds to the approach phase of the tip towards the surface of the capsule. This curve can be divided into three stages. In stage *I* the tip is at a large distance from the capsule and no force is noted. Once the capsule contacts the tip, due to the attractive forces (van der Waals or electrostatic) at stage *II*, the cantilever deflects and upon increasing the applied load, the cantilever continues deflecting until the maximum load is reached (stage *III*). After that, the retraction phase starts in which the piezo movement is reversed and the capsule starts to retract from the tip (dashed curve in Figure 5). Because of adhesion forces, the capsule will stay in contact with the tip, even though no force is applied, until the maximum adhesion force is overcome at point *IV*, after which the tip and the capsule separate and the cantilever returns to its starting point at stage *I*. To convert the deflection-distance curve shown in Figure 5 into a force-distance curve, the applied force (F) [nN] can be estimated from the deflection [nm] using Hooke's law as shown in equation 2:

$$F = -k_c \cdot d \tag{2}$$

Where k_c is the cantilever spring constant [nN/nm or N·m^{-1}], and *d* is the deflection [nm].

Figure 6 shows typical force-distance curves (approach) measurements performed on clean silica chip and hollow PLLA microcapsules prepared with dodecane, limonene and cyclohexane. The stiffness of the shell of the capsules can be calculated from the slope of the force-distance curve as described by Sboros and others [25]. According to Sboros, the deflection of a cantilever applied on elastically deformable material like a microcapsule combines two springs in series as shown in equation 3.

$$\frac{1}{k_{total}} = \frac{1}{k_c} + \frac{1}{k_s} \tag{3}$$

Where k_s is the stiffness of the shell of the capsule (effective spring constant of the shell) [N·m^{-1}], k_c is the cantilever spring constant [N·m^{-1}], and k_{total} is the overall

effective spring constant which is equivalent to the slope of the force-distance curve of the capsule shown in Figure 6.
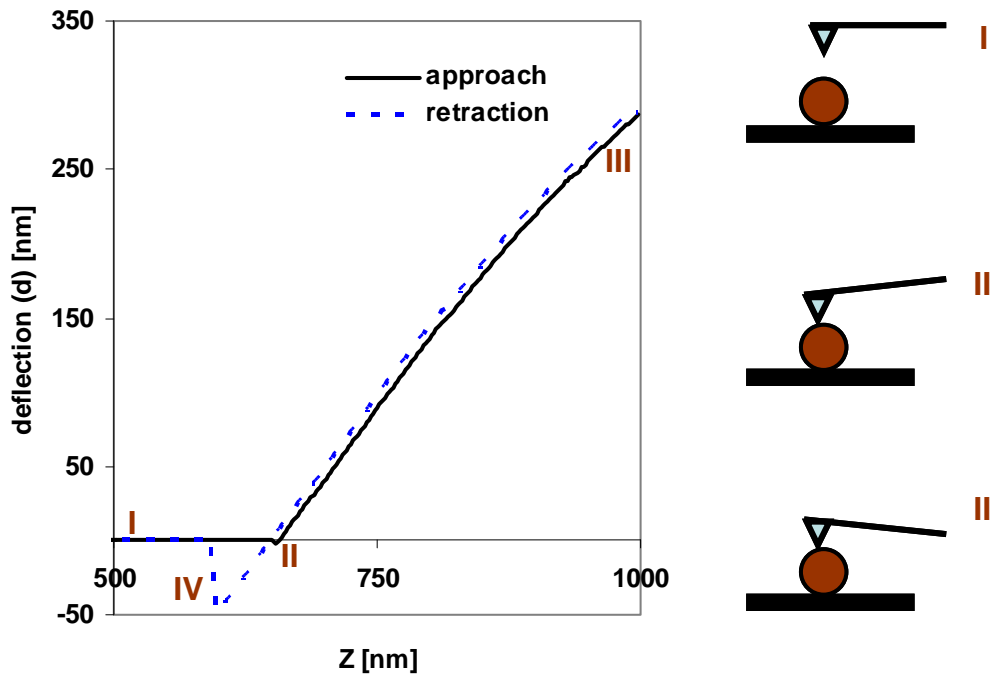
Figure 5: Typical cantilever deflection (d) vs piezo displacement (z) curve measured by AFM (left). On The right, a schematic representation of the positions of the tip and the surface of the sample at different stages during the measurements as indicated by the Roman numerals. The actual curves were measured for microparticle prepared with dodecane.
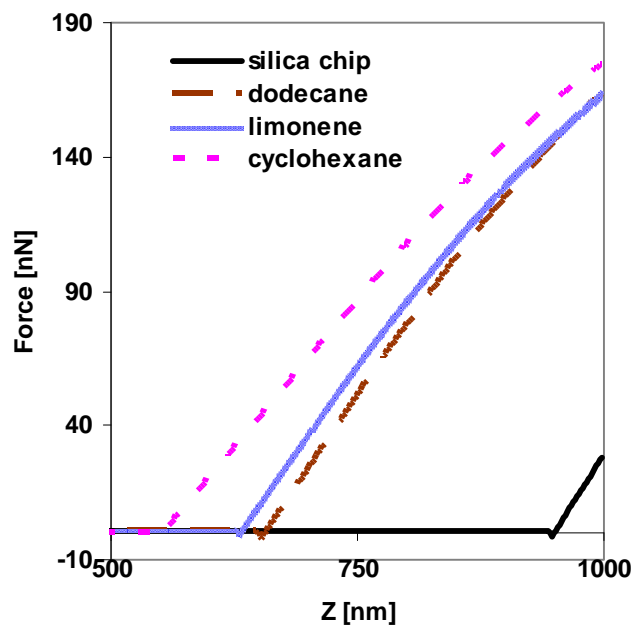
Figure 6: Force-distance curves (approach) measured for clean silica chip and PLLA microparticles prepared with dodecane, limonene and cyclohexane as oils.

The slope of the force-distance curve measured for a clean silica chip was equivalent to the spring constant of the cantilever (~0.57 N·m^{-1}). The curves for the microcapsules showed lower average slopes than the hard silica surface (0.48 ± 0.02 N·m^{-1} for dodecane, 0.44 ± 0.01 N·m^{-1} for limonene and 0.41 ± 0.01 N·m^{-1} for cyclodecane). In Figure 7, the calculated average shell stiffness of these microcapsules is shown. Capsules prepared with dodecane showed significantly higher stiffness (3.3 N·m^{-1}) than with limonene (2 N·m^{-1}) and cyclohexane (1.4 N·m^{-1}). The high stiffness of the capsules prepared with dodecane can be related to the high thermal transition temperatures of these capsules compared to those prepared with limonene and cyclohexane (see Table 1). The shells of the capsules prepared with limonene and cyclohexane were more flexible, which correlates with strong interaction between oil and polymer and higher chain mobility of the shell as was deduced from the DSC results.
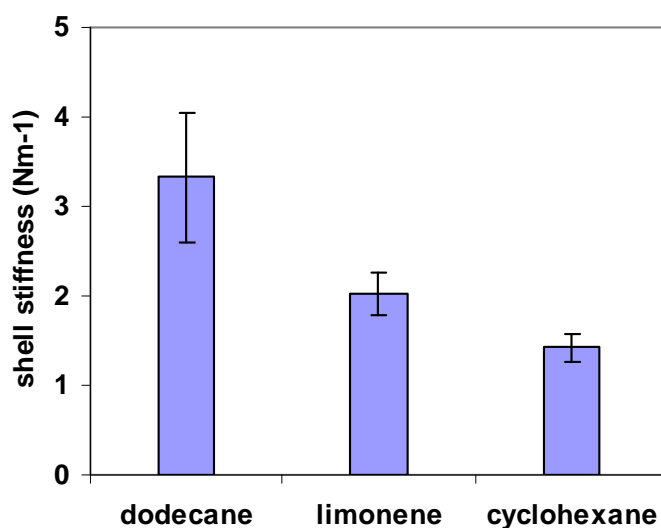
Figure 7: Average shell stiffness of PLLA microparticles prepared with dodecane, limonene and cyclohexane as oils. The average stiffness shown in the figure was measured from 5 particles of each sample. 3 force-distance curves of each particle were analyzed and the slopes were very much similar.

Comparison of the stiffness of the capsules and air-cast films shows major differences. The films prepared with cyclohexane were stiffer than those prepared with dodecane and limonene and the films prepared with limonene were the most

flexible among other films. This could be ascribed to the difference in the structure of the films and capsules. The films prepared with limonene and dodecane have much higher porosity compared to those prepared with cyclohexane, which delayed the final rupture of the films. From this, it is clear that mechanical properties of films are not good indicators for microcapsule properties.

Conclusions

Hollow PLLA microcapsules were prepared using a solution of PLLA in a mixture of good and a poor solvent (oil), emulsified into water, being nonsolvent for the polymer that is immiscible with the two solvents.

The thermal and mechanical properties of hollow PLLA microcapsules depend on the type of oil used. The presence of the oil during formation of the capsules enhanced the mobility during the formation of the shell and reduced the glass transition temperature; allowing crystallization to take place to a greater extent. The crystallinity degree of the capsules could be varied from 0% to 45% by using different oils. Hollow capsules with well-defined shell thicknesses (~ 50 nm) were obtained with all oils, except for eugenol. The stiffness of the shell of the capsules, measured with AFM, was not related to the stiffness of the PLLA films, but was highly dependent on the type of oil. Capsules prepared with dodecane were stiffer than those prepared with limonene and cyclohexane.

Acknowledgements

References

1. Drumright, R.E., Gruber, P.R., Henton, D.E., *Polylactic acid technology.* Advanced materials, 2000. **12**(23): p. 1841.

2. Lim, L.-T., Auras, R., Rubino, M., *Processing technologies for poly(lactic acid).* Progress in polymer science, 2008. **33**(8): p. 820.

3. Lam, K.H., Nijenhuis, A.J., Bartels, H., Postema, A.R., Jonkman, M.F., Pennings, A.J., Nieuwenhuis, P., *Reinforced poly(L-lactic acid) fibres as suture material.* Journal of applied biomaterials, 1995. **6**(3): p. 191.

4. Luciano, R. M., Zavaglia, C. A. C., Duek, E. A. R., Alberto-Rincon, M. C., *Synthesis and characterization of poly(L-lactic acid) membranes: Studies in vivo and in vitro.* Journal of materials science. Materials in medicine, 2003. **14**(1): p. 87.

5. Lee, S. H., Kim, B. S., Kim, S. H., Kang, S. W., Kim, Y. H., *Thermally produced biodegradable scaffolds for cartilage tissue engineering.* Macromolecular bioscience, 2004. **4**(8): p. 802.

6. Mohamed, F., Van Der Walle, C.F., *Engineering biodegradable polyester particles with specific drug targeting and drug release properties.* Journal of Pharmaceutical Sciences, 2008. **97**(1): p. 71.

7. Freiberg, S., Zhu, X. X., *Polymer microspheres for controlled drug release.* International Journal of Pharmaceutics, 2004. **282**(1-2): p. 1.

8. Liu, R., Ma, G., Meng, F.-T., Su, Z.-G., *Preparation of uniform-sized PLA microcapsules by combining Shirasu Porous Glass membrane emulsification technique and multiple emulsion-solvent evaporation method.* Journal of Controlled Release, 2005. **103**(1): p. 31.

9. Kooiman, K., Böhmer, M.R., Emmer, M., Vos, H.J., Chlon, C., Shi, W.T., Hall, C.S., de Winter, S.H.P.M., Schroën, K., Versluis, M., de Jong, N., van Wamel, A., *Oil-filled polymer microcapsules for ultrasound-mediated delivery of lipophilic drugs.* Journal of Controlled Release. **In Press, Corrected Proof**.

10. Lathia, J. D., Leodore, L., Wheatley, M. A., *Polymeric contrast agent with targeting potential.* Ultrasonics, 2004. **42**(1-9): p. 763.

11. Böhmer, M. R., Schroeders, R., Steenbakkers, J. A. M., de Winter, S. H. P. M., Duineveld, P. A., Lub, J., Nijssen, W. P. M., Pikkemaat, J. A., Stapert, H. R., *Preparation of monodisperse polymer particles and capsules by ink-jet printing.* Colloids and surfaces. A, Physicochemical and engineering aspects, 2006. **289**(1-3): p. 96.

12. Vladisavljević, G.T., Williams, R.A., *Recent developments in manufacturing emulsions and particulate products using membranes.* Advances in colloid and interface science, 2005. **113**(1): p. 1.

13. Sawalha, H., Fan, Y., Schroën, K., Boom, R.,*Preparation of hollow polylactide microcapsules through premix membrane emulsification-Effects of nonsolvent properties.* Journal of membrane science, 2008. **325**(2): p. 665.

14. Norris, D.A., Puri, N., Sinko, P.J., *The effect of physical barriers and properties on the oral absorption of particulates.* Advanced Drug Delivery Reviews, 1998. **34**(2-3): p. 135.

15. Kim, H.K., Park, T.G., *Comparative study on sustained release of human growth hormone from semi-crystalline poly(-lactic acid) and amorphous poly(,-lactic-co-glycolic acid) microspheres: morphological effect on protein release.* Journal of Controlled Release, 2004. **98**(1): p. 115.

16. Bouakaz, A., Versluis, M., de Jong, N., *High-speed optical observations of contrast agent destruction.* Ultrasound in Medicine & Biology, 2005. **31**(3): p. 391-399.

17. Grayburn, P.A., *Current and Future Contrast Agents.* Echocardiography, 2002. **19**(3): p. 259.

18. Raisinghani, A., DeMaria, A.N., *Physical principles of microbubble ultrasound contrast agents.* The American Journal of Cardiology, 2002. **90**(10, Supplement 1): p. 3.

19. Wuisman, P.I.J.M., Smit, T.H., *Bioresorbable polymers: Heading for a new generation of spinal cages.* European spine journal, 2006. **15**(2): p. 133.

20. Sawalha, H., Schroën, K., Boom, R., *Addition of oils to polylactide casting solutions as a tool to tune film morphology and mechanical properties.* Submitted, 2008.

21. Ljungberg, N., Wesslén, B., *Preparation and properties of plasticized poly(lactic acid) films.* Biomacromolecules, 2005. **6**(3): p. 1789.

22. Sawalha, H., Schroën, K., Boom, R., *mechanical properties and porosity of polylactide for biomedical applications.* Journal of applied polymer science, 2008. **107**(1): p. 82.

23. Sawalha, H., Schroën, K., Boom, R., *Polylactide films formed by immersion precipitation: Effects of additives, nonsolvent, and temperature.* Journal of Applied Polymer Science, 2007. **104**(2): p. 959.

24.   Sboros, V., Glynos, E., Pye, S.D., Moran, C.M., Butler, M., Ross, J., Short, R., McDicken, W.N., Koutsos, V., *Nanointerrogation of ultrasonic contrast agent microbubbles using atomic force microscopy.* Ultrasound in Medicine & Biology, 2006. **32**(4): p. 579.

Chapter 8

Polylactide microcapsule formation*

Abstract

Polymeric microcapsules are used for different applications. They are commonly produced through emulsion solvent-evaporation / extraction method. In this technique, the polymer (mainly polylactide) is dissolved in a good solvent and together with a poor solvent (oil) is emulsified into a nonsolvent phase. After emulsification, the solvent is removed to the nonsolvent and evaporated, which results in solidification of the polymer around the oil droplets, which is removed later when hollow capsules are required.

This paper discusses the fundamental aspects of the formation process of hollow polylactide microcapsules and its effects on the physical and chemical properties of the capsules, with emphasis on the solidification process of the polymer and the resulting properties of the shell. The scope for improvement and adaptation of the current process, including new emulsification techniques, is also discussed.

The main conclusion of this work is that the properties of the capsules can be fine-tuned through the solidification process of the polymer which can be highly influenced by the choice of the nonsolvent and oil. Since this field is hardly investigated in literature, there is room for improvement, especially if the capsules can be produced with the newest emulsification technologies that are becoming available.

Introduction

Biopolymers have been used extensively for various applications including packaging, membranes, and biomaterials [1-9]. For each product, the required properties of the materials are different from those of the pure polymer. Different routes have been found to alter the properties, especially by using different production techniques, and by using additives. Alternatively, also chemical modification, grafting, cross linking, and interpenetrating polymer networks were suggested, but these options are not considered in this paper.

Polymeric products are generally produced by melt or solution processing [3, 10-12]. During melt processing, the polymer is heated above its melting point, shaped, and then solidified by cooling [10, 12]. Different techniques have been proposed in the literature and much effort has been put into optimizing the processing conditions [10, 12]. For solution processing, the polymer is dissolved in a solvent, shaped into the desired product, and then solidified by evaporation of the solvent to air or extraction to an external nonsolvent [3, 11], which induces phase separation. In both methods, additives may be used to improve the physical and chemical properties of the resulting materials, including other polymers, plasticizers, and fillers [13-20].

We will here discuss the production of polymeric microcapsules; they can contain a liquid droplet, or a gas bubble (hollow microcapsules). These microcapsules are typically between 0.1 and 100 μm, and prepared by solvent evaporation or phase separation, as it allows lower viscosities during processing, which is important when moulding the material in very small dimensions. As the preparation process usually is a complex interplay of interactions between the polymer, and several solvents and additives, prediction of the resulting encapsulate properties is a challenge.

This paper reports on the use of 'minor' variations in the formulation, and process conditions, which can result in large differences in microcapsule properties. We will attempt to link basic phase behaviour to product properties, and these findings

are used in the outlook to give suggestions for improvement of the production method.

Polymer microcapsules – preparation and properties

Polymeric microcapsules have attracted a great deal of interest because of their application in different fields such as medicine, catalysis, cosmetics, and foods [4, 11, 21-24]. In the biomedical field, microcapsules prepared from biodegradable polymers have been frequently used to encapsulate drugs for controlled and sustained release [4, 11]. Biodegradable hollow microcapsules prepared from polylactide (PLA) were successfully used as ultrasound contrast agents (UCA's) to increase the backscatter signal of the ultrasound field and enhance the image resolution [5, 25]. It was even recently reported that microcapsules can be loaded with a drug, and at the same time be acoustically active [25]. The idea behind these capsules is that, when injected in the body, these microcapsules can be ruptured by the ultrasound field, and locally induce high dosage of the drug.

Each application of the microcapsules has specific demands regarding the properties of the capsules, such as their size, size distribution, shell thickness, mechanical characteristics, and in-vivo stability. For example, the acoustic activity of capsules, and therewith related the drug release, is expected to be influenced by the mechanical strength, thickness, and crystallinity of the shell [26-30]. In addition, size and size distribution of the capsules can highly influence their biocompatibility and circulation time within the body [31, 32]. Therefore, tuning the properties of the capsules is a challenge in every sense.

Although different techniques have been used for preparation of microcapsules, such as complex coacervation, spray drying, layer-by-layer assembly, and emulsion solvent-extraction / evaporation, we will focus on the last method, which is used most [11, 33, 34]. In this paper, we will focus further on the biodegradable polymer, polylactide (PLA), which is used often in microcapsule production, and present the effects reported for this polymer as an illustrative example for which effects can be induced in polymers through relatively small changes in the formulation and the formation process.

Phase behaviour of solvent, nonsolvent, and polymer

For the emulsion solvent extraction / evaporation technique, the polymer (i.e. polylactide) is dissolved in a mixture of a good solvent (e.g., dichloromethane, DCM) and a poor solvent (from now on called oil, since it is a higher alkane). The polymer / solvent / oil mixture is then emulsified into a non-solvent phase (water) which usually contains a stabilizer (i.e. polyvinyl alcohol, PVA). Since the solvent is in general hardly soluble in the non-solvent phase, the droplets are initially stable. However, the solvent slowly diffuses to the continuous non-solvent phase and evaporates at the surface. Hence, the droplets slowly become more concentrated.

The demixing process inside the droplets during out-diffusion of solvent is illustrated in more detail in the phase diagram shown in Figure 1. The shaded area is the miscibility gap (oil is a poor solvent for PLA), which is bordered by the binodal. Any composition in the shaded area is not stable, and will demix into a polymer poor and a polymer rich phase, which are connected by tie lines in the phase diagram (interrupted lines). For an initial solution of PLA in DCM and oil represented by point *a*, the solvent is slowly extracted to the external nonsolvent, and the composition of the droplet changes along the arrow towards the PLA-oil axis. The solution becomes richer in PLA and oil: both oil and PLA are strongly incompatible with water, and are not volatile, therefore they do not diffuse out to the nonsolvent and stay in the droplet.

As the droplet becomes more and more enriched in PLA and oil, the composition enters the miscibility gap. Since that will happen at a PLA concentration that is higher than that of the critical point, one will see nucleation of a polymer poor and oil rich phase. From this point, the droplet has two phases; each phase is located on one arm of the bimodal (the direction of the arrow in Figure 1 only represents the overall composition). Since the concentration of solvent is lowest at the interface and highest in the middle of the droplet, the nucleation of the PLA poor (oil rich) phase will be in the middle of the droplet while the polymer rich phase will be in

between the internal oil droplet and the outside nonsolvent bath. The polymer around the oil droplet will ultimately from a (solid) shell. The total volume reduction of the primary emulsion droplet is given by the amount of solvent removed, and therewith the size of the microcapsules is a priori known. The volume of the internal droplet is determined by the amount of oil present [35, 36], and therewith, the shell thickness can be tuned.
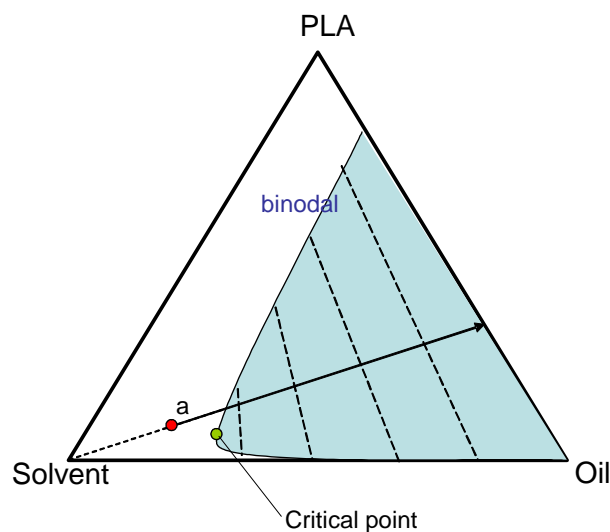
Figure 1: Schematic phase diagram of the PLA-DCM-oil system.

The ultimate solidification of the shell is for an amorphous polymer by glass transition, vitrification, or gelation [37, 38], but for a semi-crystalline polymer as PLA by crystallization [39-41]. The actual structure and properties of the shell is influenced by the rate of solvent removal and the interaction between PLA and oil (as is discussed in the next sections) [3, 39], and therewith it is clear that the mutual thermodynamic interactions between PLA, DCM, oil, and water greatly determine the ultimate properties of the microcapsule [3, 42].

Solvent removal

a. Process options

The miscibility of DCM with the nonsolvent determines its removal rate from the droplets. Water is practically immiscible with DCM, the removal rate is low, and the total formation process is slow as well, therewith allowing ample time for crystallization of PLA [11, 35, 43]. Besides, other effects, such as Ostwald ripening and coalescence, can occur, therewith increasing the polydispersity of the capsules. These drawbacks, can be considerably reduced when the solvent is removed faster.

Several attempts have been made to speed up the removal of the solvent e.g. by increasing the temperature (and hence increasing diffusion rates, DCM dissolution, and increasing its vapour pressure) or decreasing the pressure in emulsion preparation vessel (thereby increasing its evaporation rate) [43]. It was found that increasing the temperature led to larger capsules and lower encapsulation efficiency (i.e., the oil remaining in the shell was lower) [11, 43], and this could be due to less effective solidification at higher temperatures. Decreasing the pressure can enhance the evaporation of DCM to air; however, it will not speed up the transport from droplets towards the water surface, which is the rate-limiting step in the formation process, evaporation is orders of magnitude faster. Some researchers reported that the encapsulation efficiency increased with decreasing pressure whereas others reported a decrease [11, 43]. This may be due to differences in vapour pressure of the oil used; generally, the effects of pressure on encapsulation efficiency are minor, as could be expected for a system that is not limited by evaporation.

Another route is to increase the compatibility between DCM and the nonsolvent phase. Mostly a two-step process is used in literature [11, 44]; the PLA solution is first emulsified into a small amount of water, which facilitates emulsion handling, after which extra water is added. This is done in a single step or in many consecutive steps [44, 45]. Obviously, more water means that more DCM can be extracted. However, since the maximum concentration of DCM in water is quite low, this method requires large amounts of water which complicates harvesting of the capsules, and further, rather large quantities of water contaminated with DCM are produced.

b. Co-solvents

Some studies report the use of co-solvent systems to speed up the total removal of solvent from the spheres [33, 46, 47]. The polymer was here dissolved in a mixture of DCM and another solvent that is miscible with water, e.g. an alcohol. After emulsification, the alcohol is extracted to the water phase, followed by much slower extraction of the DCM. Even though the addition of alcohol will initially increase the total rate of solvent removal, the rate-limiting step in particle formation, which is the out-diffusion of DCM, is not alleviated.

c. Nonsolvent

To overcome the disadvantages of slow removal rate of the solvent, which are inherent to the use of immiscible nonsolvents such as water, it is logical to use a nonsolvent that is better miscible with the solvent. In previous papers, we reported the effects of the nonsolvent quality on the formation of PLA microcapsules and films [35, 36]. To improve the compatibility between DCM and the nonsolvent phase, a lower alcohol (e.g. methanol), which is completely miscible with DCM, was added to water. The solubility of DCM strongly increased with increasing alcohol concentration, therewith speeding up the formation process, as is shown below.

The effect of enhanced removal rate on the structure was evaluated for thin films prepared through immersion precipitation, as model system for capsule preparation [35, 39]. Thin films of PLLA/DCM/dodecane solutions were cast on a glass plate and submerged in a bath filled with different water-methanol mixtures, and phase separation was followed in time. For pure water, demixing starts after ~ 6 min, whereas the demixing time dramatically decreases with increasing methanol concentration; with pure methanol demixing starts after only 2 seconds [39]. As a result, major differences in the structure of the films were observed. With methanol, an asymmetric structure was found consisting of a solid dense top layer and a porous sub-layer (see Figure 2a) [39, 48]. With water, the morphology was completely different: symmetric spherulitic (crystalline) structures with large and irregular interstitial pores were obtained (Figure 2b). The formation of the spherulites (crystals) is ascribed to the slow out-diffusion of DCM which gives ample time for crystallization to take place in the film; the regular porous structure

of the film made with methanol indicates liquid-liquid demixing before crystallization could set in. The nonsolvent composition did not only influence the morphology but also the mechanical properties of the films. The films prepared with water were weak and fragile, while with increasing methanol concentration, the strength and ductility of the films were significantly improved [48].

It is clear, that the nonsolvent influences the rate of the demixing process strongly, and consequently, the properties of the films. Other researchers have reported that the solvent removal rate can influence the crystallinity of the capsules [49]; faster removal of the solvent can decrease the crystallinity of the capsules, as there is not enough time for crystallization to proceed. Similar effects were reported for different oils that also influence the solvent removal rate, as is discussed extensively in the following sections.
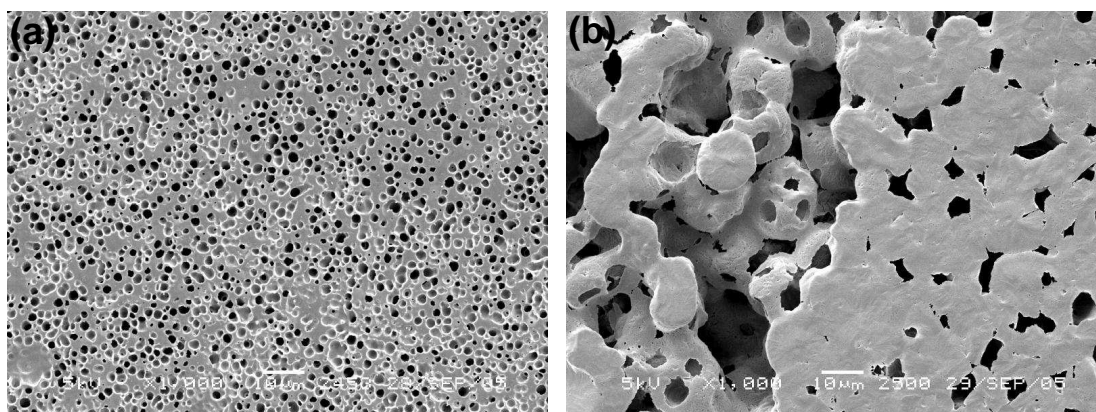
Figure 2: Typical SEM images PLLA films prepared from 10:05:85 w/w PLLA:dodecane:DCM with different non-solvents: a) methanol, b) water [48].

In our own work we found that with increasing methanol concentration, the microcapsules indeed formed faster, and as a desired side effect, their size decreased [35]. Addition of methanol up to 30% facilitated the initial removal of DCM from the droplets, which resulted in faster solidification, which preserved the original shape and size of the capsules (no coalescence was observed). The smaller size of the capsules may be caused by two effects. First, addition of methanol significantly reduces the interfacial tension of the nonsolvent, which will yield smaller droplets during emulsification; ultimately leading to smaller capsules. Second, the addition of alcohol to the nonsolvent bath will also increase the

compatibility of the oil with the nonsolvent. Consequently, some of the oil may be lost to the nonsolvent bath, and the resulting capsules will be smaller. For the combination of non-solvent and oil used in this study, the effect is expected to be only of minor influence, if any, but it may become relevant for other combinations.

At concentrations over 30% w/w, the size of the capsules became bigger, so there is a clear optimum in the alcohol concentration that can be applied. Most likely, the diffusion of methanol into the capsules increased at high methanol concentration; the capsules swell, become bigger and more porous. At methanol concentrations > 50 %, fragments of polymer aggregates were formed instead of microcapsules. Probably, the solution now enters the demixing region near the critical point, or even below it, due to much higher alcohol concentrations in the droplets, and no capsules can be formed.

Besides methanol, also ethanol and 2-propanol were used [36]. The size and the span of the microcapsules were highly dependent on the type of alcohol used. For example, use of 25% (w/w) 2-propanol in the water bath produced capsules with average size of 0.4 µm, compared to 0.8 µm with 30% ethanol, 1.4 µm with 30% methanol, and 2.2 µm with water. In contrast, the size distribution of the capsules formed with 2-propanol was broader than for ethanol and methanol (see Figure 3). The fact that the sizes of the microcapsules were different can be related to various quantities that play a role during emulsification, i.e. interfacial tension and viscosity, but also to different interactions between the polymer, solvent, and oil. How all these parameters are exactly linked is currently unknown.

The main conclusion that can be drawn on the use of different non-solvents is that the properties of the microcapsules (i.e. size, size distribution, and morphology) can be fine-tuned by adjusting the quality of the nonsolvent. An added benefit of enhanced DCM removal through appropriate choice of non-solvent is that the production process can become considerably faster, and a smaller volume of nonsolvent mixture is needed. Besides that, there is also a clear link to the production of smaller capsules, albeit not fully understood.
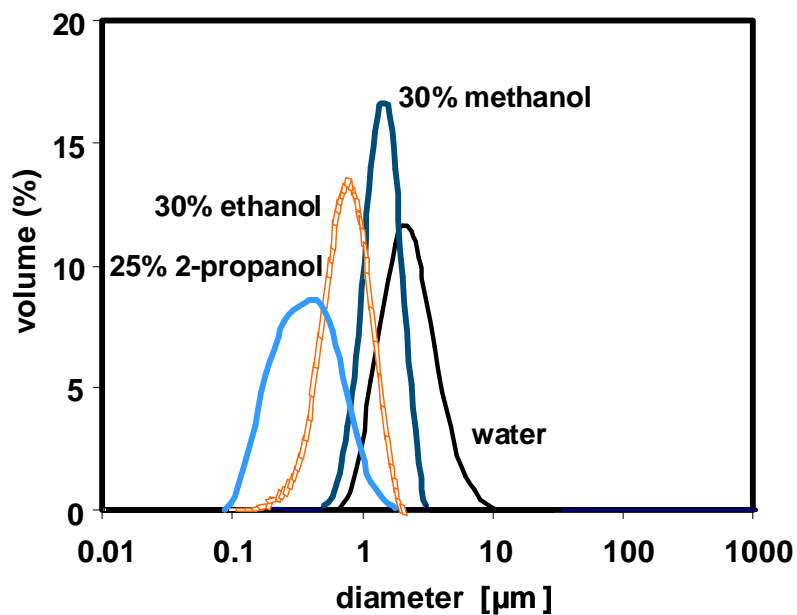
Figure 3: Typical particle size distribution of PLLA microcapsules prepared with different alcohol-water mixtures as nonsolvent [36].

Other options to influence material properties

Blending and annealing

Modification of material properties is mostly achieved through blending/mixing with other polymers or plasticizers, such as poly (ethylene glycol) PEG, polycaprolactone (PCL), poly(1,5-dioxepan) (PDOX), and chitosan. These components were used to influence (bio) degradation, and thermal behaviour of the microcapsules [33, 50-52]. Park and co-workers, showed that capsules prepared from PLLA-PEG copolymer were more hydrophilic and have lower glass transition temperature compared with those prepared with PLLA only [50]. In addition, the presence of the PEG hydrophilic group within the PLLA matrix was reported to increase the drug release rates. In another study, Edlund and Albertsson blended PLLA with PDOX and found that the crystallinity of the microcapsules decreases with increasing PDOX content in the blend [52]. Even though blending therefore seems a successful method, blending polymers has limited practicality, because of limited number of polymers that are compatible; inter-polymer phase separation during microcapsule formation can be expected, and this will not lead to integral microcapsules [53].

Sosnowsk reported that the degree of crystallinity of PLLA capsules could be controlled (0% to 60%) through annealing of the capsules [54]; however, exposing the capsules to high temperatures is not trivial, because it can also lead to major changes in the structure or even complete degradation [54].

Effects of oil

As mentioned previously, removal rate of the solvent plays an important role in the microcapsule formation process. Besides the non-solvent phase, also the oil phase is expected to be of influence on the removal rate, as is clear from Figure 1. To estimate the effects of oil on microcapsule formation, films were used as a model. Films with different dodecane concentrations were immersed in methanol baths, and the delay time of demixing (i.e., the time after which significant demixing sets in after immersion) was shorter for films with higher dodecane concentrations. Demixing starts after ~16 seconds in films prepared without dodecane, whereas demixing is almost instantaneous with 10% dodecane [39]. The presence of the oil in the PLA solution brought the initial composition much closer to the demixing gap. Thus, only a small out-flux of DCM was sufficient to induce demixing, and consequently, the morphology and mechanical properties of the films changed [39]. The presence of the oil induces porosity in the films which reduces their strength, but sometimes increases their ductility [39, 48]. Demixing in these films takes place by nucleation and growth of dodecane-rich droplets entrapped within the polymer rich phase. These droplets were the precursors of most of the pores observed. The oil can therefore play an important role in the formation process and properties of the resulting film. Consequently, it was expected that this would be similar for microcapsules, prepared by premix membrane emulsification [36, 55]. Various oils were tested including alkanes, cyclic alkanes and terpenes (limonene and eugenol), and as expected, the morphology and thermal and mechanical properties of the capsules strongly depended on the oil [55]. With all oils, hollow microcapsules with controlled shell thickness of approximately 50 nm could be formed, except with eugenol, which led to irregular, non-hollow microcapsules.

The thermal transition temperatures of the hollow capsules were lower than of solid microcapsules prepared without oil. Depending on the type of oil used, a reduction

of about 30 °C in the glass transition temperature, 20 °C in the cold crystallization temperature, and 15 °C in the melting temperature was recorded [55]. Besides, crystallinity of the microcapsules was highly dependent on the type of oil: the degree of crystallinity varied from 0% to 45 % depending on the oil used. Furthermore, the type of oil influenced the mechanical stiffness of the shell as measured with AFM: microcapsules prepared with dodecane were stiffer than when prepared with limonene and cyclohexane. Therefore, just as with the films, the mechanical properties of the very thin microcapsule shells were influenced by the type of oil used, albeit differently than for films, as will be described later [55].

The differences in the thermal and mechanical properties of the capsules can be attributed to different interactions between polymer, solvent, nonsolvent, and oil, which affect the demixing and solidification process. For example, the low thermal transition temperature of the capsules prepared with terpenes is due to the better interaction of the polymer with these oils, which delays the demixing during microcapsule formation, and gives extra mobility to the polymer chains before complete solidification of the shell (and this can lead to crystallization that is more extensive). Eugenol seems to have such a strong interaction with PLLA that the oil and the polymer did no phase separate. No separate oil droplet was formed in the middle of the capsule, and a swollen, non-hollow particle resulted.

From the above, it is clear that interactions between oil and polymer can be essential for microcapsule formation; however, also the non-solvent can have an influence as discussed in previous sections. Although indirectly, influence of nonsolvent in-diffusion on the solidification process could be estimated from a comparison of results for microcapsules and air cast films [55, 56]. Most of the oils induced porosity and reduced the thermal transition temperatures, and the maximum strength of the films, while the ductility improved [56]. As for capsules, the thermal transitions of the films were lowest with terpenes, and highest with alkanes, in spite of the absence of the nonsolvent. This implies that the interaction between the polymer and most of the oils is a dominant effect during solidification. The crystallinity of the films did not show the same trend as for microcapsules. For instance, capsules prepared with limonene and water as nonsolvent were much more crystalline (~ 45%) than air-cast films prepared with the same oil (~ 15%).

This may well be due to the nonsolvent; the removal of DCM from the capsules through the external water phase is much slower than for air-cast films (direct evaporation of DCM), which allows more time for crystallization in the capsules. Further, a major difference in the stiffness of the capsules and films was observed. In contrast to the microcapsules, films prepared with limonene and dodecane were much more ductile than those prepared with cyclohexane. This can be attributed to the porosity of the first mentioned films, which allows more dissipation of fracture energy during extension [56].

The effects of the oils on the thermal and mechanical properties of the capsules and films indicate a plasticizing effect of the oil on the polymer chains; the effects are quite similar to those reported in the literature for plasticizers. This is interesting since it was thought that the main purpose of the oil in the current process was to form a template for the shell, resulting in control over the shell thickness, whereas from the effects described earlier it is clear that it is just as important for tuning the thermal and mechanical properties.

In summary, the major effects in phase behaviour seem to be caused by the nonsolvent and oil; properties of PLA microcapsules can be tuned, and this may extend their range of application.

Emulsification methods

Next to the mechanical properties of the microcapsule walls, also size and size distribution are important. Various existing options for production of the primary emulsions have been reported, which will be discussed below. In addition, some newer technologies will be mentioned in the outlook section, and their potential for capsule formation will be discussed.

Existing methods
a. Pre-mix emulsification
Currently, pre-mix membrane emulsification seems to be the method of choice for microcapsule production, because of its simplicity, versatility, and productivity.

The method involves mixing of the ingredients and repeated passage through a membrane. The microcapsules that are produced have a relatively sharp distribution, because of repeated passage through the membrane. However, there is a limit to the rate of phase separation, since the droplet should remain fluid during repeated passage through the membrane. As mentioned previously, proper choice of the non-solvent may help in optimising this.

Pre-mix emulsification also allows production of microcapsules that have combined functionalities. For example, microcapsules can be produced that are only partially filled with oil, which carries a lipophilic drug, and shows acoustic activity, as demonstrated by Kooiman and co-workers [25]. In this way, the capsules can be used for diagnostics and therapy. The emulsification step does not have to be adjusted; only the PLA solution should contain a mixture of oils, of which one is not removed by freeze-drying.

An issue that still needs to be resolved is how pre-mix emulsification can be scaled up. For a niche product like microcapsules, the current method is sufficient, but if larger volumes are to be produced, obviously, the critical times for the various processes to take place need to be adjusted, to allow handling of the larger volumes, and this is still considered a challenge.

b. Cross-flow emulsification

Although the capsule size distribution obtained for pre-mix membrane emulsification is relatively narrow, further improvement would be useful. In literature, cross flow emulsification is used for regular oil-in-water and water-in-oil emulsions, particles, and capsule formation, and with this technology, good results could be obtained [21, 57-60]. For cross-flow emulsification, the oil is pressed through the membrane, and the oil droplets which emerge from the topside of the membrane, are carried away by the cross-flowing continuous phase. In general, low interfacial tensions (as reported for alcohol / water mixtures) facilitate production of smaller droplets by cross-flow emulsification. The membrane of choice is Shirazu porous glass, which works well in various applications. A critical point for this method is that phase separation should not take place inside the membrane, since this would lead to blockage of pores and loss of productivity. Besides, the

membrane area needed for larger production rates could be a drawback, as was the case for pre-mix emulsification.

c. Ink jetting method

A different method is ink jetting as described by Böhmer and co-workers [34]. Very monodisperse particles and capsules could be obtained, as is illustrated in Figure 4. The productivity, of the technique is quite high; up to 600,000 capsules per second could be made with one nozzle. The size of the capsules is uniform, and could be slightly tuned through the choice of the emulsification nozzle. In general, the generated droplets are large and relatively low polymer concentrations have to be used to allow sufficient reduction in size through removal of the solvent. Although the productivity of one nozzle is high, scale-up of this technology is a major challenge, as is the reduction of the amount of solvent that is currently needed.
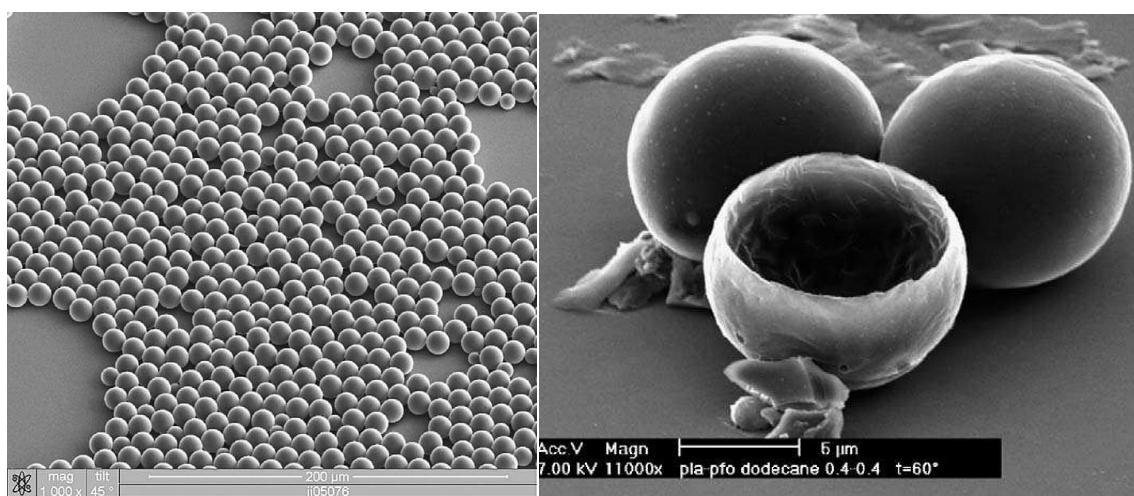
Figure 4: SEM images of products prepared through ink jetting. Solid particles are shown on the left, on the right hollow particles are shown that were obtained by freeze drying of oil filled particles [34].

Outlook

Microcapsules

For each application, the PLA microcapsules will need to meet specific requirements. The size of UCA's, together with the ductility, and mechanical strength of the shell are expected to highly influence acoustic behaviour. For instance, a ductile shell is expected to allow the bubble to resonate better and longer in the acoustic field than stiffer shells before bursting completely, which would be important for imaging purposes. The mechanical strength of the shell is expected to determine the maximum acoustic pressure needed to burst the microbubble. Its strength should be sufficient but not too high, since the bubble should burst at medically safe pressures. In drug delivery, a fast and controlled release of the drug is preferred in some cases, whereas in other cases slow release is required. The various factors discussed in the previous sections showed that control of structure, crystallinity, glass transition, and mechanical strength, are within reach, and therewith, optimising the properties for specific application may become feasible.

One of the main problems that occurred during preparation of drug-loaded capsules was that the drug encapsulation efficiency was insufficient, due to out-diffusion of the encapsulated drug during microcapsule formation. A faster solidification of the polymer through faster removal is expected to improve encapsulation efficiency considerably. Use of alcohol-water mixtures as non-solvent system seems to be a promising road for that.

The properties of the capsules strongly depend on the demixing and solidification process of the polymer, which can be controlled by the choice of nonsolvent and oil. A window of operation that links the properties of the capsules with the solidification process of the polymer can lead to a straightforward route for optimization of the properties of the microcapsules. To establish that, the phase separation behaviour of the polymer with different oils, solvents, and nonsolvent systems needs to be studied quantitatively. Although this sounds like a very straightforward way to go, construction of phase diagrams, and investigation of microcapsule properties, is a time consuming task. However, given the possibilities that it opens, it may be well worth the (time) investment.

Although ideally, all interactions are taken into account as described above, some general rules of thumb are obvious from the previous sections. The solvent–nonsolvent interaction is expected to dominate the initial stages of the phase separation, and therewith the size and the morphology of the microcapsules. Whereas, the oil-polymer interaction is expected to be most relevant for the solidification processes (i.e. crystallization, vitrification or glassification), which will determine the mechanical and thermal properties of the shell.

Although this paper focuses on PLA, it is expected that similar effects will play a role for microcapsules from other polymers. The nonsolvent-solvent interactions will determine the solvent removal rate, and therewith the size and morphology. The solidification process and consequently the properties of the capsules or films will mostly depend on the polymer and its interactions with oil.

Emulsification methods

Within the field of microtechnology, various new emulsification technologies have been proposed, and some of these seem to be well suited for the preparation of monodisperse capsules, albeit that they have not been tested for this specific purpose. Here we give a small overview of those methods that would allow up- or outscaling to realistic productivities (see Table 1).

Table 1: Comparison of two of micro technological devices for capsule production.

Technique	Formation mechanism	Productivity	Scalable	Issues	Feasibility
T-junctions	Shear forces detach droplets	High	Yes	Surface interactions	+
Micro channels	Spontaneous droplet formation	Medium	Yes	Surface interactions	+

Microsieves and microchannels with T-shaped (see Figure 5) or Y-shaped junctions, use the shear force by a cross-flowing phase to detach droplets, as was the case for cross-flow membrane emulsification [61]. The main advantage of the micro technological device is that the shear forces can be precisely controlled, and therefore, uniform droplets are formed. The productivity per junction is high, up to 1000's of droplets per second, depending on the choice of the components used. Outscaled systems (i.e., systems using many microchannels working in parallel) have been reported in literature. Nisisako and Torii [62], developed a system with 256 parallel junctions, while Van der Graaf, and Abrahamse used microsieves featuring many pores actively simultaneously [63, 64].
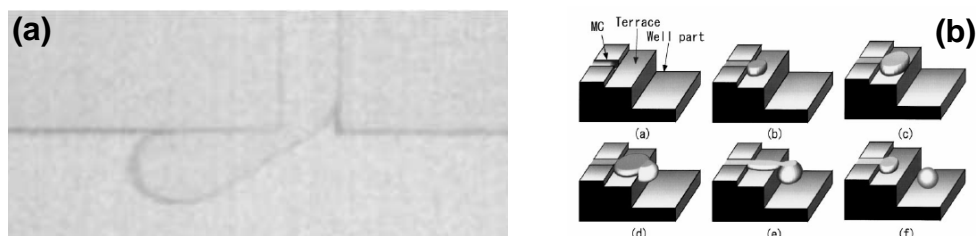
Figure 5: Scalable micro technological methods for the production of droplets. A: T-junction where the oil is pushed from the small channel into the larger channel that hosts the cross-flowing continuous phase [61]. B. Microchannel, where the oil is pushed onto a terrace where it forms a disk. Once the disk reaches the end of the terrace, it can form a spherical droplet, which subsequently detaches [65].

In microchannel emulsification, first presented by Sigiura and co-workers [65], and scaled-up by Kobayashi c.s., oil is first pushed onto a so-called terrace, where it assumes a disk-like shape. This disk grows through the continuous oil supply, and eventually reaches the end of the terrace, where it can assume a spherical shape. Because of the Laplace pressure differences that are involved in this change in shape, the droplet will snap off spontaneously; at low throughputs, the size of the droplets is determined by the design of the terrace only. Very monodisperse emulsions can be produced with these systems. Although the productivity is not as high as for shear- based systems, the method is scalable and does have the advantage that only the oil phase needs to be controlled. Out-scaled versions of microchannels have been developed and were discussed in literature [62].

Although various other microtechnological methods are known from literature, only microchannel emulsification, cross-flow emulsification with microsieves, and to a lesser degree, T- and Y-shaped microchannel systems can be outscaled. As all these systems inherently feature a very high surface-to-volume ratio, interaction of the polymer solutions with the surface of the device is a matter of concern. Surfaces that are not sufficiently hydrophilic or that would change their properties during processing will lead to plugged microchannels and process failure. Various modification methods are known from literature, and the surfaces of glass and Si (typical materials used for micro devices) can be modified seemingly at will [66-69]. However, reliable application of these methods inside a microstructure is still a challenge.

Conclusion: The 'ideal' process

In an ideal production system for polylactide microcapsules, small, and relatively uniform capsules can be produced. Further, it is possible to control the thermal and mechanical properties of the shell. And even more ideally, the process is flexible and has a high throughput.

Premix membrane emulsification combines many of these aspects; it has high throughput and acceptable control over the size and size distribution. Through adjustment of the nonsolvent composition, solidification of the polymer can be controlled, the original size and morphology of the capsules can be preserved better, and it is expected that also encapsulation efficiency can be enhanced. The properties of the microcapsules can even be fine-tuned through the choice of the added 'oil'. And therewith, pre-mix emulsification has many benefits.

In the future, it is expected that premix emulsification can be replaced by other micro-technological devices such i.e. micro-channel or micro-sieve systems, which give sharper size distributions. For cross-flow systems, the size of the particles can even be reduced further when using a non-solvent with a low interfacial tension (given that there is sufficient time before solidification sets in). In microchannel

systems, a non-solvent with a high interfacial tension (i.e. water) needs to be used to produce small droplets. For further tuning of the microcapsule properties, different stages including other non-solvent baths, could be an option, albeit that this would lead to more complex microcapsule harvesting as indicated in previous sections. For both technologies, it is clear that out-scaling and surface modification of these systems to make them more compatible with polymer solutions is still a major challenge, but once these hurdles are taken, a new generation of truly monodisperse microcapsules will become available.

References

1.   Mohamed, F., Van Der Walle, C.F., *Engineering biodegradable polyester particles with specific drug targeting and drug release properties.* Journal of Pharmaceutical Sciences, 2008. **97**(1): p. 71.

2.   Auras, R., Harte, B., Selke, S., *An overview of polylactides as packaging materials.* Macromolecular bioscience, 2004. **4**(9): p. 835.

3.   Van de Witte, P., Dijkstra, P. J., Van den Berg, J. W. A., Feijen, J., *Phase separation processes in polymer solutions in relation to membrane formation.* Journal of Membrane Science, 1996. **117**(1-2): p. 1.

4.   Freiberg, S., Zhu, X. X., *Polymer microspheres for controlled drug release.* International Journal of Pharmaceutics, 2004. **282**(1-2): p. 1.

5.   Lathia, J. D., Leodore, L., Wheatley, M. A., *Polymeric contrast agent with targeting potential.* Ultrasonics, 2004. **42**(1-9): p. 763.

6.   Karageorgiou, V., Kaplan, D., *Porosity of 3D biomaterial scaffolds and osteogenesis.* Biomaterials, 2005. **26**(27): p. 5474.

7.   Lam, K.H., Nijenhuis, A.J., Bartels, H., Postema, A.R., Jonkman, M.F., Pennings, A.J., Nieuwenhuis, P., *Reinforced poly(L-lactic acid) fibres as suture material.* Journal of applied biomaterials, 1995. **6**(3): p. [d]191.

8.   Luciano, R. M., Zavaglia, C. A. C., Duek, E. A. R., Alberto-Rincon, M. C., *Synthesis and characterization of poly(L-lactic acid) membranes: Studies in vivo and in vitro.* Journal of materials science. Materials in medicine, 2003. **14**(1): p. 87.

9.   Lee, S. H., Kim, B. S., Kim, S. H., Kang, S. W., Kim, Y. H., *Thermally produced biodegradable scaffolds for cartilage tissue engineering.* Macromolecular bioscience, 2004. **4**(8): p. 802.

10.   Rhim, J.-W., Mohanty, A.K., Singh, S.P., Ng, P.K.W., *Effect of the processing methods on the performance of polylactide films: Thermocompression versus solvent casting.* Journal of applied polymer science, 2006. **101**(6): p. 3736.

11.   Freitas, S., Merkle, H.P., Gander, B., *Microencapsulation by solvent extraction/evaporation: Reviewing the state of the art of microsphere preparation process technology.* Journal of Controlled Release, 2005. **102**(2): p. 313

12. Lim, L.-T., Auras, R., Rubino, M., *Processing technologies for poly(lactic acid).* Progress in polymer science, 2008. **33**(8): p. 820.

13. Broström, J., Boss, A., Chronakis, I.S., *Biodegradable films of partly branched poly(L-lactide)-co-poly(ε-caprolactone) copolymer: Modulation of phase morphology, plasticization properties and thermal depolymerization.* Biomacromolecules, 2004. **5**(3): p. 1124.

14. Sheth, M., Kumar, R.A., Davé, V., Gross, R.A., Mccarthy, S.P., *Biodegradable polymer blends of poly(lactic acid) and poly(ethylene glycol).* Journal of applied polymer science, 1997. **66**(8): p. 1495.

15. Ke, T., Sun, S.X., Seib, P., *Blending of poly(lactic acid) and starches containing varying amylose content.* Journal of applied polymer science, 2003. **89**(13): p. 3639.

16. Labrecque, L.V., Kumar, R.A., Davé, V., Gross, R.A., Mccarthy, S.P. , *Citrate esters as plasticizers for poly(lactic acid).* Journal of applied polymer science, 1997. **66**(8): p. 1507.

17. Jacobsen, S., Fritz, H.G., *Plasticizing polylactide - the effect of different plasticizers on the mechanical properties.* Polymer engineering and science, 1999. **39**(7): p. 1303.

18. Martin, O., Avérous, L., *Poly(lactic acid): plasticization and properties of biodegradable multiphase systems.* Polymer, 2001. **42**(14): p. 6209.

19. Ljungberg, N., Wesslén, B., *Preparation and properties of plasticized poly(lactic acid) films.* Biomacromolecules, 2005. **6**(3): p. 1789.

20. Leszczyńska, A., Njuguna, J., Pielichowski, K., Banerjee, J.R., *Polymer/montmorillonite nanocomposites with improved thermal properties: Part I. Factors influencing thermal stability and mechanisms of thermal stability improvement.* Thermochimica Acta, 2007. **453**(2): p. 75.

21. Vladisavljević, G. T., Williams, R. A., *Recent developments in manufacturing emulsions and particulate products using membranes.* Advances in colloid and interface science, 2005. **113**(1): p. 1.

22. Johnston, A.P.R., Cortez, C., Angelatos, A.S., Caruso, F., *Layer-by-layer engineered capsules and their applications.* Current Opinion in Colloid & Interface Science, 2006. **11**(4): p. 203.

23. Buonomenna, M.G., Figoli, A., Spezzano, I., Davoli, M., Drioli, E., *New PVDF microcapsules for application in catalysis.* Applied Catalysis B: Environmental, 2008. **80**(3-4): p. 185.

24.   Morganti, P., Ruocco, E., Wolf, R., Ruocco, V., *Percutaneous absorption and delivery systems.* Clinics in Dermatology, 2001. **19**(4): p. 489.

25.   Kooiman, K., Böhmer, M.R., Emmer, M., Vos, H.J., Chlon, C., Shi, W.T., Hall, C.S., de Winter, S.H.P.M., Schroën, K., Versluis, M., de Jong, N., van Wamel, A., *Oil-filled polymer microcapsules for ultrasound-mediated delivery of lipophilic drugs.* Journal of Controlled Release. **In Press, Corrected Proof**.

26.   Kim, H.K., Park, T.G., *Comparative study on sustained release of human growth hormone from semi-crystalline poly(-lactic acid) and amorphous poly(,-lactic-co-glycolic acid) microspheres: morphological effect on protein release.* Journal of Controlled Release, 2004. **98**(1): p. 115.

27.   Grayburn, P.A., *Current and Future Contrast Agents.* Echocardiography, 2002. **19**(3): p. 259.

28.   Norris, D.A., Puri, N., Sinko, P.J., *The effect of physical barriers and properties on the oral absorption of particulates.* Advanced Drug Delivery Reviews, 1998. **34**(2-3): p. 135.

29.   Bouakaz, A., Versluis, M., de Jong, N., *High-speed optical observations of contrast agent destruction.* Ultrasound in Medicine & Biology, 2005. **31**(3): p. 391.

30.   Raisinghani, A., DeMaria, A.N., *Physical principles of microbubble ultrasound contrast agents.* The American Journal of Cardiology, 2002. **90**(10, Supplement 1): p. 3.

31.   Gref, R. R., Minamitake, Y., Peracchia, M. T., Trubetskoy,V., Torchilin,V., Langer, R., *Biodegradable long-circulating polymeric nanospheres.* Science, 1994. **263**(5153): p. 1600.

32.   Chu, L. Y., Park, S. H., Yamaguchi, T., Nakao, S. I., *Preparation of Micron-Sized Monodispersed Thermoresponsive Core-Shell Microcapsules.* Langmuir, 2002. **18**(5): p. 1856.

33.   Lassalle, V., Ferreira, M.L., *PLA Nano- and Microparticles for Drug Delivery: An Overview of the Methods of Preparation.* Macromolecular Bioscience, 2007. **7**(6): p. 767.

34.   Böhmer, M. R., Schroeders, R., Steenbakkers, J. A. M., de Winter, S. H. P. M., Duineveld, P. A., Lub, J., Nijssen, W. P. M., Pikkemaat, J. A., Stapert, H. R., *Preparation of monodisperse polymer particles and capsules by ink-jet printing.* Colloids and surfaces. A, Physicochemical and engineering aspects, 2006. **289**(1-3): p. 96.

35. Sawalha, H., Purwanti, N., Rinzema, A., Schroën, K., Boom, R., *Polylactide microspheres prepared by premix membrane emulsification-Effects of solvent removal rate.* Journal of membrane science, 2008. **310**(1-2): p. 484.

36. Sawalha, H., Fan, Y., Schroën, K., Boom, R.,*Preparation of hollow polylactide microcapsules through premix membrane emulsification-Effects of nonsolvent properties.* Journal of membrane science, 2008. **325**(2): p. 665.

37. Wienk, I. M., Boom, R. M., Beerlage, M. A. M., Bulte, A. M. W., Smolders, C. A., Strathmann, H., *Recent advances in the formation of phase inversion membranes made from amorphous or semi-crystalline polymers.* Journal of Membrane Science, 1996. **113**(2): p. 361.

38. Young, T. H., Cheng, L. P., Lin, D. J., Fane, L., Chuang, W. Y., *Mechanisms of PVDF membrane formation by immersion-precipitation in soft (1-octanol) and harsh (water) nonsolvents.* Polymer, 1999. **40**(19): p. 5315.

39. Sawalha, H., Schroën, K., Boom, R., *Polylactide films formed by immersion precipitation: Effects of additives, nonsolvent, and temperature.* Journal of Applied Polymer Science, 2007. **104**(2): p. 959.

40. Bulte, A. M. W., Mulder, M. H. V., Smolders, C. A., Strathmann, H., *Diffusion induced phase separation with crystallizable nylons. II. Relation to final membrane morphology.* Journal of Membrane Science, 1996. **121**(1): p. 51.

41. Cheng, L. P., Young, T. H., You, W. M., *Formation of crystalline EVAL membranes by controlled mass transfer process in water-DMSO-EVAL copolymer systems.* Journal of Membrane Science, 1998. **145**(1): p. 77.

42. Van De Witte, P., Dijkstra, P.J., Van Den Berg, J.W.A., Feijen, J., *Phase behavior of polylactides in solvent-nonsolvent mixtures.* Journal of Polymer Science Part B: Polymer Physics, 1996. **34**(15): p. 2553.

43. Li, M., Rouaud, O., Poncelet, D., *Microencapsulation by solvent evaporation: State of the art for process engineering approaches.* International Journal of Pharmaceutics, 2008. **363**(1-2): p. 26.

44. Jeyanthi, R., Thanoo, B.C., Metha, R.C., DeLuca, P.P., *Effect of solvent removal technique on the matrix characteristics of polylactide/glycolide microspheres for peptide delivery.* Journal of Controlled Release, 1996. **38**(2-3): p. 235.

45. Yang, Y.-Y., Chung, T.-S., Bai, X.-L., Chan, W.-K., *Effect of preparation conditions on morphology and release profiles of biodegradable polymeric microspheres containing protein fabricated by double-emulsion method.* Chemical Engineering Science, 2000. **55**(12): p. 2223.

46. Maia, J.L., Santana, M.H.A., Ré, M.I., *The effect of some processing conditions on the characteristics of biodegradable microspheres obtained by an emulsion solvent evaporation process.* Brazilian Journal of Chemical Engineering, 2004. **21**: p. 01.

47. Peltonen, L., Koistinen, P., Karjalainen, M., Häkkinen, A., Hirvonen, J., *The effect of cosolvents on the formulation of nanoparticles from low-molecular-weight poly(I)lactide.* AAPS PharmSciTech, 2002. **3**(4): p. 52.

48. Sawalha, H., Schroën, K., Boom, R., *mechanical properties and porosity of polylactide for biomedical applications.* Journal of applied polymer science, 2008. **107**(1): p. 82.

49. Izumikawa, S., Yoshioka, S., Aso, Y., Takeda, Y., *Preparation of poly(l-lactide) microspheres of different crystalline morphology and effect of crystalline morphology on drug release rate.* Journal of Controlled Release, 1991. **15**(2): p. 133.

50. Park, S.-J., Kim, S.-H., *Preparation and characterization of biodegradable poly(l-lactide)/poly(ethylene glycol) microcapsules containing erythromycin by emulsion solvent evaporation technique.* Journal of Colloid and Interface Science, 2004. **271**(2): p. 336.

51. Garkhal, K., Verma, S., Jonnalagadda, S., Kumar, N. , *Fast degradable poly(L-lactide-co-ε-caprolactone) microspheres for tissue engineering: Synthesis, characterization, and degradation behavior .* Journal of Polymer Science Part A: Polymer Chemistry, 2007. **45**(13): p. 2755.

52. Edlund, U., Albertsson, A.-C., *Morphology engineering of a novel poly(L lactide)/poly(1,5-dioxepan-2-one) microsphere system for controlled drug delivery.* Journal of Polymer Science Part A: Polymer Chemistry, 2000. **38**(5): p. 786.

53. Hu, Y., Hu, Y.S., Topolkaraev, V., Hiltner, A., Baer, E., *Aging of poly(lactide)/poly(ethylene glycol) blends. Part 2. Poly(lactide) with high stereoregularity.* Polymer, 2003. **44**(19): p. 5711.

54. Sosnowski, S., *Poly(-lactide) microspheres with controlled crystallinity.* Polymer, 2001. **42**(2): p. 637.

55. Sawalha, H., Schroën, K., Boom, R., *Hollow polylactide microcapsules with controlled morphology and thermal and mechanical properties.* Submitted, 2008.

56.   Sawalha, H., Schroën, K., Boom, R., *Addition of oils to polylactide casting solutions as a tool to tune film morphology and mechanical properties.* Submitted, 2008.

57.   Vladisavljevic, G.T., Schubert, H., *Preparation and analysis of oil-in-water emulsions with a narrow droplet size distribution using Shirasu-porous-glass (SPG) membranes.* Desalination, 2002. **144**(1-3): p. 167.

58.   Ma, G. H., Omi, S., Dimonie, V. L., Sudol, E. D., El-Aasser M. S., *Study of the preparation and mechanism of formation of hollow monodisperse polystyrene microspheres by SPG (Shirasu Porous Glass) emulsification technique.* Journal of applied polymer science, 2002. **85**(7): p. 1530.

59.   Ma, G., Nagai, M., Omi, S., *Preparation of uniform poly(lactide) microspheres by employing the Shirasu Porous Glass (SPG) emulsification technique.* Colloids and surfaces. A, Physicochemical and engineering aspects, 1999. **153**(1-3): p. 383.

60.   Liu, R., Ma, G., Meng, F.-T., Su, Z.-G., *Preparation of uniform-sized PLA microcapsules by combining Shirasu Porous Glass membrane emulsification technique and multiple emulsion-solvent evaporation method.* Journal of Controlled Release, 2005. **103**(1): p. 31.

61.   Van Der Graaf, S., Steegmans, M.L.J., Van Der Sman, R.G.M., Schroën, C.G.P.H., Boom, R.M., *Droplet formation in a T-shaped microchannel junction: A model system for membrane emulsification.* Colloids and Surfaces A: Physicochemical and Engineering Aspects, 2005. **266**(1-3): p. 106.

62.   Nisisako, T., Torii, T., *Microfluidic large-scale integration on a chip for mass production of monodisperse droplets and particles.* Lab on a Chip - Miniaturisation for Chemistry and Biology, 2008. **8** (2): p. 287.

63.   Van Der Graaf, S., Schroën, C.G.P.H., Van Der Sman, R.G.M., Boom, R.M., *Influence of dynamic interfacial tension on droplet formation during membrane emulsification.* Journal of Colloid and Interface Science, 2004. **277**(2): p. 456.

64.   Gijsbertsen-Abrahamse, A.J., Boom, R.M., Van Der Padt, A., *Why liquid displacement methods are sometimes wrong in estimating the pore-size distribution.* AIChE Journal, 2004. **50**(7): p. 1364.

65.   Sugiura, S., Nakajima, M., Tong, J., Nabetani, H., Seki, M., *Preparation of Monodispersed Solid Lipid Microspheres Using a Microchannel Emulsification Technique.* Journal of Colloid and Interface Science, 2000. **227**(1): p. 95.

66. Sieval, A.B., Linke, R., Heij, G., Meijer, G., Zuilhof, H., Sudhölter, E.J.R., *Amino-Terminated Organic Monolayers on Hydrogen-Terminated Silicon Surfaces.* Langmuir, 2001. **17**(24): p. 7554.

67. De Smet, L.C.P.M., Stork, G.A., Hurenkamp, G.H.F., Sun, Q.-Y., Topal, H., Vronen, P.J.E., Sieval, A.B., Wright, A., Visser, G.M., Zuilhof, H.,Sudhölter, E.J.R., *Covalently Attached Saccharides on Silicon Surfaces.* Journal of the American Chemical Society, 2003. **125**(46): p. 13916.

68. Arafat, A., Schroën, K., De Smet, L.C.P.M., Sudhölter, E.J.R., Zuilhof, H., *Tailor-Made Functionalization of Silicon Nitride Surfaces.* Journal of the American Chemical Society, 2004. **126**(28): p. 8600.

69. Rosso, M., Arafat, A., Schroën, K., Giesbers, M., Roper, C.S., Maboudian, R., Zuilhof, H., *Covalent Attachment of Organic Monolayers to Silicon Carbide Surfaces.* Langmuir, 2008. **24**(8): p. 4007.

Summary

Summary

Polylactide (PLA) is a biodegradable, biocompatible, and nontoxic polyester, which has various applications i.e. in the biomedical, and pharmaceutical field. In the biomedical field, PLA is used to prepare different types of biomaterials e.g. sutures, bone screws, scaffolds, films for tissue engineering, and microcapsules for controlled drug delivery systems. Besides, hollow PLA microcapsules can be used as ultrasound contrast agent (UCA). Imaging of the body with ultrasound can be significantly improved when UCA's are used because these capsules can resonate in the acoustic field which increases the backscatter signal of the ultrasound. Loading the UCA's with drugs gives extra benefits as the drug can be released at the desired location by bursting the capsules with the ultrasound. Successful application of these capsules in the body requires control over various properties including size, size distribution, structure, and thermal and mechanical properties; therefore, these aspects will be discussed extensively in the following chapters. The overall aim of the thesis is to produce hollow microcapsules with tuneable properties.

Various emulsification techniques can be used to prepare PLA microcapsules such as sonication, high-pressure homogenizers, and (pre-mix) membrane emulsification. Since pre-mix membrane emulsification offers the best combination of control over size and size distribution of the primary emulsion droplets and high throughput, this method was used to prepare the microcapsules. For microcapsule preparation, a solution containing PLA, dichloromethane (solvent for the polymer), and an oil (poor solvent for the polymer) is used. This solution is mixed with a non-solvent phase (water) to give the coarse pre-mix. The pre-mix, is repeatedly pushed through a membrane, and upon passage of the membrane, the large droplets are broken into smaller ones. After emulsification, the solvent is slowly extracted from the droplets to the water phase, and the solution becomes unstable and phase separates. Because the oil is poorly compatible with water, it will from a droplet inside the original droplet; the polymer between the internal oil droplet and the external water phase will eventually solidify, forming a shell around the oil droplet. Removal of the oil by freeze-drying eventually leads to formation of hollow microcapsules.

Although the emulsification process determines the size and size distribution of the emulsion that is initially formed, the solidification process determines whether size and size distribution can be conserved. Therefore, the effects of nonsolvent and oil on the solidification process of the polymer are first studied in a model system for microcapsules: PLA films prepared by immersion precipitation (chapter 2). PLA/DCM/dodecane solutions are cast on a glass plate and submersed in different water-methanol mixtures that are used as nonsolvent. With water, the solidification of the polymer occurs very slowly, whereas the phase separation rate significantly increases with increasing methanol concentration in the nonsolvent. This results in different morphologies of the films, and as shown in chapter 3, in major differences in the mechanical properties of the films. Weak and fragile films are obtained with water, while the strength and ductility of the films considerably increase with increasing methanol concentration in the nonsolvent. The insights obtained in chapters 2 and 3, are applied to microcapsules in the following two chapters.

In chapter 4 and 5, results are shown for PLA microcapsules prepared with premix membrane emulsification using different water-alcohol mixtures as nonsolvent. The solvent removal process is characterised experimentally and by computer simulation based on a Maxwell-Stefan model for non-ideal, multi-component mass transfer. It was shown that addition of alcohol speeds up the formation process of the capsules through faster extraction of DCM from the droplets to the nonsolvent because of increased solubility of DCM in the nonsolvent phase (DCM is fully miscible with the pure alcohol). This leads to faster solidification and preservation of the droplet size; the particles prepared with alcohol have a smoother surface than those prepared with water. As an added benefit, the alcohol lowers the interfacial tension, which decreases the size and span of the capsules, and enhances the emulsification efficiency.

Besides the effect of nonsolvent, also, the effects of various oils on morphology and other properties are investigated. In chapter 6, results for air-cast films are presented, and in chapter 7, results for microcapsules are shown. The tested oils are linear alkanes, cyclic alkanes, and two terpenes (limonene and eugenol). Addition of most of the oils induces extra porosity in the films, and results in hollow

microcapsules. The thermal and mechanical properties of the films and particles are strongly dependent on the oil; the glass transition temperatures of the films and hollow capsules are lower when prepared with oil. The oil induces extra mobility in the structure, which allows crystallization to start at lower temperatures, and therewith crystallinity of the films and capsules is influenced. As a result, the mechanical strength and elastic modules of the films are lower, whereas ductility is improved. The stiffness of some of the capsules is measured with AFM, and again a relation with the oil used is found, albeit that the relation is slightly different from the one found for films.

In chapter 8, various factors that are discussed in the previous chapters are brought together. Fundamental aspects of the formation process of hollow PLA microcapsules through emulsion solvent/evaporation are discussed, in relation to both phase separation phenomena and emulsion preparation. The main effects of the nonsolvent and oil on the solidification process of the polymer and on the physical and chemical properties of the capsules are summarised and compared with literature. It is expected that the solvent/non-solvent interactions determine the size of the microcapsules and the polymer/oil interactions the mechanical properties. Besides, different emulsification methods for preparation of microcapsules are presented and evaluated, and finally, improvements and adaptations for the current process are presented which lead to the proposed 'ideal' production system for the microcapsules.

Samenvatting

Samenvatting

Polymelkzuur, dat ook bekend staat onder de naam polylactide (PLA), is een biologisch afbreekbare, biocompatibele, niet toxische polyester die verschillende toepassingen kent in het biomedische en farmaceutische veld. In het biomedische veld wordt PLA gebruikt om verschillende biomaterialen te maken, zoals hechtingen, schroeven die in botten gebruikt kunnen worden, dragermateriaal om cellen op te laten groeien, films voor 'cel engineering', en microcapsules voor de gecontroleerde vrijgave van medicijnen. Los daarvan kunnen holle PLA microcapsules gebruikt worden als ultrageluid-contrastmiddel; de beeldkwaliteit van een echograaf kan aanzienlijk worden verbeterd als deze contrastmiddelen gebruikt worden omdat de capsules resoneren in het akoestische veld waardoor de signalen versterkt worden. Als de contrastmiddelen beladen worden met medicijnen kan dit extra voordelen geven omdat de medicijnen lokaal kunnen worden 'afgeleverd' door de capsules open te laten barsten met het ultrageluid. Om tot een succesvolle toepassing van deze capsules in het lichaam te komen, moeten verschillende eigenschappen van de capsules goed beheerst kunnen worden, zoals de grootte, de grootteverdeling, de structuur, en de thermische en mechanische eigenschappen, vandaar dat deze aspecten uitvoerig worden besproken in de verschillende hoofdstukken van dit proefschrift. Het uiteindelijke doel van dit onderzoek was om holle microcapsules te produceren waarvan de eigenschappen naar wens kunnen worden ingesteld.

Verschillende emulgeertechnieken kunnen worden gebruikt om microcapsules te bereiden zoals sonificeren, homogeniseren bij hoge druk, en (premix) membraanemulgeren. Aangezien premix membraanemulgeren de beste combinatie geeft van controle over de grootte en grootteverdeling van de primaire emulsie, en tevens een hoge productiviteit heeft, is deze methode gebruikt om de capsules te vervaardigen. Voor de bereiding van de microcapsules wordt een oplossing van PLA in di-chloro-methaan (DCM: goed oplosmiddel voor het polymeer) gemaakt, en daaraan wordt een olie toegevoegd (de olie is een slecht oplosmiddel voor het polymeer). Deze oplossing wordt gemengd met een non-solvent fase (water) zodat een grove premix emulsie ontstaat. De premix wordt vervolgens herhaaldelijk door een membraan geperst, en tijdens het passeren van het membraan worden de grote

emulsiedruppels opgebroken in kleinere. Nadat het emulgeren is voltooid, zal het oplosmiddel langzaam uit de druppels naar de waterfase worden geëxtraheerd; de oplossing wordt instabiel en fasescheiding treedt op. Omdat de olie slechts weinig compatibel is met water, zal zich een oliedruppel in de emulsiedruppel vormen, waarbij het polymeer dat zich tussen de interne oliedruppel en de externe waterfase bevindt vast zal worden en zo een schil vormt rond de oliedruppel. De olie kan verwijderd worden door vriesdrogen waarna holle microcapsules ontstaan.

Het emulgeerproces bepaalt de grootte en grootteverdeling van de emulsie die initieel gevormd wordt, maar het fasescheidingsproces bepaalt of deze ook behouden blijven. Daarom zijn eerst de effecten van nonsolvent en olie op het solidificatieproces van het polymeer onderzocht aan de hand van een modelsysteem voor microcapsules: polymeerfilms die bereid zijn via immersieprecipitatie (hoofdstuk 2). Van een PLA/DCM/dodecane oplossing wordt een film gemaakt op een glasplaat die vervolgens wordt ondergedompeld in een water/methanol mengsel dat gebruikt wordt als nonsolvent. Met alleen water voltrekt de solidificatie zich erg traag, terwijl de fasescheiding aanzienlijk sneller wordt met toenemende hoeveelheid methanol in het nonsolvent. Hierdoor worden films met verschillende morfologie gevormd, en, zoals in hoofdstuk 3 wordt geïllustreerd, ook films met hele verschillende mechanische eigenschappen. Zwakke en fragiele films worden verkregen met water als nonsolvent terwijl de sterkte en rekbaarheid van films aanzienlijk toeneemt met toenemende hoeveelheid methanol in het nonsolvent. De inzichten verkregen in hoofdstukken 2 en 3 worden toegepast op microcapsules in de volgende twee hoofdstukken.

In hoofdstukken 4 en 5 worden resultaten gepresenteerd voor PLA microcapsules die bereid zijn via premix membraanemulgeren waarbij verschillende water/alcohol mengsels als nonsolvent zijn gebruikt. De verwijdering van het oplosmiddel DCM is gekarakteriseerd, zowel experimenteel als modelmatig door computersimulaties gebaseerd of een Maxwell-Stefan model voor niet-ideaal, multi-component massa transport. Toevoeging van alcohol versnelt het vormingsproces van de capsules door sneller extractie van DCM naar de nonsolvent-fase waarin DCM beter oplost (DCM is volledig mengbaar met pure alcohol). Dit leidt tot een snellere solidificatie en behoud van de druppelgrootte; capsules die bereid zijn met alcohol

hebben een gladder oppervlak dan capsules die met water bereid zijn. Als toegevoegd voordeel verlaagt alcohol de grensvlakspanning, waardoor kleinere capsules gemaakt kunnen worden en hun grootteverdeling scherper wordt: met andere woorden, de emulgeerefficiency wordt hoger.

Behalve het effect van nonsolvent is ook het effect van de olie onderzocht op onder andere de morfologie. In hoofdstuk 6 worden resultaten gepresenteerd voor films die aan de lucht gemaakt zijn, en in hoofdstuk 7 worden resultaten weergegeven voor microcapsules. De getest oliën zijn lineaire alkanen, cyclische alkanen, en twee terpenen (limoneen en eugenol). Toevoeging van de meeste oliën leidt tot extra porositeit in de films, en resulteert in holle microcapsules. De thermische en mechanische eigenschappen van de films en deeltjes zijn sterk afhankelijk van de gebruikte olie. De glasovergang van de films en holle capsules gebeurt bij lagere temperaturen als olie gebruikt is bij de bereiding. De olie zorgt voor extra mobiliteit in de structuur waardoor kristallisatie al bij lagere temperatuur kan beginnen en de kristalliniteit van de films en capsules wordt beïnvloed. Het resultaat is dat de mechanische sterkte en elasticiteitsmodulus van de films lager wordt terwijl de rekbaarheid groter wordt. De stijfheid van sommige capsules is gemeten met AFM, en opnieuw is een relatie gevonden met de gebruikte olie, al is deze relatie anders dan die voor films.

In hoofdstuk 8 worden verschillende factoren die in de eerdere hoofdstukken zijn gepresenteerd bediscussieerd en samengebracht. Fundamentele aspecten van het vormingsproces van holle PLA microcapsules door emulsie solvent/verdamping worden besproken in relatie tot fasescheiding en emulsiebereiding. De hoofdeffecten van nonsolvent en olie op het solidificatieproces van het polymeer, en op de fysische en chemische eigenschappen van de capsules worden samengevat en vergeleken met de literatuur. De verwachting is dat de solvent/non-solvent interacties de grootte van de capsule bepalen en de polymeer/olie interacties de mechanische eigenschappen. Verder worden verschillende emulgeermethoden gepresenteerd en geëvalueerd, en uiteindelijk worden verbeteringen en aanpassingen voor het huidige proces gepresenteerd die moeten leiden tot het 'ideale' productiesysteem voor microcapsules.

Acknowledgments

Alhamdulillah, doing a PhD was a dream for me since my childhood and I worked hard to achieve that. Achieving this dream is a great grace of almighty (Allah) who provided me with the power, health, and patience to accomplish my PhD. All praises and thanks goes to you Allah for everything and I pray day and night to accept this work from me.

I am profoundly grateful to my mother and father for their never ending support and encouragement all through my life. Without your prayers, it would have not been possible to accomplish this work.

I would like to thank all of my brothers and sisters. I am especially indebted to my brothers Abd Al-Salam, Hafez, Fareed and late brother Mahmoud. This achievement is yours as it is mine, you contributed to it since I was a little child by making everything possible to continue my education, only Allah can reward you for all that you have done for me, thanks a lot my brothers.

My dearest and lovely wife Amal, you are a major contributor to this success. You took all the troubles and difficulties to let me concentrate only on my PhD. You took good care of our house and little daughters (Amra and Salsabeel) and in the mean time you were busy with your master degree, so you had to fight at many fronts in the same time, but you were successful in all of them, Alhamdulillah. I am very grateful to you and to Amra and Salsabeel, and at the same time I am very proud of you.

I like also to thank Allah that he brought me to Wageningen University to do my PhD with such kind people like Karin and Remko. My dear daily supervisor, Karin, I don't know if these few words would be enough to express my deep gratitude for all what you have done for me and family during our stay in the Netherlands. Generally, the paper work concerning visa application is a hassle for most of the overseas students but for a student coming from Palestine is an absolute challenge, as Palestine is not yet considered a state in the Netherlands. However, you didn't give up and have tried your best to convince the immigration office (IND) to grant us the visa and finally we could come to the Netherlands. In the mean time, you arranged the accommodation and every thing that can make our life easy and comfortable and that allows me actually to smoothly start my work in the group. During my daily work, I got all the help, support, and encouragement from you

which were a real drive for success. I learned many things from you, especially how to write in a concise and scientific manner. Thanks a lot Karin!

I like to abundantly thank my promoter Remko. Dear Remko, your smart ideas and valuable comments have given the work extra value and the enthusiasm you showed in my work has motivated me to do my best in the project. I have learned a lot about polymers form you and I highly appreciate your help with the constructions of the phase diagrams. Finally, it was an honor for me to be part of your research team.

To my colleagues at the process engineering group in the 6th floor, Biotechnion, I deeply thank all of you for the joyful and '*gezellige*' atmosphere. Being with nice colleagues like you has left in mind a lot of nice memories which I will never forget, especially form the lovely '*labuitjes*'. A special thank goes to Francisco Rossier, for the kind help with the cover and with the AFM measurements. I wish also to especially thank my roommates (room 621, Biotechnion), Mohammed, Sayam, Petra, and Lieke for the friendly and pleasant environment in our office.

I like to thank all the BSc and MSc students who helped me during my PhD. I express my thanks here to Nanik Purwanti, Zheng Ke, Yuxuan Fan, and Shuang Liu for their valuable contributions to my thesis.

I would like to express my sincere thankfulness to the BURST team, Marcel, Ceciel, Klazina, Nico, Annemieke, and Michel for the fruitful discussions, brilliant ideas, and kind help over the period of the project.

The laboratory and technical support is very essential for any PhD student; I wish here to thank Jos Sewalt for his help with the equipment in the lab. Thanks are also expressed to Herman Teunis, Addrian van Aelst and Jacqueline Donkers for their help with SEM images and Herman de Beukelaer for his help with the DSC experiments.

Back home in my lovely country Palestine, I would like to thank all of my relatives, uncles, aunts, sisters and brothers in-law, mother in-law, nephews, nieces (Shireen, Sharihan, Boshra, Maraam, …), teachers, and friends, for their encouragement and support.

My deep and warm thanks and gratitude to my best friends in Wageningen and the Netherlands, with whom my family and I spent the most joyful and pleasant times in the Netherlands: The families of Abu Osama, Rafat, Ahmad Altatari, Sami, Mohammed Tayem, Abu Ibrahim, Mustafa, Shahrul, Feras and Mohammad. Also

Publication list

1. Hassan Sawalha, Yuxuan Fan, Karin Schroën and Remko Boom, Preparation *of hollow polylactide microcapsules through premix membrane emulsification-Effects of nonsolvent properties.* Journal of membrane science, 2008. 325(2): p. 665-671.

2. Hassan Sawalha, Nanik Purwanti, Arjen Rinzema, Karin Schroën and Remko Boom, *Polylactide microspheres prepared by premix membrane emulsification-Effects of solvent removal rate.* Journal of membrane science, 2008. 310(1-2): p. 484-493.

3. Hassan Sawalha, Karin Schroën and Remko Boom, *Mechanical properties and porosity of polylactide for biomedical applications.* Journal of applied polymer science, 2008. 107(1): p. 82-93.

4. Hassan Sawalha, Karin Schroën and Remko Boom, *Polylactide films formed by immersion precipitation: Effects of additives, nonsolvent, and temperature.* Journal of applied polymer science, 2007. 104(2): p. 959-971.

5. Hassan Sawalha, Karin Schroën and Remko Boom*, Addition of oils to polylactide casting solutions as a tool to tune film morphology and mechanical properties.* Submitted for publication

6. Hassan Sawalha, Karin Schroën and Remko Boom*, Hollow polylactide microcapsules with controlled morphology and thermal and mechanical properties.* Submitted for publication.

7. Hassan Sawalha, Karin Schroën and Remko Boom*, Polylactide microcapsules formation.* To be submitted for publication

Conferences

1. Hassan Sawalha, Karin Schroën and Remko Boom, *Preparation of Polylactide microspheres for use as ultrasound contrast agents,* 8th World Biomaterials Congress, 28 May - 1 June, 2008, Amsterdam, The Netherlands.

2. Hassan Sawalha, Karin Schroën and Remko Boom, *Polylactide particles for ultrasound imaging,* advanced nanomaterials conference, 21-25 June, 2008, Aveiro, Portugal.
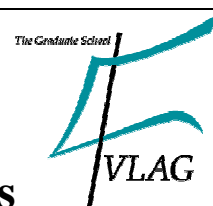
Overview of completed training activities

Discipline specific activities	Year	ECTS
Courses		
Lattice Boltzmann simulation for particulate systems, Wageningen university	2005	1.4
Bionanotechnology, VLAG	2006	1.5
Unified approach to mass transfer, OSPT/VLAG	2007	1.4
Meetings		
Netherlands Process Technology Symposium, the Netherlands	2005/2007	2.2
11th NMG Posterday, Ede, the Netherlands	2005	0.8
Dies symposium on Bionanotechnology, Wageningen,	2006	0.3
8th World Biomaterials Congress, Amsterdam	2008	2.0
Advanced nanomaterials conference, Aveiro, Portugal	2008	2.0
Microbubbles for Ultrasound Imaging and Drug Delivery workshop, Eindhoven, the Netherlands	2008	0.3

General courses

	Year	ECTS
Techniques for writing and presenting a scientific paper, Wageningen University	2007	1.2
Supervising student thesis, Wageningen University	2007	0.7

Optionals

	Year	ECTS
Preparation PhD research proposal		6.0
Group theme meetings		3.0
Project theme meetings		3.0
PhD trip Denmark and Sweden	2006	1.7
PhD trip Japan	2008	2.5
Brian storm week	2005	1.4

Total		**31.4**

About the author

Hassan Sawalha was born in Bani Naim, Hebron, Palestine, on August 5th, 1979. In 1997, he graduated from secondary school (Bani Naim secondary school) and in the same year, he joined An-Najah National University, Nablus, Palestine, to study Chemical Engineering. In 2002, he obtained his BSc. degree in Chemical Engineering. Shortly after that, Hassan was employed as research assistance at Hebron University, Palestine. In August 2003, he received a scholarship from the Swedish Institute to do his master degree at Chalmers University of Technology, Gothenburg, Sweden in the international master program of 'Environmentally Sustainable Process Technology'. Hassan obtained his MSc. degree from Chalmers University in December 2004. In April 2005, he started his PhD. Project, entitled 'Bubbles for Ultrasound and Therapy (BURST)', at the Food and Bioprocess Engineering Group of Wageningen University, the Netherlands. The results of this PhD. research are presented in this thesis. Hassan can be reached through his email address: hassan.sawalha@gmail.com.

الفصلان السادس و السابع يلخصان تأثير نوع الزيت المضاف إلى محلول المبلمر على الصفات التركيبية و الميكانيكية و الحرارية لكريات و صفائح المبلمر. لعمل هذه الدراسة، قمنا باستخدام أنواع مختلفة من الزيوت (الديكانات و الديكانات الحلقية و كذلك بعض الزيوت العطرية). دللت النتائج أن لنوعية الزيت تأثير كبير على صفات المبلمر وأن غالبية أنواع الزيوت المستخدمة أدت إلى تكون صفائح مسامية و كريات مفرغة. بينت الدراسة كذلك أنه يمكن التحكم بشكل فعال في الصفات الميكانيكية (القوة و المرونة) و الحرارية من خلال نوعية الزيت المضاف. عُزي الاختلاف في تأثير هذه الزيوت على صفات المبلمر إلى اختلاف التفاعل الجزيئي لمبلمر حامض اللبنيك مع هذه الزيوت.

الفصل الثامن من هذه الدراسة يلخص النتائج التي تم التوصل إليها في الفصول السابقة مع التركيز بشكل أكبر على تأثير نوع غير المذيب و الزيت على التفاعل الجزيئي مع المبلمر و تأثيره على صفات الكريات الناتجة.
في النهاية تم تقديم اقتراح لعملية تحضير نموذجية لكريات مبلمر حامض اللبنيك مبنية بشكل أساسي على النتائج التي تم التوصل إليها في هذه الرسالة و توفر تحكماً جيداً في الصفات الأساسية لهذه الكريات.

تمت بحمد ألله.

مختلفة و غير متناسقة مما يؤثر على فعالية استخدامها الطبي. لذلك قمنا في هذه الدراسة باستخدام طريقة حديثة تم اختراعها مؤخراً و توفر قدراً كبيراً من التحكم في حجم الكريات الناتجة. تحضير الكريات بهذه الطريقة يتم على النحو التالي: بعد خلط محلول المبلمر بالماء باستخدام الخلاط الميكانيكي نقوم بتمرير الخليط الناتج من محلول المبلمر و الماء داخل غشاء مسامي "منخل" ذو فتحات صغيرة و متساوية في الحجم نسبياً. مرور قطرات المبلمر داخل هذه الفتحات يؤدي إلى تكسير القطرات الكبيرة إلى قطرات أصغر و للحصول على أحجام متساوية يتم تمرير الخليط عدة مرات خلال فتحات الغشاء المسامي.

إن صفات كريات المبلمر لا تعتمد فقط على طريقة التحضير و لكن العمليات اللاحقة، كاستخلاص المذيب من الكريات و ترسب المبلمر يمكن أن تؤثر تأثيراً كبيراً في صفات هذه الكريات. في هذا البحث تمت دراسة العوامل المؤثرة على خصائص الكريات بشكل منظم و تفصيلي.

يلخص الفصل الثاني و الثالث من هذه الدراسة تأثير نوعية غير المذيب و تركيز الزيت على عملية ترسب المبلمر. تمت هذه الدراسة على صفائح من المبلمر تم تحضيرها تحت ظروف مشابهة لتلك التي يتم تحضير الكريات فيها. تحضير هذه الصفائح تم عن طريق دهن جزء من محلول مبلمر حامض اللبنيك المحتوي على زيت الديكان على قطعة من الزجاج و التي تم غمسها في محاليل غير مذيبة محتوية على تراكيز مختلفة من محلول الميثانول في الماء. استخلاص المذيب (ثاني كلوريد الميثان) من محلول المبلمر أدى إلى ترسب المبلمر على شكل صفيحة دقيقة. بينت النتائج أن إضافة الميثانول إلى الماء أدى إلى زيادة سرعة استخلاص المذيب مما سرع في عملية ترسب المبلمر بشكل كبير و هذا أدى إلى إحداث تغير كبير في الصفات التركيبية و الميكانيكية للصفائح. الصفائح التي تم تحضيرها في غير مذيب يحتوي على الماء فقط كانت هشة و غير مرنة، في حين أنه بزيادة تركيز الميثانول في الماء زادت قوة هذه الصفائح و زادت مرونتها. كذلك أوضحت النتائج أن تركيز الزيت يلعب دوراً مهماً في عملية ترسب المبلمر. زيادة تركيز زيت الديكان داخل محلول المبلمر أدى إلى زيادة مسامية الصفائح مما أضعف من قوتها الميكانيكية و لكن مرونتها تحسنت. النتائج التي تم الحصول عليها من الصفائح تم تطبيقها على الكريات كما وضح ذلك في الفصل الرابع و الخامس من هذه الرسالة.

في البداية تم دراسة تأثير صفات غير المذيب على سرعة استخلاص المذيب من الكريات من خلال التجربة عن طريق تحضير الكريات في عدة محاليل غير مذيبة محتوية على الماء و الكحول و كذلك نظرياً باستخدام نموذج رياضي مبني بشكل أساسي على قانون انتقال المادة. وضحت النتائج أن استخدام الكحول مع الماء في محاليل غير المذيب أدى إلى الإسراع في إستخلاص المذيب من الكريات و ذلك بسب أن المذيب (ثاني كلوريد الميثان) ذائب بشكل كامل مع الكحول في حين أن ذائبيته في الماء قليلة جداً. سرعة إستخلاص المذيب هذه أدت إلى الإسراع في ترسب المبلمر مما أدى بالتالي إلى تكون الكريات بشكل أسرع و الذي ساعد بدوره على تحسين صفات هذه الكريات. بالإضافة إلى ذلك، فان إضافة الكحول إلى غير المذيب أدى إلى تكوين كريات ذات أحجام صغيرة و أكثر تناسقاً.

الملخص العربي

يعتبر التشخيص الناجح لأي مرض من الخطوات المهمة بل و الحاسمة في عملية العلاج. إلا أن الآلية الحالية لاكتشاف و تشخيص الأمراض تعتمد بشكل أساسي على وجود تغيير في شكل أو حجم الخلية أو الجهاز المصاب و لكن البداية الحقيقية للمرض تكون قبل ذلك بمراحل. و لعلاج هذه الأمراض علاجاً ناجعاً لابد من اكتشافها في مراحلها الأولية. هنالك طرق متعددة تم و يتم استخدامها للكشف عن الأمراض لعل أهمها التصوير بالأشعة فوق الصوتية و التي تتمتع بمميزات مهمة من حيث رخص ثمنها نسبياً و توفرها بأعداد كبيرة و خلوها من الأشعة الضارة مقارنة مع طرق التصوير الأخرى. على الرغم من هذه المميزات، إلا أن هناك مشكلة تواجه الأطباء عند تشخيص الجسم بهذه الأشعة، ذلك أن الدم لا يستطيع عكس هذه الأشعة بشكلٍ كافٍ مما يؤثر على وضوح الصورة. للتغلب على هذه لذلك يتم حقن الجسم بمواد مساعدة تقوم بعكس هذه الأشعة بشكل جيد مما يزيد في وضوح الصورة و يساهم في تشخيص الأمراض تشخيصاً دقيقاً. هذه المواد هي عبارة عن كريات من المبلمر حجمها مماثل لحجم كريات الدم الحمراء (١- ٥ ميكروميتر) مفرغة من الداخل و محتوية على الهواء. وجود الهواء داخل هذه الكريات يمكنها من الاهتزاز في المجال الصوتي مما يزيد من انعكاس الأشعة و يحسن عملية التشخيص بشكل كبير. إضافة إلى استخدامها في عمليات التشخيص، يمكن تطوير هذه الكريات بحيث يتم حقنها بالدواء و باستخدام الأشعة يمكن إفراغ هذا الدواء في الخلايا و الأجهزة المصابة مما يزيد من فعالية العلاج و يقلل من الآثار الجانبية للدواء. إن الاستخدام الطبي الفعال لهذه الكريات يتطلب التحكم الجيد بأحجامها و أشكالها و صفاتها الميكانيكية و الحرارية.

إن الهدف الأساسي لهذه الرسالة هو تصميم كريات من مبلمر حامض اللبنيك "اللاكتيك، بولي لاكتيك أسيد" ذات أحجام صغيرة متساوية نسبياً وتتمتع بصفات تركيبية و ميكانيكية و حرارية محددة. لهذا الغرض قمنا باستخدام مبلمر حامض اللبنيك لتحضير هذه الكريات و ذلك لتمتعه بصفات مميزة أهلته لأن يكون من أكثر المبلمرات استخداماً في المجالات الطبية. فهذا المبلمر غير سام و قابل للتحلل الحيوي داخل الجسم كما أنه مسموح باستخدامه طبياً، حيث تم استعماله في تصنيع الكثير من المواد الطبية مثل خيوط خياطة الجروح وكذلك في تحضير الصفائح و الكريات المستخدمة في العمليات العلاجية.

تبدأ عملية تحضير كريات المبلمر بإذابة مبلمر حامض اللبنيك في مذيب جيد "ثاني كلوريد الميثان" ثم يتم إضافة القليل من الزيت "ديكان ثقيل" إلى هذا المحلول. بعد ذلك يتم خلط كمية معينة من محلول المبلمر مع محلول آخر يسمى غير المذيب و الذي عادة ما يكون الماء. استخلاص المذيب من قطرات محلول المبلمر بواسطة محلول غير المذيب (الماء) و تبخره لاحقاً يؤدي إلى ترسب المبلمر حول قطرات الزيت مكونةً كريات مبلمر ممتلئة بالزيت. بعد ذلك يتم جمع هذه الكريات باستخدام جهاز الطرد المركزي ثم يستخرج الزيت من داخل هذه الكريات بواسطة جهاز التبريد المجفف مما يؤدي إلى تكون كرات مبلمر ممتلئة بالهواء. إن عملية خلط محلول المبلمر بالماء تتم عادةً باستخدام أجهزة تقليدية مثل الخلاط الميكانيكي و التي غالباً ما ينتج عنها قطرات ذات أحجام

ألإهداء

إلى ينبوع الحنان و العطاء. . .

أمي و أبي

إلى روح الحبيب محمود

إلى نبع الوفاء و التفاني. . .

عبد السلام و حافظ و فريد

إلى اخوتي و أخواتي

إلى زوجتي الحبيبة أمل

إلى عمرة و سلسبيل

إلى جميع الأهل و الأصدقاء

إليكم جميعا اهدي هذا العمل المتواضع

بسم الله الرحمن الرحيم

كريات وصفائع ميلمر حامض اللبنيك: التحضير و الخصائص

رسالة دكتوراه مقدمة من

حسن اسماعيل محمود صوالحة

قسم هندسة الغذاء و العمليات الحيوية
جامعة فاخننجن

فاخننجن ـ هولندا

ربيع الأول / ١٤٣٠، الموافق أذار / ٢٠٠٩

In the name of Allah the most gracious most merciful

(وقل ربّ زدني علما)

"O my Lord! advance me in knowledge."

Cover: modified scanning electron microscope images of polylactide microspheres (see Figure 8a, chapter 4) and film (see Figure 2d, chapter 3). The images were embedded within Arabic architecture.